Essays on Interlocking Directorates and Speculative Dynamics

Inaugural-Dissertation
zur Erlangung des akademischen Grades eines Doktors
der Wirtschafts- und Sozialwissenschaften
der Wirtschafts- und Sozialwissenschaftlichen Fakultät
der Christian-Albrechts-Universität zu Kiel

vorgelegt von

MSc Ricardo Giglio

aus São Paulo, Brasilien

Kiel, September 2015

Gedruckt mit Genehmigung der Wirtschafts- und Sozialwissenschaftlichen Fakultät der Christian-Albrechts-Universität zu Kiel

Dekan: Professor Dr. Achim Walter

Erstberichterstattender: Professor Dr. Thomas Lux

Zweitberichterstattender: Professor Dr. Martin Quaas

Drittberichterstattender: Professor Dr. Johannes Bröcker

Tag der Abgabe der Arbeit: 18.03.2015

Tag der mündlichen Prüfung: 08.09.2015

"And the woman which thou sawest is that great city, which reigneth over the kings of the earth."

Revelation 17:18

CHRISTIAN-ALBRECHTS-UNIVERSITÄT ZU KIEL

Abstract

Faculty of Business, Economics and Social Sciences
Department of Economics

Doctor of Philosophy

Essays on Interlocking Directorates and Speculative Dynamics

by Ricardo Giglio

This thesis is composed by four chapters which can be classified in two broad topics. The first and second chapters deal with the properties of the networks created by interlocking directorates, while the third and fourth chapters with the so-called Efficient Market Hypothesis. Connecting these two topics is the notion of a stylized fact (also called a universal property) which is not accounted for by the currently stablished theory. The first chapter shows that the existence of a very well connected dominant community is not explained by the traditional preferential attachment models. In addition, it is also shown that the patterns of accumulation of board positions by single individuals observed in empirical data cannot be explained by a simple random binomial procedure.

An in depth analysis of a time framed interlocking directorates dataset from Spain is presented in order to argue that board linkages might have generated some kind of special conditions for lending that would not exist if based on economic criteria only. In addition, the effects of a new gender equality regulation are investigate to conclude that women are still under represented in the boards of directors, although an increase in their absolute number could be observed.

Finally, surrogate linearity tests and microscopic (agent based) models are applied in order to explain the stylized facts not account for by the Efficient Market Hypothesis. More specifically, with respect to the class of microscopic models called Structural Stochastic Volatility models, it is shown that the introduction of inactive traders increases the model ability to explain the stylized facts. Additionally, taking advantage of this model contest, it is argued that a simulation horizon one allows a model to run in order to estimate its parameters higher than what was previously assumed in not necessary in order to compare different models.

Acknowledgements

I wish to acknowledge the help provided by my supervisor, Dr. Thomas Lux, during the whole period of my research. His extremely qualified suggestions surely made the path for this research easier and much more interesting. I would also like to thank Dr. Simone Alfarano for the support and for the discussions during my stay in Spain. Special and kind thanks should be given to my wife Paula for the patience during these years of hard work, and to my family for their support and encouragement throughout my study, as it has always been in my life. Last but not least, thanks to Joseph for showing me that problems are always smaller than they look like.

Contents

List of Figures

List of Tables

Dedicated to Paula, to my family, and to everybody who has written it with me

Introduction

This thesis is composed by four chapters which can be divided into two broad topics. The first two chapters deal with the properties of the networks created by interlocking directorates, while the last two are concerned with the so-called Efficient Market Hypothesis. Connecting these two topics is the notion of a stylized fact, also called a universal property, which is not accounted for by the currently stablished theory. With respect to the first topic, the existence of a very well connected dominant community is not explained by the traditional preferential attachment models, while for the second topic, the Efficient Market Hypothesis fails to explain several of the statistical properties presented in financial data.

The first chapter, called *The Topology of the Global Interlocking Directorates* is organized as follows: first, it presents a literature review on interlocking directorates and their sources and effects on the economy. Afterwards, it highlights the small-world phenomenon, which consists of very large networks presenting both high average clustering coefficients and small average shortest path lengths. This is related to informal notion of *six degrees of separation*. The third section deals with communities by depicting why one should carefully choose a random network benchmark in order to assess whether some features observed in empirical networks are somehow unexpected or not. The fourth section presents two of the most applied random benchmark models to stress their resemblances and differences with respect to empirical interlocking networks.

Finally, the last section of the chapter introduces the rich club coefficient as a measure of intra-hub connectivity to show that the topology of the interlocking networks cannot be completely described by the simple interaction of nodes in a preferential attachment scenario. It is then argued that another explanation for the structure and

the emergence of a dominant interconnected hierarchy may have to do with attaining specific goals rather than with the *rich-gets-richer* effect.

The second chapter, called *Interlocking Directorates in Spain: Evidence from a Comprehensive Data Set* consists basically of two parts. The first part revisits the argumentation of the first chapter, in the light of a richer dataset concerning Spanish board networks, comprising seven years from 2004 to 2010. These findings add to the growing literature stressing the fundamental similarities (or stylized facts) between interlocking networks from a diverse set of countries. The second part provides an in depth analysis of this data set by highlighting the most influential nodes, companies, and sectors of activity, to stress the special role of financial institutions in the social network of board members.

In addition to that, a significant inverse relation between centrality and leverage of non-financial institutions could be observed during the period, suggesting that board linkages might have generated some kind of special conditions for lending that would not exist if based on economic criteria only. On the other hand, no significant relation between centrality and economic performance was found.

Moreover, the role of the highly capitalized Ibex companies in the network, gender differences, and the participation of politicians in company boards are investigated in the remaining section. It could be seen, for instance, (a) that more than half of the directors holding two or more board positions serve in at least one Ibex board, (b) that women's participation is increasing, although they still have smaller average centrality then men, and (c) that politicians are more likely to get a second positions than non politicians.

The third chapter, called *Investigation on the Simulation Horizon Requirement for Estimation of Agent Based Models* is organized as follows. The first section presents some selected stylized facts which will be used in the estimation of the models. The second section of the investigation briefly overview Agent Based Model (ABM) methodology, which is claimed to take into account the so-called stylized facts to a great extent, and, thus, could be viewed as an alternative to the Efficient Market Hypothesis theoretical background.

In doing so, selected recent empirical findings are highlighted, and a brief taxonomy for ABMs is presented. Then, in the following sections specific microscopic models are discussed in more detail while focusing on their ability to explain some of the stylized facts. Afterwards, the estimation of these models by the method of simulated moments is introduced and an investigation on the simulation horizon requirements is carried out by means of an example of model contest assessing the difference in goodness of fit of allowing inactive traders in one of the Structural Stochastic Volatility (SSV) models proposed by [5]. It is observed that (a) the augmented SSV model with inactive traders outperforms its default version with respect to the quantitative reproduction of some stylized facts, and (b) that a longer simulation horizon then the one assumed by [5] seems to be unnecessary in order to run model contests.

The fourth and last chapter, called *Testing for non-linear structures in artificial financial data: A Recurrence Quantification Approach*, generally deals with the stylized facts the Efficient Market Hypothesis fails to explain.More specifically, this chapter adds to the work presented in [3], which uses tradicional non-linearity measures in order to check for non-linearity or chaos in artificial financial data generated from the Lux-Marchesi model [6].

In this sense, this chapter presents an alternative method proposed based on Recurrence Quantification Analysis (RQA). Recurrence quantification analysis is a nonlinear method of analyzing dynamical systems. It is carried out by calculating some measures on the so-called Recurrence Plot, which is a graphical representation of how often in time a trajectory visits the neighbor regions of its phase space.

Afterwards, I present both the Recurrence Plots and the Recurrence Quantification Analysis in detail, to finally introduce the surrogate test for linearity which is used to assess the existence of non-linearities or chaos. The last section of the essay presents the application of these surrogate linearity test based on RQA measures to a synthetic data set generate from two agent based (microscopic) models. For instance, in the same way as pointed out by [3] and [2], the hypothesis of chaos or linearity is rejected for the majority of the subsamples, indicating that, if there is a deterministic process ruling the data, it is more complicated than the dynamics from low dimensional chaotic systems.

Chapter 1

The Topology of the Global Interlocking Directorates

Introduction

Random models based on network growth and preferential attachment have gained lots of attention in the recent literature [7]. This class of models is particularly interesting due to the generation of scale-free networks, that is, graphs in which the degree distribution of the nodes follows at least roughly a power law process. Scale-free networks are found in several and very diverse contexts, such as the internet, the World Wide Web, protein networks, communication systems, and many social networks [8]. The preferential attachment process, which is just about a preference of new nodes to attach to already highly connected nodes, implies the existence of massive hubs (i.e., very well connected nodes) forming an aristocratic network, in contrast to a more egalitarian one where node degrees do not vary wildly. This feature guarantees the relatively short average shortest path lengths observed in many natural and social networks, and make it resistant to naive, undirected attacks or failures. However, aristocratic networks are not necessarily safe against clever attacks in which the hubs are targeted. In some cases, after the removal of some important hubs, the network collapses to a large number of small and disconnected components. This fact highlights the important role the topology plays in sustaining a network.

Although corporate interlocks are supposed to be scale-free at least partially [9] (that is, part of its degree range is believed to follow approximately a power-law), they cannot be fully explained by a simple preferential attachment process due to an observed high intra-hub connectivity. This is the so-called rich-club phenomenon [10, 11], some nodes are rich (they are the hubs) and highly inter connected to each other at the same time (they form a club). This feature is not found in many of the natural and social scale-free networks [12], and makes it very robust to targeted attacks: given the high inter connectivity of the hubs, the removal of several of them does not result in network fragmentation.

The remaining of the chapter is organized as follows: the first section presents a literature review on interlocking directorates and their possible sources and effects on the economy. The second highlights the small-world phenomenon, which consists of very large networks presenting both high average clustering coefficients and small average shortest path lengths, found in many real world social networks. The third section deals with communities by depicting why one should carefully choose a random network benchmark in order to assess whether some features observed in empirical networks are somehow unexpected or not. The fourth section presents two of the most often applied random benchmark models to stress their resemblances and differences to empirical interlocking networks. Finally, the last section introduces the rich club coefficient as a measure of intra-hub connectivity to show that the topology of interlocking networks cannot be completely described by the simple interaction of nodes in a preferential attachment scenario. It is then argued that another explanation for the structure and the emergence of a dominant interconnected hierarchy may have to do with attaining specific goals rather than with the *rich-gets-richer* effect [13].

1.1 Interlocking directorates

Whether or not interlocking directorates have economic importance has been topic of long-term academic debate (for an overview, see [14]). Typically, the impact of these linkages has been examined on organizational performance in terms of collusion, control, information flows, profitability, financing, and reduction of uncertainty [15]. However,

it seems that there is still no consensus about the relevance of interlocks for such matters, because mixed and contradictory results with respect to performance have been found [16]. In fact, a large literature finds rather a negative (if any) effect from having directors who serve on multiple boards on measures of firm performance [17]. As a possible explanation for such unsolved debate, [18] suggests ambiguity in casual ordering: interlocks can be both cause and result of performance. In addition, there has been an assumption that interlocks affect performance uniformly, while some interlocks might be more influential than others, and some partners might be more influential than others.

In this sense, interlocks may have consequences for organizational behavior regardless of whether they were established for primary organizational purposes. In a slightly different perspective, [19] suggests that board interlocks are a low-cost channel of information and communication across firms, meaning they are a way to deal with uncertainty, to provide legitimacy, and to have information about business practices. In this sense, interlocks would not exist primarily for direct control but rather as a tool for performing *business scans* [20] of best managerial practices. It has been shown that the adoption of a given practice by an organization depends on whether other companies are adopting it [21], and interlocks are a good way of facilitating diffusion. The argument is that potential adopters increase their evaluation of a new practice of uncertain value after observing others adopt it, which leads to institutionalization of the new practice.

In a survey called *What do interlocks do?*, [18] points to an interesting result with regard to the replaceability of corporate interlocks. The frequency with which accidentally broken interlocks (e.g., by death or retirement) between firms were reconstituted was considered as an indicator of the extent to which such interlocks represented significant links between the firms in question. Interestingly, it was noted that the majority of accidentally broken interlocks were not reconstituted with the same firm, suggesting that interlocks were not primarily organizational phenomena. It was then suggested they could reflect intraclass social ties rather than inter-organizational resource dependence or control ties. In this sense, another interesting result is the persistence of these tight connections over long time horizons. As pointed out by [22], the network core of the most capitalized companies in Germany persisted from 1993 to 2005 regardless of personal turnover. In the next chapter, a comprehensive and time-framed dataset on board affiliation in Spain will be used to assess impacts both on performance and persistence

of the core.

More recently, some researchers have also explored these interlocks in terms of the possible emergence of a global business community [23, 24]. This different perspective implies there might be reasons for interlocks to happen, which may be not captured by performance measures. The *inner circle*, because of their multiple and diverse affiliations, would be likely to maximize overall profits, rather than to protect the welfare of particular companies. Nevertheless, one fact that does not seem to be a matter of debate is the surprisingly small number of steps required to connect almost any two companies in the networks [9]. If interlocks convey information, then the particular position of a firm in the topology of the network is at least as important as its direct connections.

1.2 Graph theory

The purpose of this section is to present basic graph theory concepts. For doing so, it considers the example graph S illustrated in figure 1.1. The graph S consists of a set of 7 nodes $N(S)$ and a set of 6 edges $M(S)$ as shown below.

$$N(S) = [0, 1, 2, 3, 4, 5, 6]$$

$$M(S) = [\{0, 1\}, \{0, 2\}, \{1, 2\}, \{0, 3\}, \{3, 4\}, \{5, 6\}]$$

Each edge presents the incidence relation between two end-point nodes. Two nodes are called adjacent if they are the end-points of an edge (nodes 0 and 1, for example). An edge is called incident with a node if it is an end-point of that edge (node 0 and edge $\{0, 1\}$, for example). Two edges are called incident if they have a common end-point (edges $\{0, 1\}$ and $\{0, 2\}$, for example).

The degree of a node n_i of S, denoted by $deg(n_i)$, is the number of edges incident with that node. It can be seen, for example, that $deg(n_0) = 3$, and $deg(n_1) = 2$. Since each edge has two end-points, the sum of node-degrees of S is twice the number of its edges, given by the so-called handshaking lemma. The sum of node-degrees in the example graph S is 12. The density of a graph is defined as the ratio between the number of edges in that graph over the number of its possible edges, given by

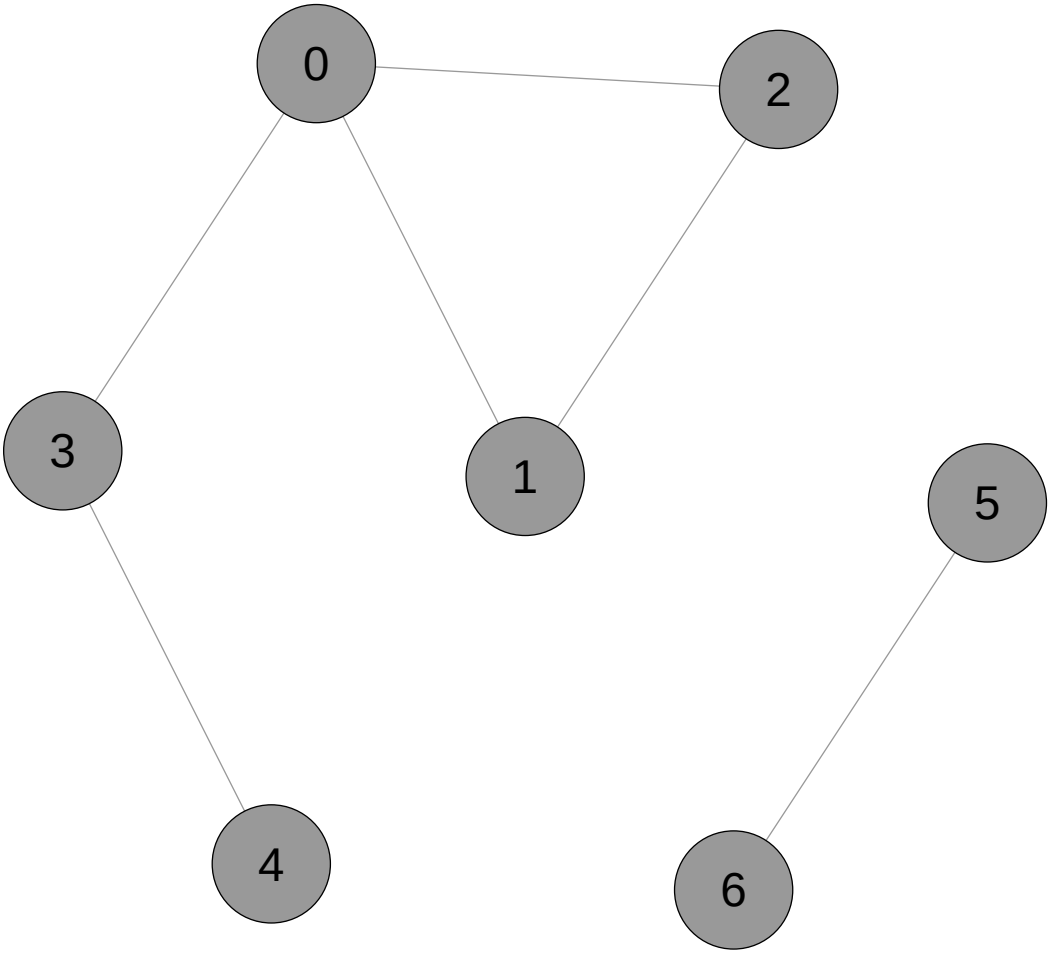

FIGURE 1.1: Example graph S, consisting of a set of 7 nodes $N(S) = [0, 1, 2, 3, 4, 5, 6]$ and a set of 6 edges $M(S) = [\{0, 1\}, \{0, 2\}, \{1, 2\}, \{0, 3\}, \{3, 4\}, \{5, 6\}]$.

$$density(S) = \frac{2|M(S)|}{|N(S)|(|N(S)| - 1)} \tag{1.1}$$

where the operator $|X|$ stands for the size of X. The density of S is approximately 0.2857.

A walk w of S, is a finite sequence $w = [n_0, m_1, n_1, ..., m_k, n_k]$ whose terms are alternately nodes n_i and edges m_i of S for $1 \leq i \leq k$, and n_{i-1} and n_i are the two ends of m_i. As an example, the sequence $[0, \{0, 1\}, 1, \{1, 2\}, 2, \{0, 2\}, 0, \{0, 1\}, 1]$ is a walk in S. A trail t in S, is a walk in which no edge of S appears more than once (ex: $[0, \{0, 1\}, 1, \{1, 2\}, 2, \{0, 2\}, 0, \{0, 3\}, 3]$). A path P in S, is a trail in which no node appears more than once (ex: $[0, \{0, 1\}, 1, \{1, 2\}, 2]$).

Two nodes n_i and n_j are said to be connected in S if there exists a path between these nodes. In the example graph S, nodes 1 and 2 are connected, but 1 and 6 are not. A graph is called connected if all pairs of its nodes are connected (thus S is not connected). A component is defined by a subgraph where all nodes are mutually reachable by some path. It can be seen that S presents two components $[0, 1, 2, 3, 4]$ and $[5, 6]$. The component containing more nodes is called the largest connected component (LCC). For S, the LCC consists of the nodes $[0, 1, 2, 3, 4]$ and the edges $[\{0, 1\}, \{0, 2\}, \{1, 2\}, \{0, 3\}, \{3, 4\}]$.

The length of a path P_i denoted by $L(P_i)$ is taken as the number of its edges. The length of the path $[0, \{0, 1\}, 1, \{1, 2\}, 3]$ is 2. P_i is called the shortest path between the two nodes n_0 and n_k, if for any other path P_j between these nodes $L(P_i) \leq L(P_j)$. As an illustration, consider the two paths in S from node 2 to node 4, $[2, \{0, 2\}, 0, \{0, 3\}, 3, \{3, 4\}, 4]$ and $[3, \{1, 2\}, 1, \{0, 1\}, 0, \{0, 3\}, 3, \{3, 4\}, 4]$, being the first one the shortest of them.

The distance between two nodes of a graph is defined as the length of the shortest path connecting them. In the example graph S the distance between nodes 2 and 4 is 3). This distance is also referred to as geodesic distance. The eccentricity of a node is given by the length of the longest shortest path between this node and any other node, to capture the idea of how far a node is from his furthest connection. In the LCC of S, the eccentricity of nodes 0 and 2 are respectively 2 and 3.

Finally, the diameter of a connected graph is given by the maximal eccentricity among

its nodes, and its radius by the minimal eccentricity. Diameter and radius for the LCC of S are, respectively, 3 and 2. Eccentricity is not defined for disconnected graphs such as S, thus it is conventionally assumed they have infinite diameter.

While observing that both radius and diameter might be very sensitive to extreme cases, it is then common to think about the small-world phenomena considering average shortest path lengths defined as follows:

$$a = \sum_{n_i, n_j \in V} \frac{d(n_i, n_j)}{N(N-1)} \tag{1.2}$$

where $d(n_i, n_j)$ is the length of the shortest path connecting nodes n_i and n_j, N is the number of nodes in the connected graph V. The average shortest path length in the example graph S is 1.7.

The degree centrality of a node i is simply given by its degree, as follows:

$$\text{degree centrality}_i = \sum_{n_j \in V} a_{n_i, n_j} \tag{1.3}$$

where a_{ij} is the entry of the adjacency matrix A for the nodes i and j, being equal to 1 if the nodes are connected and 0 otherwise. For example, the degree centrality of node 0 is 3, and it is the node with the highest degree centrality of the graph

The closeness centrality applies the definition of distance based on the length of the shortest path between two nodes. In detail, the farness of a node is given by the sum of the distances between this node and all the other nodes. Then, the closeness centrality is given by the inverse of the farness of a node. Closeness centrality concerns the amount of steps needed in order for information to spread sequentially from a given node, and is given by:

$$\text{closeness centrality}_i = \left[\sum_{\substack{n_j \in V \\ j \neq i}} \frac{d(n_i, n_j)}{N-1} \right]^{-1} \tag{1.4}$$

In order to calculate such measure, one must pre calculate the shortest distances between all pairs of nodes. This can be efficiently accomplished by means of the Floyd-Warshall algorithm [25], for example. Given the incomputability of distance between unconnected nodes, this measure is only defined for connected graphs. As an example, the closeness centrality of node 0 is 0.8 because it is connected to 4 other nodes, being 1 step away from three of them and 2 steps away from two of them, yielding an average distance of 1.25 and, thus, a closeness centrality of 0.8.

Another related but fundamentally different definition of centrality is the betweenness centrality. The betweenness centrality of a node is given by the number of times it appears as a step of a shortest path between two given nodes. The intuition is that nodes are more central if they are in the fastest route between many pairs of nodes. The betweenness definition of centrality is calculated as follows:

$$\text{betweenness centrality}_i = \sum_{\substack{n_i,n_j,n_k \in V \\ i \neq j, i \neq k, j \neq k}} \frac{\sigma_{n_j,n_k}(n_i)}{d(n_j,n_k)} \tag{1.5}$$

where the term $\sigma_{n_j,n_k}(n_i)$ is the number of shortest paths from j to k that pass through node i. It can be seen that the betweenness centrality for node 0 is 4, and for node 1 is 0.

Finally, the eigenvector centrality of a node extends the idea of the degree centrality (that is, nodes are more central the more connections they have) to indirect connections. The intuition is that the centrality of a node depends on the centrality of its direct connections. In this sense, being connected to a very well connected node increases more the centrality of a node than being connected to a poorly connected node. Specifically, considering the adjacency matrix A, the eigenvector centrality of a given node i is defined as the i-th entry in the normalized eigenvector belonging to the largest eigenvalue of A. Formally, the eigenvector centrality of node i is given by:

$$\text{eigenvector centrality}_i = \mu \sum_{\substack{n_j \in V \\ j \neq i}} a_{i,j} x_j \tag{1.6}$$

where $x = \frac{1}{\lambda} Ax$ (solving $Ax = \lambda x$) and $\mu = \frac{1}{\lambda}$ (proportionality factor) so that eigenvector centrality of node i is proportional to the sum of similarity scores of all nodes

connected to it. In the present context, it suffices to find the eigenvector belonging to the largest eigenvalue, which can be calculated by means of the power iteration method [26]. As an illustration, the eigenvector centrality of node 0 is approximately 0.604.

Apart from these measures of node importance, several other measures are related to the mixing patterns in networks. More specifically, assortativity is a general tendency of nodes to attach to other nodes which are considered similar, at least with regard to some precise definition. As an example, one can think of degree assortativity as the tendency of nodes having high degrees to be more connected to other nodes with high degree than to nodes with low degrees. More formally, the degree assortativity can be defined by the Person's correlation coefficient for degrees of nodes at either end of an edge. As an illustration, the degree assortativity of graph S is 1/3. A positive (negative) degree assortativity means nodes with high degree are more (less) likely to connect to other nodes with high degree than to nodes with low degree.

1.3 Data description

Data was collected from the *Investing Business Week* website in May 2012. More specifically, at the bottom of the index page there is the possibility of browsing companies by the starting letter of their names. Data from both public and private companies presenting valid board membership information was collected from specific pages such as http://investing.businessweek.com/research/ stocks/people/board.asp?ticker=DBK:GR for Deutsche Bank, as an example.

It is worth to mention that such pages label each person into one of the three following labels: a board member, an executive, or an insider. This chapter treats all of the three labels indistinctly. By doing this, it considers a broader definition of a board member when compared to the consideration of the Advisory and/or Executive boards only, which allows the identification of personal relations that can go beyond the formal key representatives. However, no information on other committees (such as the Audit, Compensation, Nominating, etc.) that are presented in pages such as http://investing.businessweek.com/research/ stocks/people/committees.asp?ticker= was considered in this chapter.

Board membership information was represented by means of incidence matrices, which allow for the calculation of network measures. Two directors are said to be connected if they occupy seats in a same company, and two companies are said to be connected if they have a same director in their boards. In this sense, the evaluation of the network can be done in two directions, namely considering directors as nodes or considering companies as nodes. In both cases, the incidence matrix M is the same, but the respective adjacency matrices can be accessed by the projections $D = MM^T$ and $C = M^TM$.

A peculiar feature of the network of board affiliations D is the existence of nodes communities by construction (the boards), resulting in complete subgraphs in which all nodes (the board members) are connected to each other. This feature has an impact on some specific network properties: the existence of such communities produces trivially high average clustering coefficients, for example. In addition, the degree of a node depends on the size of the boards in which she/he has a position. Hence, two members in equally connected but differently sized boards have different degree centralities. This issue will be further addressed in the forthcoming sections.

In this sense, the subgraph formed by the network of board members holding at least $b = 2$ positions (referred to as D_2) keeps all important information with regard to information flow in the entire network, but removes the noise from disproportionality between board sizes. Thus, here only the network of members holding multiple (at least two) positions is considered. It is worthwhile to note that this definition of b-core (b for board positions) is different from that of k-core (k for degree). A k-core (or k-degenerate graph) is the (unique) maximal induced subgraph with minimum degree at least k. Alternatively, the k-core is the (unique) result of iteratively deleting nodes that have degree less than k, in any order.

In total, there are $738,571$ board members holding $846,659$ board positions, yielding an average number of board positions 1.146. If completely isolated directors are excluded (that is, the only member of a disconnected board), $652,570$ directors with at least one connection remain. If considering only those directors holding at least two board positions (these are responsible for the links between companies), $70,230$ directors remain. In addition to these restrictions, when only the largest connected component (LCC) of

D_2 is considered, 55,219 directors remain.

The total number of companies is 247,632, being 40,899 (16.5%) public and 206,733 (83.5%) private. The number of not completely isolated companies falls to 76,806 in total, divided in 29,183 (38%) public and 47,623 (62%) private. While considering only the LCC of C there are 50,320 companies, being 23,676 (47.1%) public and 26,644 (52.9%) private. These raw numbers show that engaging in inter companies interlocks is not an activity of public companies only, but rather that there is a strong interaction between them and the private companies. There are records of companies from 200 countries, but presenting a high degree of concentration of companies among a small set of them. For instance, more than 90% of the companies are from only 27 countries. The five countries presenting more companies are (in order) United States, United Kingdom, Canada, Germany, and France.

1.4 Random benchmark for the accumulation of board positions

With respect to German board membership data for several time periods, [27] points out that the pattern of accumulation of board positions by single individuals cannot be plausibly seen as a chance outcome of random draws from the pool of directors for filling the excess of board positions over the number of directors, and, thus, there are systemic tendencies at work favoring that a small number of individuals assembles a comparatively high number of simultaneous board positions.

The idea is to check whether this degree of concentration of positions is statistically significantly different from what one would get under random assignment of director positions to the pool of individuals (which by construction would mean that with X directors assigned to Y board positions and $X < Y$, a certain number of persons had to end up with multiple positions). The random benchmark used, and reproduced here, considers the binomial probability of observing multiple board membership in an independent sequence of k Bernoulli trials with probability p, being k and p given by, respectively, the number of board positions minus the number of directors and one over the number of directors, as shown in equation 1.7.

$$P(X = k) = \binom{k}{b} p^b (1-p)^{k-b} \tag{1.7}$$

Figures 1.2 and 1.3 show the relative frequency of empirical multiple board membership (red circles) and the random binomial benchmark (blue x's) for eight selected countries. The semi-log scale reveals deviations of increasing orders of magnitude for $b > 3$, confirming that the characteristic presented in [27] for German data can also be seen for other (both developed and developing) countries. Figure 1.4 shows that the same relation also holds for different perspectives on the global network of board members. Table 1.1 presents the number of directors and positions, and the values of k and p for the same selected countries and the global network.

TABLE 1.1: Number of directors, positions, and values of k and p for eight selected countries and the global network. In total, there are 738,571 board members holding 846,659 board positions (A), resulting in an average number of board positions of 1.146. If completely isolated directors are excluded (that is, the only member of a disconnected board), 652,570 directors with at least one connection remain (B). If considering only those directors holding at least two board positions (these are the responsible for the links between companies), 70,230 directors remain (C). In addition to these restrictions, when only the *LCC* of D_2 is considered, 55,219 directors remain (D).

Network	Directors	Positions	k	p
Global (A)	738,571	846,670	108,099	1.35e-06
Global (B)	652,570	759,320	106,750	1.53e-06
Global (C)	70,230	176,980	106,750	1.42e-05
Global (D)	55,219	144,338	89,119	1.81e-05
Germany	25,844	28,422	2,578	3.86e-05
France	17,924	19,670	1,746	5.57e-05
United States	291,959	322,516	30,557	3.42e-06
United Kingdom	44,589	48,266	3,677	2.24e-05
Brazil	3,244	3,598	354	3.08e-04
Russia	10,332	11,191	859	9.67e-05
India	31,912	37,687	5,775	3.13e-05
China	24,056	25,528	1,472	4.15e-05

1.5 Small worldness

In the last section, it was shown that the empirical accumulation of board positions could not be explained by a benchmark based on the uniform random assignment of directors to positions. This fact is also found to be true with respect to several countries, both developed and developing, suggesting that this *excess* accumulation of positions is a stylized fact of board membership networks. The present section introduces two

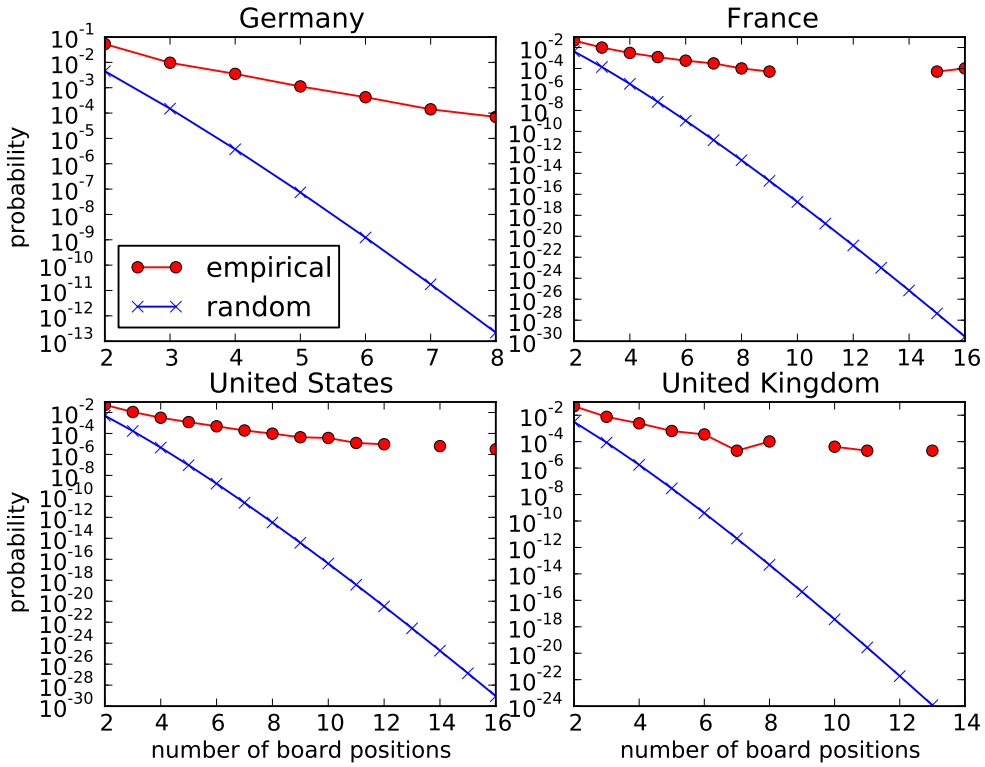

FIGURE 1.2: Relative frequency of empirical multiple board membership (red circles) and the random binomial benchmark (blue x's) for four selected developed countries.

additional important stylized facts of interlocking networks, namely, the existence of communities and the small diameter. These two features combined form what is called *small world* networks.

The small-world experiment [28] comprised several experiments conducted by Stanley Milgram and other researchers examining the average path length for social networks of people in the United States. The research was groundbreaking in that it suggested that human society is a small-world-type network characterized by short path-lengths. Many other networks, both natural and social, were found to possess that same property [7].

Additionally to the smallworldness, another stylized fact found in interlocking networks is the existence of a large connected component (referred to as LCC). This section introduces the concepts of random and ordered graphs in order to explain how small world networks can be created by simple models, and also for assessing how surprising it is to find a LCC in graphs such as the interlocking networks. It is shown that both

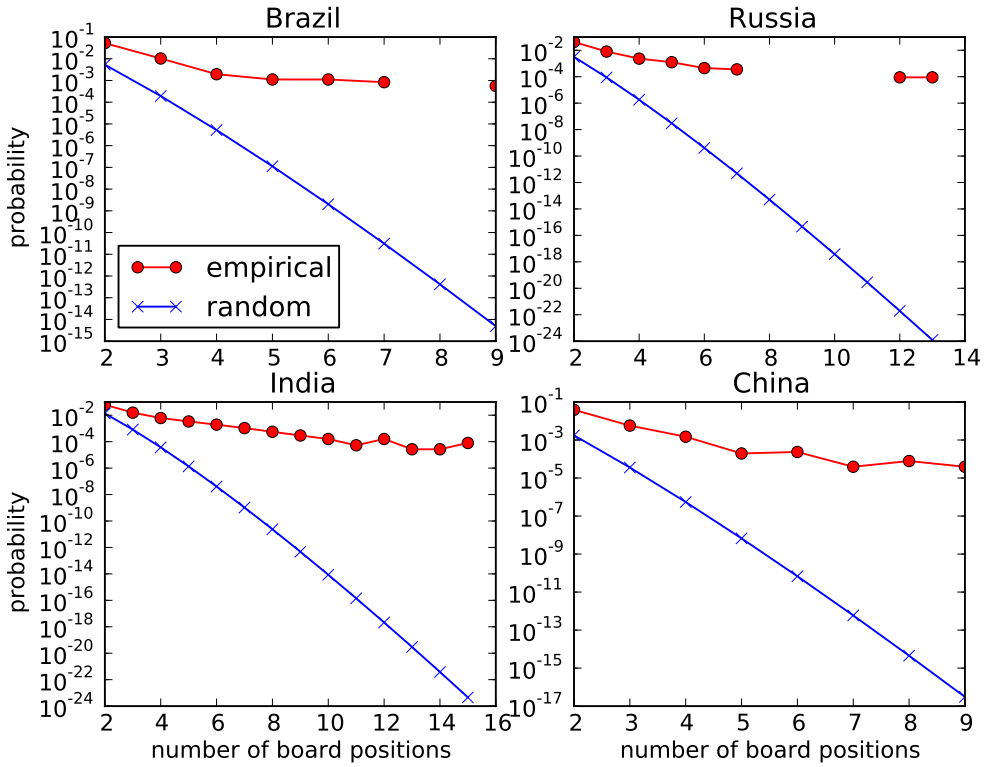

FIGURE 1.3: Relative frequency of empirical multiple board membership (red circles) and the random binomial benchmark (blue x's) for four selected developing countries.

the small average paths and the existence of a LCC can be described by simple random benchmarks, but also that these features are still just part of the topology.

1.5.1 Communities

Despite the pattern of multiple board accumulation shown in the last section, all these networks also present the most common symptoms of small-worldness: short diameters and average shortest path lengths. Table 1.2 presents some basic statistics for the LCC of the network of companies C, and also for selected countries.

It seems uncontroversial that both network types (D and C) derived from board membership connections are small-world networks, regardless whether analyzed at the global or country level. However, is it really a surprising feature that all 760 directors serving the boards of French companies are distant to each other on average by less than five personal connections?

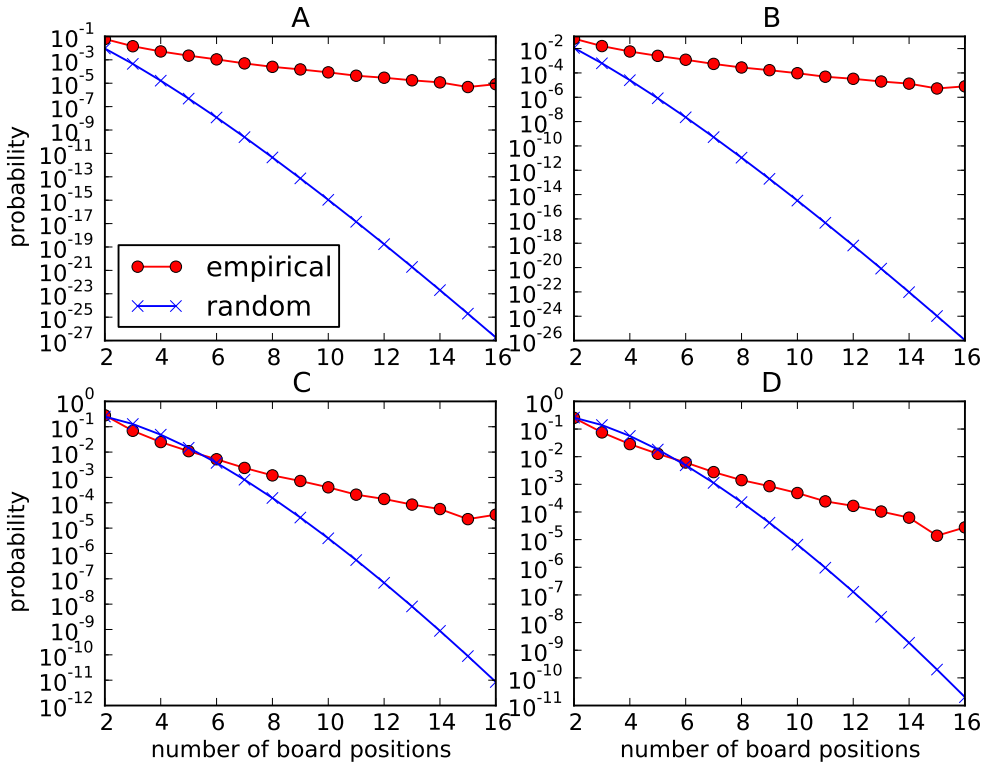

FIGURE 1.4: Binomial benchmark and empirical frequencies of multiple board positions. (A) all directors, (B) directors with at least one connection, (C) directors holding at least two board positions, and (D) only the *LCC* is considered.

TABLE 1.2: Number of nodes and edges, average degree and shortest path length, diameter, radius, and density for the *LCC* of the network of companies C, and for the networks of companies from selected countries.

Network	nodes	edges	$\bar{deg}$	$\bar{L}$	Diam.	Rad.	Dens.
$LCC(C)$	50,320	132,857	5.28	7.60			0.0001
Germany	1,191	6,492	10.90	5.03	16	9	0.0091
France	760	4,090	10.76	4.19	14	7	0.0141
United States	15,162	67,835	8.95	6.09	20	11	0.0006
United Kingdom	1,516	3,930	5.18	7.68	25	13	0.0034
Brazil	187	650	6.95	4.05	11	6	0.0373
Russia	357	1,381	7.73	5.04	15	8	0.0217
India	2,778	13,156	9.47	4.66	17	9	0.0034
China	700	1,521	4.34	7.64	20	10	0.0062

Many complex networks are single networks in the sense that their structure is unique not one of several. In general, we do not have the equivalent of a physical law to verify if the statistical measures obtained from a single network are expected or exceptional. Network models serve as a foundation to understanding interactions within empirical complex networks. Various random graph generation models produce network structures that may be used in comparison to real-world complex networks.

As it was shown in the last section, the accumulation of board positions is not explained by a binomial process. This section highlights another fundamental property of the board membership networks (and also of many other social networks) - the formation of communities - and its impact on the choice of a random benchmark. In doing so, the concept of random and ordered graphs will be presented. Then it will be shown that the small average shortest path lengths and the large size of the LCC of C and D_2 are not so surprising when compared to classic random graphs.

Before talking about communities, it is worth to give some definitions related to clustering. For a given node n_i, the ego network corresponds to a sub-graph where only its adjacent neighbors and their mutual edges are included. A graph has as many egos as it has nodes. The ego network of node 2 is given by the nodes $[1, 2, 3]$ and the edges $[\{1, 2\}, \{1, 3\}, \{2, 3\}]$.

A subgraph of S is called a clique if all its nodes are connected to themselves (that is, a clique is a complete subgraph). A clique of size 3 is also referred to as a triangle. The clustering coefficient of a node is the ratio between its actual and possible triangles, as shown in equation 1.8.

$$C(n_i) = \frac{2|M_i|}{|N_i|(|N_i| - 1)} \tag{1.8}$$

where $C(n_i)$ stands for the clustering coefficient of node n_i, M_i and N_i together represent the ego network of n_i, and the operator $|X|$ stands for the size of X. In words, the clustering coefficient of a node is given by the density of its ego network. It ranges from 0 to 1 and may be also interpreted as follows: suppose board members A and B are both connected to C, then the clustering coefficient is the probability that A and B are also connected to each other.

Communities are found among many other social networks, including one describing US board membership [29] which presents results similar to the ones depicted here. Table 1.3 presents the number of triangles and the average clustering coefficient for the LCC of C and for the LCC of the networks of companies from selected countries, showing that the existence of board communities is a widespread stylized fact of interlocking networks.

TABLE 1.3: Number of triangles and average clustering coefficient for the LCC of the network of companies C, and for the networks of companies from selected countries.

Network	triangles	Avg. Cluster. Coeff.
Global (LCC of C)	1,988,823	0.60
Germany	84,660	0.65
France	31,596	0.61
United States	464,712	0.58
United Kingdom	13,230	0.56
Brazil	3,891	0.70
Russia	8,394	0.67
India	77,892	0.61
China	3,999	0.56

1.5.2 Random Graphs

The most basic random benchmarks which can be used to verify whether the observed properties of an empirical network are somehow unexpected are the classic Erdős-Rényi random graphs [30, 31]. The original concern of the authors was to analyze several properties of a graph as its number of edges N grows with respect to a fixed large number of nodes n. This situation can be considered in two following different though equivalent ways.

First, one can think about choosing a graph at random among all possible graphs which can be formed with N edges and n nodes. Considering N edges being randomly selected from all the $\binom{n}{2}$ possible edges that can be formed given n, so that all possible graphs $C_{n,N} = \binom{\binom{n}{2}}{N}$ are equally likely to be chosen. The second and equivalent method is to start with a set of n disconnected nodes, and sequentially attach two nodes by selecting an edge among all possible and remaining edges $\binom{n}{2} - k$, being k the numbers of edges created so far in the sequential process, until $k = N$.

In this sense, the same authors [30, 31] say a given property holds for *almost all graphs* if the probability of a randomly selected graph having such property tends to 1 as $n \to \infty$. Among several properties they have analyzed, figure 1.5 presents as illustration simulation results from the behavior of the number of components and the size of the largest component. The solid vertical line indicates the threshold $c = \frac{N}{n} \sim \frac{1}{2}$ highlighted by the authors. For instance, with respect to the number of components, if $c < \frac{1}{2}$ the number of components reduces linearly with the increase in N, while for $c > \frac{1}{2}$ this is no longer the case. The empirical network D shows $c = \frac{738{,}571}{2{,}815{,}319} \approx 0.26$, only a half of the threshold, thus making the existence of a LCC of size $55,219$ (7.4% of all nodes) not a huge surprise. That is, the existence of such a large connected component can be explained by a network growth process based on the connection of two randomly and independently chosen nodes at each time step.

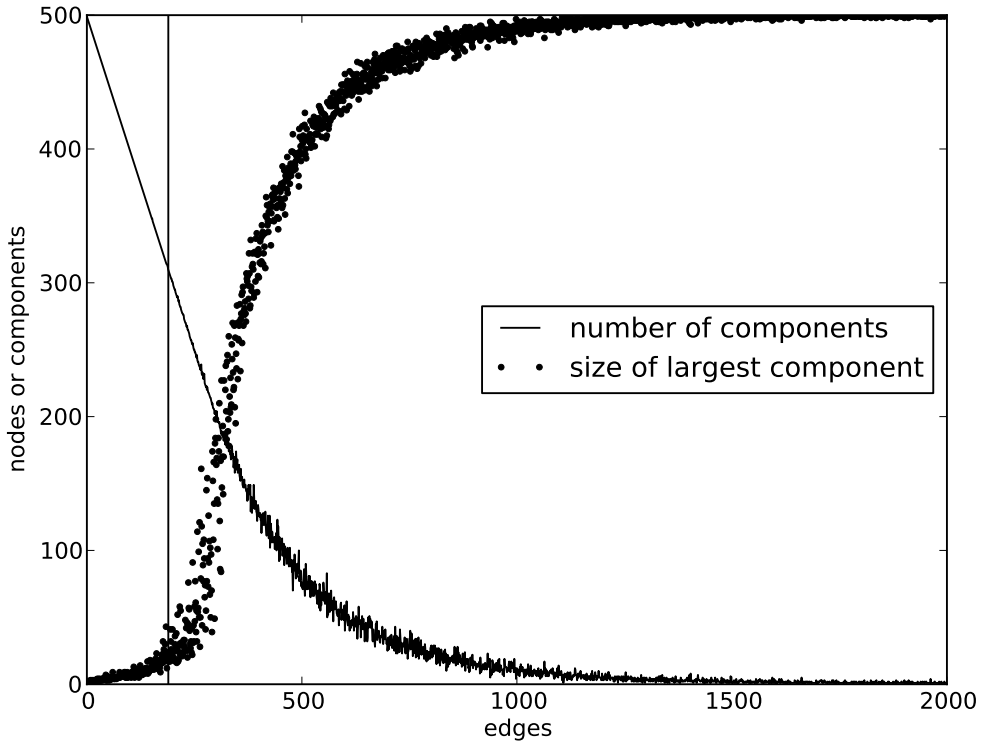

FIGURE 1.5: Illustrational simulation results for the behavior of the number of components and the size of the largest component in an ER random graph. The solid vertical line indicates the threshold $c = \frac{N}{n} \sim \frac{1}{2}$. For instance, with respect to the number of components, if $c < \frac{1}{2}$ the number of components reduces linearly with the increase in N, while for $c > \frac{1}{2}$ this is no longer the case.

There are two methods of generating random graphs. The $E(n, m)$ version selects a graph from all possible graphs which can be formed with given n nodes and m edges.

This is done by assigning equal probability $\binom{\binom{m}{2}}{n}^{-1}$ to all graphs with exactly m edges and n nodes. The $E(n,p)$ version is constructed by connecting nodes randomly, with probability p and independently from every other edge (i.e., following a binomial probabilistic model). Every possible edge occurs independently with probability $0 < p < 1$, and the probability of a random graph with m edges being selected is $p^m(1-p)^{n-m}$. This version can be viewed as a snapshot at a particular time m of the random graph growth process which starts with n vertices and no edges, and at each step adds one new edge chosen uniformly from the set of missing edges. The former is used here for assessing whether observed empirical properties are expected under a classic random graph benchmark, specifically the size of the largest connected component and the average clustering coefficient.

Table 1.4 presents a comparison between an $ER(n,m)$ random network with the same number of nodes and edges of the LCC of C, showing that the empirical number of triangles is of several orders of magnitude higher than one might expect if edges are created randomly between existing nodes. It is clear from such results that classic random graphs ignore communities, important feature present in many social networks. Normally, most of our friends are friends themselves, thus random rewiring is not appropriated as a benchmark for analyzing social networks. These random networks are conceivable, but nor real. Both versions of the Erdős-Rényi random graph generator are based on the assumptions that a) edges are independent, and b) each edge is equally likely to exist. In practice this implies that they generate networks with Poisson degree distributions.

TABLE 1.4: Comparison between an $ER(n,m)$ random network with the same number of nodes and edges of the LCC of C, showing that the empirical number of triangles is of several orders of magnitude higher than one might expect if edges are created randomly between existing nodes.

	Global (LCC of C)	$ER(n,m)$
Nodes	50,320	50,320
Edges	132,857	132,857
Average degree	5.28	5.28
Density	1.0494e-4	1.0494e-4
Triangles	1,988,823	93
Average clustering coefficient	0.60	1.4967e-4

1.5.3 Ordered Graphs

On the other hand, ordered graphs as the one depicted in figure 1.6 exhibit large clustering coefficients and communities, but they are not small world. In this sense, it can be seen a clear dichotomy between randomness (making the graph smallworld-like) and order (forming communities).

The power of an edge to reduce the diameter of a graph by several orders of magnitude is inversely related by the neighborhood connection of the two connected nodes. This is the so-called *strength of weak ties* [32]. The underlying idea is that if one removes an edge forming a triangle, very little effect will be observed in the structural properties of the graph, because an alternative linking route is directly available. Strong links form triangles, while the weak links, the bridges connecting different and remote communities together making the graph smaller. As an illustration, [33] asked high school juniors for a rank with their eight best friends. Then he constructed two networks, one by considering only the top two and another the bottom two best friends, to notice that the second one connects the school much more tightly because top two best friends are strong links, and very likely to form triangles.

These are examples of how topology is important, and that there is a dichotomy between order and randomness changing network length. The next section will address this dichotomy explicitly, stressing why one should be careful when choosing random benchmarks to analyze empirical networks.

1.5.4 Country level interlocks

According to [24], the literature presents vast support for the idea that within each advanced capitalist country the directors of the largest corporations form close communities. In this section, the international interlocks are considered, that is, the fact that some directors serve on boards of different nationalities. To begin with, table 1.7 presents the number of positions, directors, and companies for the top 50 countries by the number of directors. The last two columns show the average number of board positions per director and the average board size in number of positions.

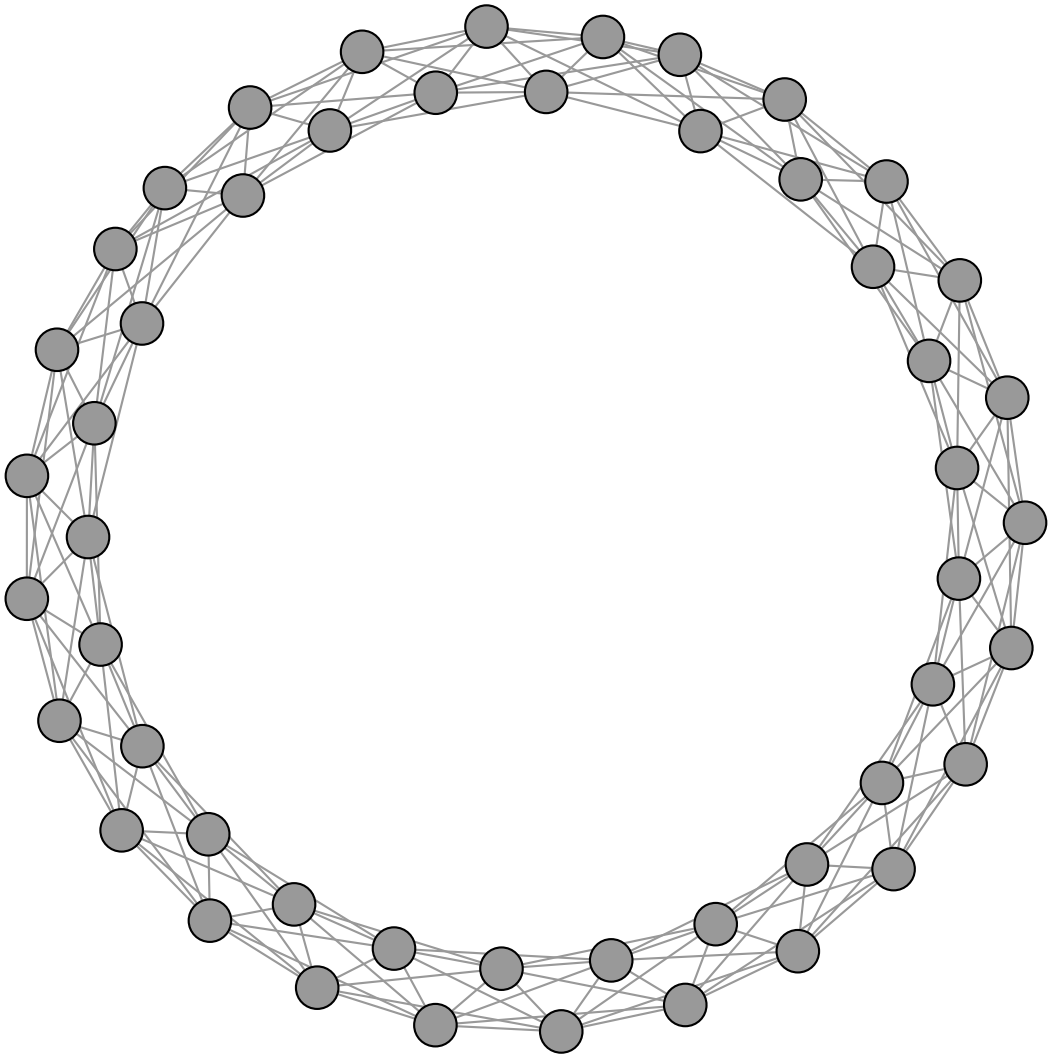

FIGURE 1.6: An example of ordered graph which exhibits large clustering coefficients and communities, but it is not small world.

In the remaining of this section a network is defined by having countries as nodes, and weighted edges proportional to the number of directors holding simultaneous positions in companies from both countries sharing that edge. In this sense, directors whose all positions are in companies of the same country are discarded. Figure 1.7 illustrates this network and its most important actors (nodes are sized and colored by their correspondent eigenvector centralities). The network is composed of 167 nodes (countries), $1,828$ weighted edges summing up to $6,140$ connections. This very dense network shows that the majority of the countries are to some degree engaged in international interlocks.

Table 1.5 presents a different perspective, not based on centrality, but rather on the relation between national and international interlocks. The first column presents the ratio between the number of foreigners and domestic interlocks, while the second presents the normalized Shannon entropy of the distribution of connections as a measure of how *globalized* a country is in contrast to strong local connections to one or few other countries. The normalized Shannon entropy of a discrete random variable X with N possible values $x_1, \ldots, x_n$ and probability mass function $P(X)$ is given by

$$H(X) = \frac{-\sum_{n=1}^{N} P(x_i) log(P(x_i))}{log(N)} \tag{1.9}$$

where H ranges from 0 (when all connections have the same country as an end-point) to 1 (when the connections are equally distributed among all countries).

The Channel Islands, Luxembourg, Ireland, Bermuda, The Netherlands, Switzerland, and Belgium presented more international interlocks than domestic ones. This fact, along with a high entropy value (as a measure diversification of connections), indicates these are the most open countries.

Another interesting point of view deals with the average profile of the firm who engages in international interlocks. Assortativity is the preference of nodes to attach to others that are similar with regard to some attribute [34]. The classic example is the degree assortativity, given by the Person correlation coefficient between the degrees of nodes at either end of the edges. As a correlation coefficient, it ranges from -1 (perfect dissortativity) to 1 (perfect assortativity). In the specific case, the network of companies C presents positive country assortativity, in the sense that on the average, companies

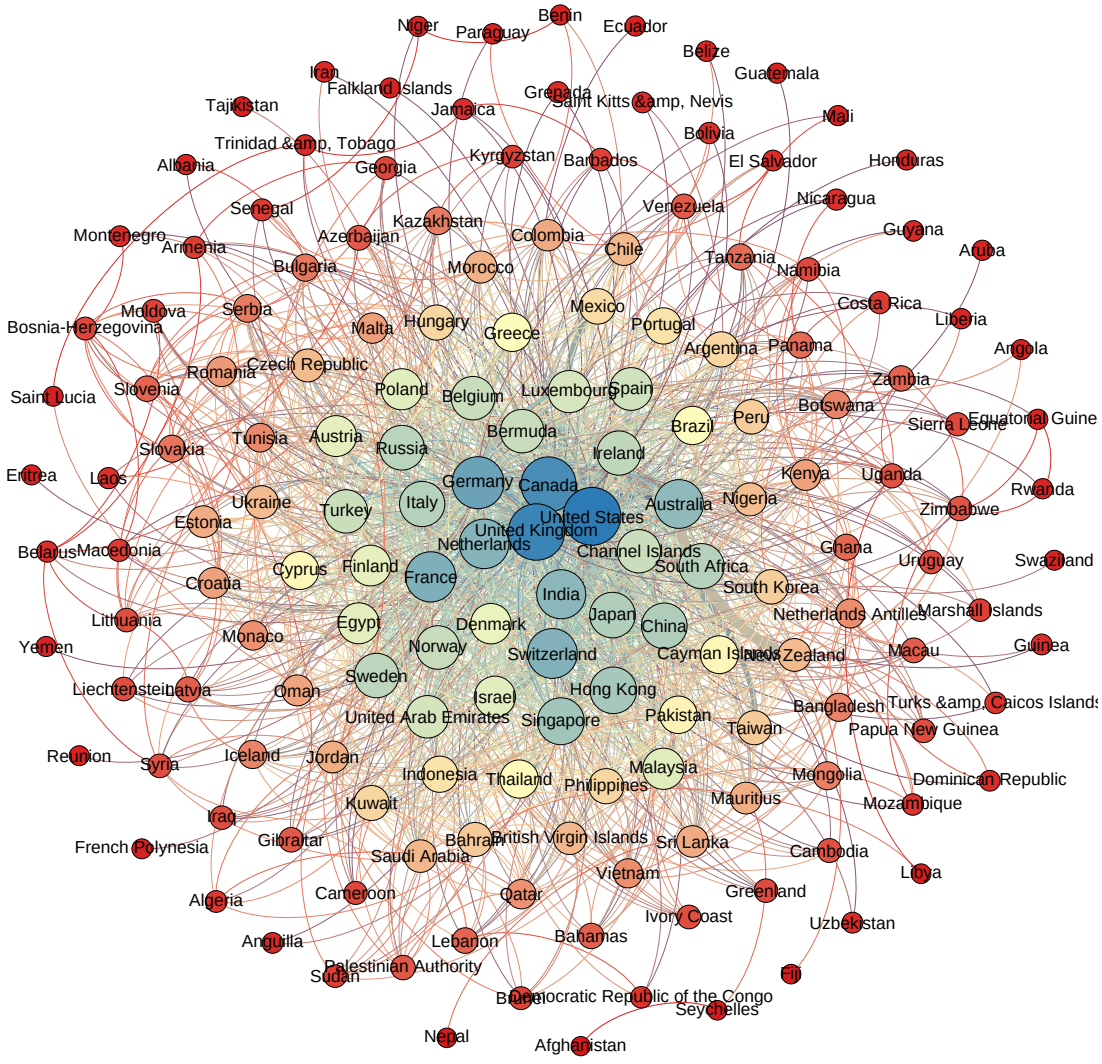

FIGURE 1.7: Country level aggregation of international interlocks. The weighted connection between two countries is defined by the number of directors holding simultaneous positions in companies from both countries. Directors whose all positions are in companies of the same country are discarded. Nodes are sized and colored by eigenvector centrality.

TABLE 1.5: Top and bottom ten countries ordered by the diversity of connections with regard to nationality. The first column presents the ratio between the number of foreigners and domestic interlocks, while the second presents the entropy of the distribution of connections as a measure of how *globalized* a country is in contrast to strong local connections to one of few other countries. The Channel Islands, Luxembourg, Ireland, Bermuda, The Netherlands, Switzerland, and Belgium presented more international interlocks than domestic ones. This fact, along with a high entropy value (as a measure diversification of connections), indicates these are the most open countries.

Country	Ratio	Entropy
Channel Islands	6.64	0.71
Luxembourg	6.03	0.77
Ireland	2.82	0.56
Bermuda	2.36	0.61
Netherlands	1.56	0.59
Switzerland	1.34	0.55
Belgium	1.15	0.54
United Arab Emirates	0.93	0.58
China	0.83	0.39
United Kingdom	0.82	0.45
...	...	...
Canada	0.20	0.17
United States	0.20	0.20
Japan	0.20	0.22
Malaysia	0.18	0.21
Philippines	0.13	0.19
Thailand	0.11	0.17
Pakistan	0.11	0.18
India	0.10	0.14
Bangladesh	0.10	0.18
Sri Lanka	0.07	0.11

are more likely to attach to other companies of the same country. Figure 1.8 presents the country assortativity mixing of the network of companies for varying thresholds of minimum degree, that is, for each degree k the country assortativity is calculated considering only those nodes with degree higher than k. It can be seen a consistent decrease in assortativity for growing values of k meaning that the higher the number of connections, the higher the chances of engaging in international interlocks.

1.5.5 Sector connectivity

To begin with, 1.8 presents the number of positions, directors, and companies by sectors of economic activity. The last two columns show the average number of board positions per director and the average board size in number of positions. It can be clearly seen

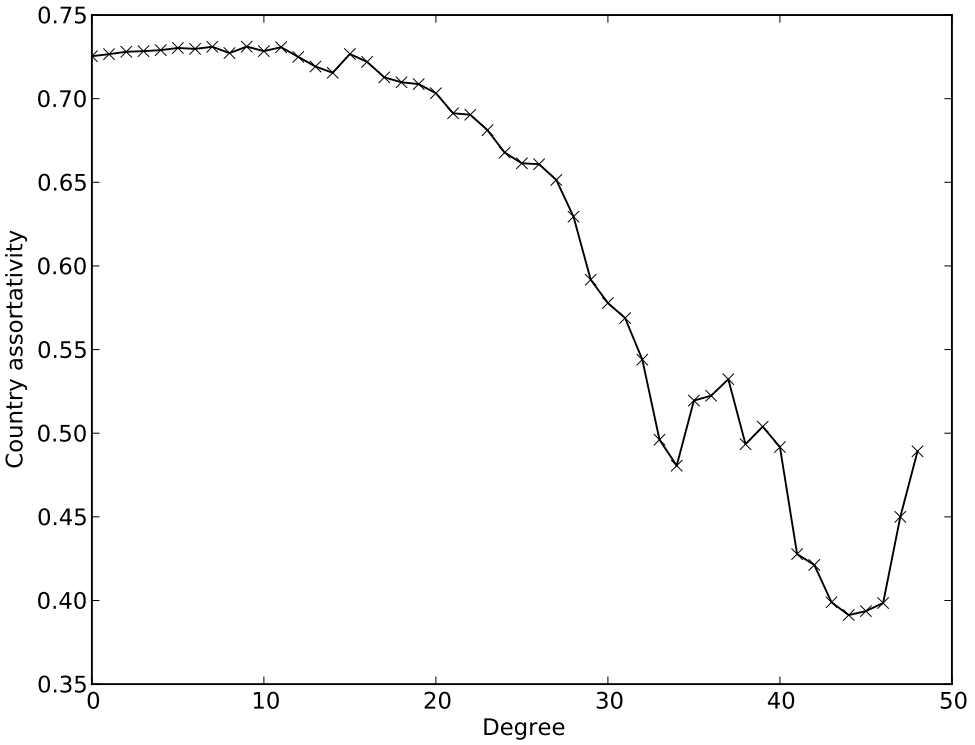

FIGURE 1.8: Country assortativity mixing of the network of companies for varying thresholds of minimum degree, that is, for each degree k the country assortativity is calculated considering only those nodes with degree higher than k. It can be seen a consistent decrease in assortativity for growing values of k meaning that the higher the number of connections, the higher the chances of engaging in international interlocks.

that both the Banking and the Insurance industries present an average board size significatively higher than the others. According to [35], financial institutions depend more on the business scan than the other companies, so for them it is worthwhile to maintain a large body of board directors.

There is vast literature supporting the prominent role of financial institutions in the networks formed by interlocking directorates (see [9] for some examples). Table 1.9 presents the eigenvector centrality (first column) and the diversity of connections (second column) by sector of economic activity. While the eigenvector centrality shows which are the most central sectors of activity in the network, the diversity of its connections indicate whether the sector influences just a few other related sectors or a large part of the network. The diversity of the connections is defined as the normalized Shannon Entropy of the weighted connections (as defined in equation 1.9). That means it will be close to 0 when the sector basically connects to one or just a few other sectors (like

Metals and Mining, for example), and it will be close to 1 if the sector connects more or less equally to all other sectors (like Financial Services, for example).

Drawing on 100 large US industrial corporations between 1969 and 1979, [36] hypothesize that interlocks with banks should be positively associated with corporate performance and debt/equity ratios. However, their findings revealed a negative association between bank interlocks and most measures of profitability. In this sense, [37] speaks about financial hegemony: banks would play a central role in unifying the network of corporations linked through shared directors. The inner circle, because their multiple and diverse affiliations, are likely to maximize overall profits, rather than protect the welfare of particular companies. In a different perspective, [38] points out that no evidence of performance gains by the Financial sector has been found. Thus, it is argued that the Financial institutions are not necessarily central, but different: banks are special in the sense they are holders and distributors of social capital.

1.6 Kinds of small

In the last section, it was shown that topology is important: the dichotomy between order and randomness in the distribution of neighbor connections can drastically change the network length. This section presents the model proposed by [39], which can be used to generate graphs that are at the same time clustered (that is, they present communities) and small world. The basic idea is that if one performs a few random rewires in an ordered graph, its typical shortest path length is reduced by several orders of magnitude. Afterwards, an investigation on the distribution of connections among the nodes is performed to introduce another random model [7] based on network growth and preferential attachment claimed to take into account the existence of massive hubs (nodes with many connections) found in many natural and social networks.

1.6.1 Watts/Strogatz small world graphs

The algorithm takes the following inputs: number of nodes N, the average degree K, and rewiring probability β. The output is a graph with N modes and $\frac{NK}{2}$ edges built in the following way: a ring lattice is constructed, linking the nodes to its K neighbors, $\frac{K}{2}$

on each side ($k-1$ neighbors if k is odd). Then, for each edge of each node, rewire it to another uniformly random node with probability β. In this sense, β can be understood as a tuning parameter between order and randomness: if $\beta = 0$, no rewiring is performed and the ordered ring lattice is maintained; if $\beta = 1$, all edges are uniformly shuffled and the result is an $ER(n,p)$ random graph with N nodes and probability $p = \frac{NK}{2\binom{N}{2}}$. The underlying lattice structure of the model produces a locally clustered network, and the random links dramatically reduce the average path lengths.

For the ring lattice, the average shortest path length is $l = \frac{N}{2K}$ and scales linearly with system size, while for the $ER(n,p)$ graph its value is given by $l = \frac{\log N}{\log K}$. For the intermediate region $0 < \beta < 1$, l converts very quickly to its limiting value. The clustering coefficient of the ring lattice is given by $C = \frac{3(K-2)}{4(K-1)}$ and tends to $\frac{3}{4}$ when K grows. For the random graphs, the clustering coefficient is $C = \frac{K}{N}$. When ranging β from 0 to 1, the clustering coefficient stays close to its original (ring lattice) value, only being reduced for high values of β. The combination of these two features (reduced average shortest path lengths and persistent clustering coefficient) is what makes the Watts/Strogatz's model able to produce small-world networks. No matter how many points, a small number of random rewiring ties the network together and produces small world and large connected components.

When a random graph is generated by such a procedure, and calibrated to present the same number of nodes and (approximately) the same average degree of the empirical networks C and D_2 (recalling that C stands for the network of companies, and D_2 for the network of directors holding at least two board positions), the same short average shortest path lengths and clustering coefficient emerge. This remarkable feature of reducing average shortest path lengths with a few random rewiring operations is argued to allow such networks to store information in a much better fashion, to stand up in the face of faults, and to reduce by thousands the number of connections needed to synchronize [39].

Such theoretical random benchmark does explain a lot of what is observed in empirical interlocking directorates networks. However, communities and smallworldness are just part of the topology. For instance, highly clustered and small world networks can possibly be of hierarchical or fishnet types. The next section presents another investigation on the topological properties of interlocking directorates networks, namely, the

distribution of the connections.

1.6.2 The distribution of connections

To begin with, figures 1.9 and 1.10 present, respectively, the degree distribution for the $ER(m, n)$ and for the WS networks. As it is expected, the $ER(m, n)$ random graph presents the degree distribution following a Poisson process (given the binomial distribution of the connections). For the WS, if $\beta = 0$ (that is, the ring lattice), the degree distribution follows as Dirac delta function centered in the number of nodes K. If $\beta = 1$, the result is a pure $ER(m, n)$ random graph, thus following a Poisson process. For $0 < \beta < 1$, the degree distribution is relatively homogeneous with all nodes having approximately the same degree [1].

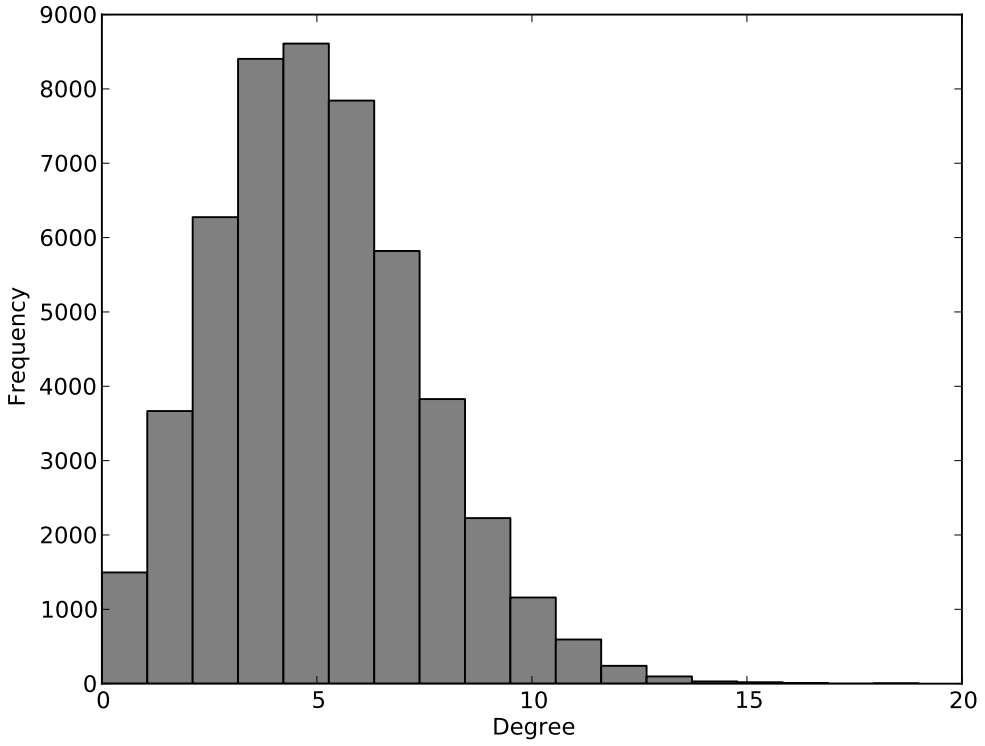

FIGURE 1.9: Degree distribution for the $ER(m, n)$ network. As it is expected, the $ER(m, n)$ random graphs presents degree distribution following a Poisson process (given the binomial distribution of the connections).

However, figure 1.11 shows a dramatically different picture of the degree distribution of the empirical network C. This fact makes it clear that the WS random model, although reproducing observed empirical clusters and short diameters, is not able to account for

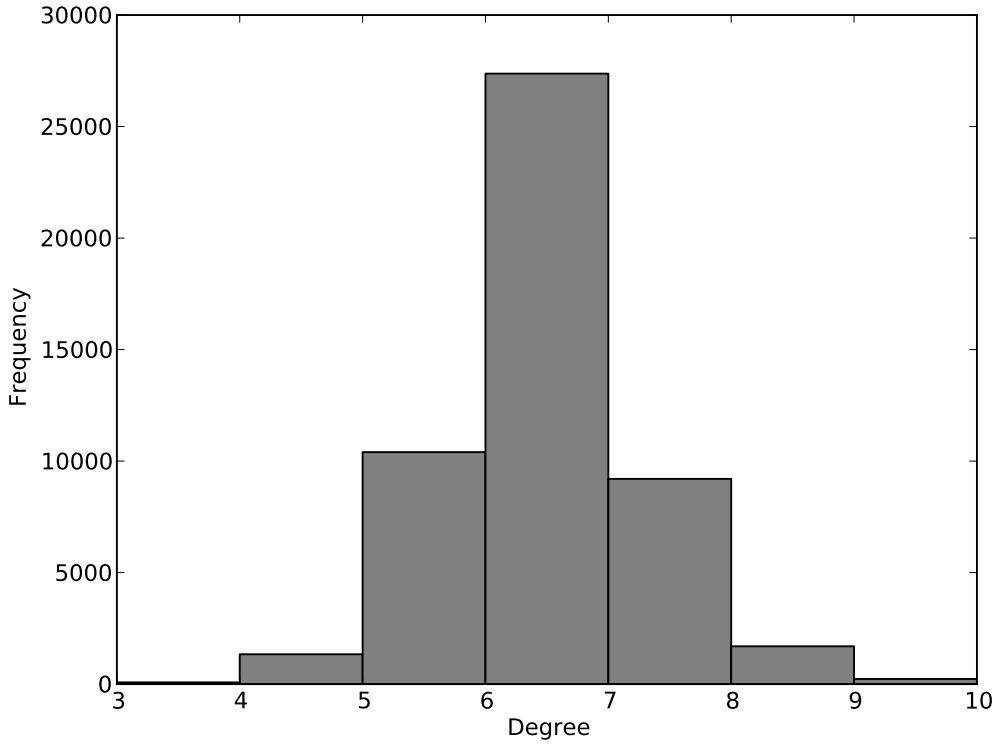

FIGURE 1.10: Degree distribution for the WS network. If $\beta = 0$ (that is, the ring lattice), the degree distribution follows as Dirac delta function centered in the number of nodes K. If $\beta = 1$, the result is a pure $ER(m, n)$ random graph, thus following a Poisson process. For $0 < \beta < 1$, the degree distribution is said to be relatively homogeneous with all nodes have more or less the same degree [1].

an immense disproportionality with regard to the number of connections among the nodes. This fact, a high level of concentration of connections between few nodes, is also found in a large number of other natural and social networks [7]. For instance, for the World Wide Web it has been shown that $80 - 90\%$ of the links have one side in just a small fraction of nodes, making the architecture dominated by a few well-connected hubs.

The next section presents an alternative model based on preferential attachment and growth proposed by [7], the Barabási-Albert (BA) model, which produces scale-free networks. Scale-free networks are characterized by presenting a power-law process ruling the degree distribution of their nodes. The last section presents a series of tests to check whether the degree distribution of the empirical networks do follow a power-law, or if there is another distribution presenting a better goodness of fit to empirical data.

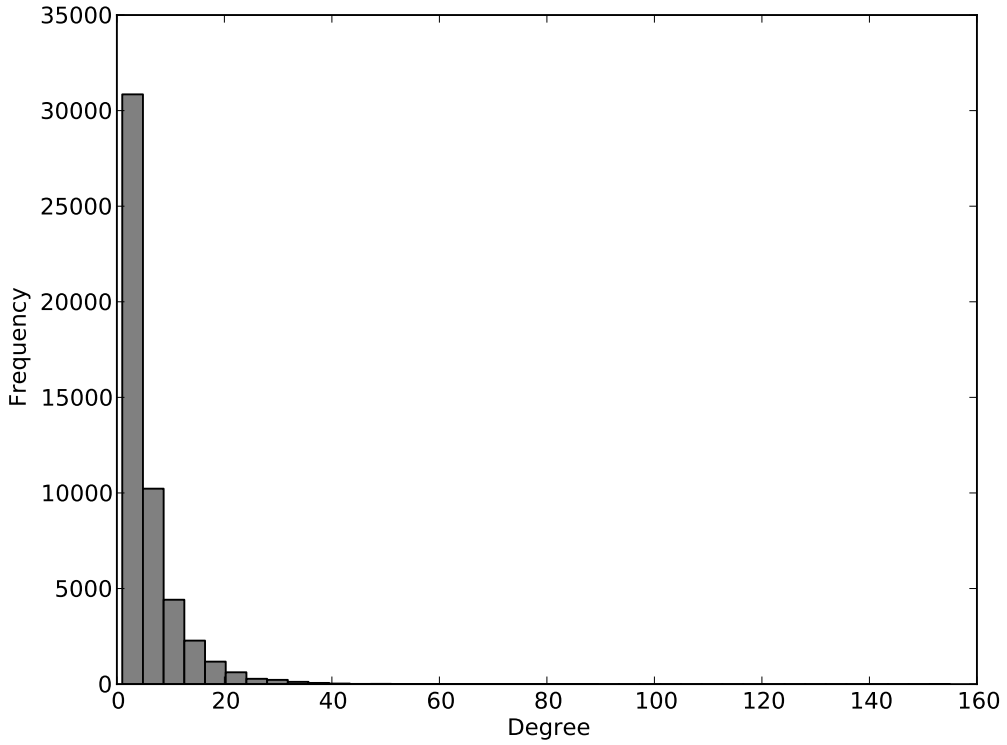

FIGURE 1.11: Degree distribution for the empirical network C. It is clear that the WS random model, although reproducing observed empirical clusters and short diameters, is not able to account for an immense disproportionality with regard to the number of connections among the nodes.

1.6.3 Preferential attachment and growth

Many observed networks fall into the class of scale-free networks, meaning that they have power-law (or scale-free) degree distributions, while random graph models such as the Erdős-Rényi (ER) model and the Watts-Strogatz (WS) model do not exhibit power laws. The Barabási-Albert model is one of several proposed models that generate scale-free networks. It incorporates two important general concepts: growth and preferential attachment. Both growth and preferential attachment exist widely in real networks. Growth means that the number of nodes in the network increases over time. Preferential attachment means that the more connected a node is, the more likely it is to receive new links. Nodes with higher degree have stronger ability to grab links added to the network.

Intuitively, the preferential attachment can be understood if we think in terms of social networks connecting people. Here a link from A to B means that person A knows or is acquainted with person B. Heavily linked nodes represent well-known people with lots

of relations. When a newcomer enters the community, she/he is more likely to become acquainted with one of those more visible people rather than with a relative unknown. Similarly, on the web, new pages link preferentially to hubs, i.e., very well known sites such as Google or Wikipedia, rather than to pages that hardly anyone knows. If someone selects a new page to link to by randomly choosing an existing link, the probability of selecting a particular page would be proportional to its degree.

This explains the preferential attachment probability rule. Preferential attachment is an example of a positive feedback cycle where initially random variations (one node initially having more links or having started accumulating links earlier than another) are automatically reinforced, thus greatly magnifying differences. This is also sometimes called the Matthew effect, the rich get richer, and, in chemistry, autocatalysis.

The network begins with an initial connected network of m_0 nodes. New nodes are added to the network one at a time. Each new node is connected to $m \leq m_0$ existing nodes with a probability that is proportional to the number of links that the existing nodes already have. Formally, the probability p_i that the new node is connected to node i is:

$$p_i = \frac{k_i}{\sum_j k_j} \tag{1.10}$$

where k_i is the degree of node i and the sum is made over all pre-existing nodes j (i.e., the denominator results in the current number of edges in the network). Heavily linked nodes (hubs) tend to quickly accumulate even more links, while nodes with only a few links are unlikely to be chosen as the destination for a new link. The new nodes have a preference to attach themselves to the already heavily linked nodes.

The average shortest path length if a BA network is given by $l \sim \frac{\log N}{\log \log N}$. While there is no analytical result for the clustering coefficient of the BA model, the empirically determined clustering coefficients are generally significantly higher for the BA model than for random ER networks. The clustering coefficient also scales with network size following approximately a power law in the form $C \sim N^{-0.75}$. However, the most interesting fact about the BA model is that it produces scale-free networks, that is, with

degree distribution following a power-law in the form $P(k) \sim k^{-3}$.

1.6.4 Power law fitting

The purpose of this section is to show that neither the power-law nor the binomial distributions present a satisfactory fit to empirical distribution of degrees. For validating this hypothesis, pair wise comparisons between the power-law and selected alternative distributions are carried out with respect to their relative goodness of fit.

Power laws are theoretical probability distributions in the form $p(x) \propto x^{-\alpha}$. Empirical power laws hold only approximately or over a limited range. According to [40], the first step of fitting a power law is to determine what portion of the data to fit. If the initial, small values of the data, do not follow a power law distribution one may opt to disregard them. The methods of [41] find this optimal initial value by creating a power law fit starting from each unique value in the dataset, then selecting the one that results in the minimal Kolmogorov-Smirnov distance, D, between the data and the fit. For the empirical network this was found to be 20, meaning that nodes holding more than 20 connections were discarded in the fitting procedure. The fitted exponent for the empirical network is 5.85.

It is frequently insufficient and unnecessary to answer the question of whether a distribution really follows a power law. Instead the question is whether a power law is the best description available. In this sense, for deciding whether or not a power-law is the best fit available for empirical data at hand, one has to compare it to other distributions with regard to goodness of fit.

The exponential distribution is the absolute minimum alternative candidate for evaluating the heavy-tailedness of the distribution. The reason is definitional: the typical quantitative definition of a heavy-tail is that it is not exponentially bounded [40]. Thus, if a power law is not a better fit than an exponential distribution (as in the above example) there is scarce ground for considering the distribution to be heavy-tailed at all, let alone a power law.

However, the exponential distribution is, again, only the minimum alternative candidate

distribution to consider when describing a probability distribution. However, sometimes the rich cannot get richer forever. There could be a gradual upper bounding effect on the scaling of the power law. An exponentially truncated power law could reflect this bounding. To test this hypothesis, the empirical fit of the distribution is then compared to a pure exponential, normal, and logistic references, as shown in table 1.6. It can be seen that the hypothesis of a power law process governing the distribution of connections a company has can be ruled out, as shown by the poor fit with respect both to exponential and logistic distributions.

TABLE 1.6: Anderson-Darling test statistic and its correspondent critical value at 1% for data coming from selected distributions. It can be seen that normal, exponential, and logistic distributions can be ruled out at 1% significance level.

Distribution	Statistic	Critical 1%
Exponential	2248.226	1.957
Normal	1163.326	1.092
Logistic	1041.240	0.906

1.7 Network core

So far, it has been shown that ER random models are able to explain the existence of large connected components and the relatively short average shortest path lengths observed in the board membership networks. However, this class of models do not produces another important feature found in most empirical social networks, namely, the existence of communities. Then, the WS random models were introduced as a way to mix randomness from the ER models with order from the ordered graphs to obtain networks which are at the same time small and clustered. Notwithstanding, it has been also shown that empirical board membership networks display the existence of hubs - highly connected nodes - in contrast to the more balanced degree distribution presented by both ER and WS random models. Finally, the scale-free BA model based on network growth and preferential attachment was presented as a way to generate random benchmarks with account for the existence of massive hubs as well.

As pointed out by [12], the degree distribution of the nodes (that is, the probability $P(k)$ of a given node in the network share an edge with k other nodes) received lots of attention in the literature as a way to discriminate between different structural orders. However, the degree distribution is only part of the topology: a deeper investigation of

the connectivity patterns requires the study of the degree correlation functions.

The *BA* random model based on preferential attachment is argued to account quite well for the topology of the World Wide Web [42], which was shown to be a network of the aristocratic type, with the dominance of a few but extremely massive hubs. In the *WWW* context, this picture is somewhat expected since there are many small and unpopular websites pointing to a few, very large and popular hubs. However, the lack of inter-hub connectivity is also expected in the *WWW*, and it is a result by construction from the preferential attachment process. In this sense, the next two sections deal with the so-called rich club phenomena (in the sense that the hubs - the rich nodes - form a tightly connected community - the club), to show that a simple process of network growth by preferential attachment is not able to explain this important part of the board membership network topology.

1.7.1 The most important nodes

At the node level, there are basically four definitions of centrality which attempt to capture different definitions for measuring the importance of a node in a network. The *degree* centrality is given by the number of edges that a given node is an endpoint of, hence capturing how connected is the node in absolute terms. The *closeness* centrality is defined as the average (shortest) path from a given node to all others, measuring how distant in terms of connections the node is from all the other nodes on average.

While *degree* centrality weights all edges equally, the *eigenvector* centrality considers each connected node proportionally to its respective connections and thus it is a measure that depends on the entire pattern of the graph, and not only on the directly connected nodes. Finally, the *betweenness* centrality captures the number of shortest paths that go through the node, hence giving an idea of how often the node is used as a step of a shortest path between two other nodes.

Table 1.10 shows the most important board members of the global network. The list presents the 19 most important board members according to betweenness and eigenvector centrality (the top-10 members according to each definition, with an overlap of one member).

1.7.2 The rich club phenomena

The rich-club phenomenon refers to the tendency of the dominant elements of the system to form tightly interconnected communities and it is one of the most important properties with respect to the formation of dominant communities in both natural and social sciences [12]. As pointed out by [34], the rich club phenomenon is not necessarily associated with the degree assortative mixing. A positive (negative) degree assortative mixing implies nodes with high degrees tend to be connected to other nodes of high (low) degree. The fact these two properties (degree assortativity and rich club) are not trivially related can be understood by considering a rich club formed by a clique of size four, in which each of the rich nodes is connected to other ten different and small nodes, as depicted in figure 1.12. This example network presents rich club phenomena and negative degree assortativity at the same time. Large nodes are more likely to connect to small nodes than to other large nodes (negative degree assortativity), while the interconnectivity among the large nodes is higher than the connectivity among small nodes (rich club phenomena).

The presence or absence of the rich-club phenomenon might have deep impacts on several aspects of a complex network [12]. For example, in a scientific collaboration network, the presence of the rich club phenomena would imply that famous scientists in that field are frequently coauthors with other influential scientists in the same field. With respect to the network formed by protein interaction, the absence of the phenomena can possibly mean that the hubs (the proteins with large connectivity) control different aspects of network functioning. Considering power-grid networks, the presence of the rich club phenomena reduces drastically the impact of a clever attack which aims part of the hubs, since other neighboring hubs can replace the attacked ones quickly.

In scale-free networks the connectivity of the rich-club plays an important role in the functionality of the network, for example, in the transmission of rumors in social networks or the efficient delivery of information on the Internet [43]. In a social context, for example, a rich-club coefficient increasing with the degree k indicates the dominance of an oligarchy of highly connected and mutually communicating individuals, as opposed to a structure consisting of many loosely connected and relatively independent

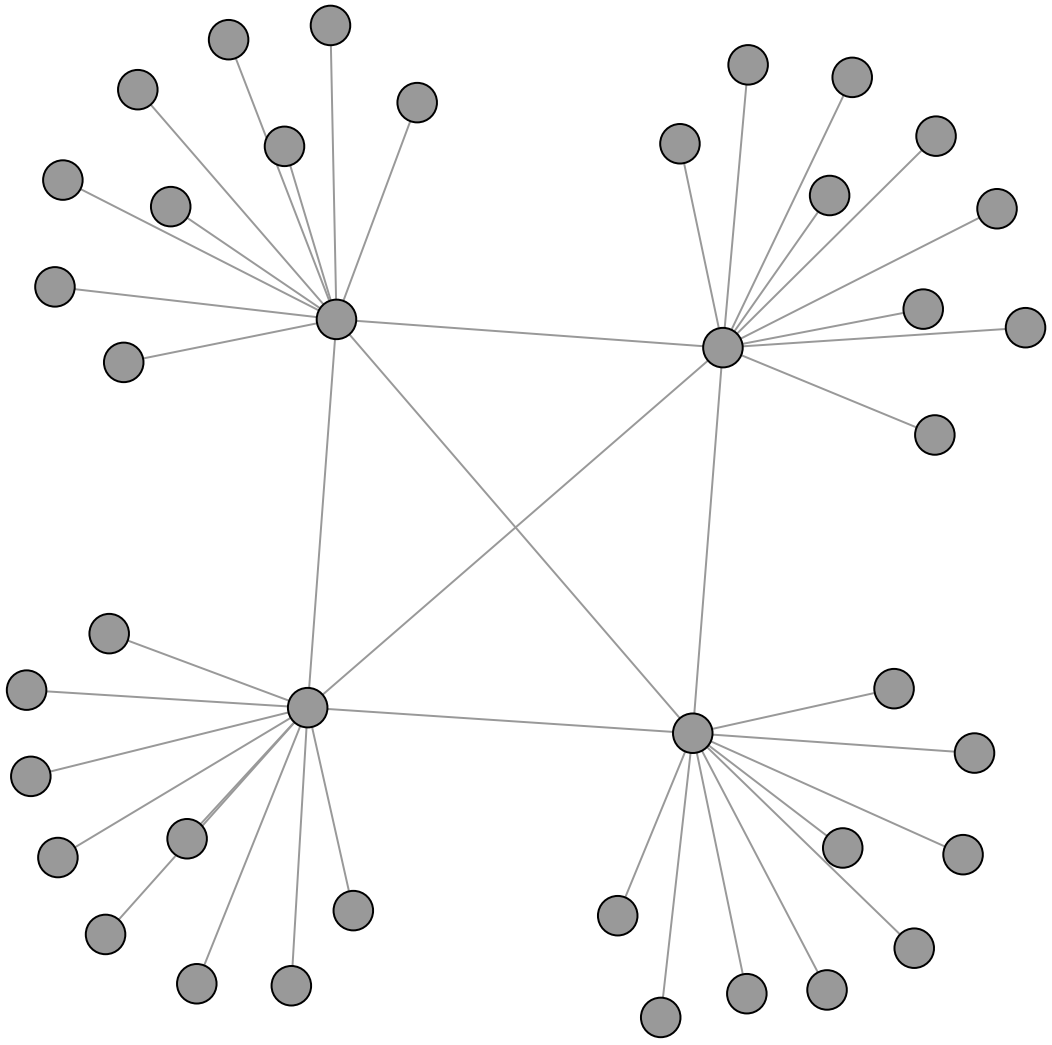

FIGURE 1.12: This example network presents rich club phenomena and negative degree assortativity at the same time. Large nodes are more likely to connect to small nodes than to other large nodes (negative degree assortativity), while the interconnectivity among the large nodes is higher than the connectivity among small nodes (rich club phenomena).

sub-communities [43]. Considering the effects of the rich club phenomena in Human Connectome data, [44] found it to produce highly resilient and stable networks.

1.7.3 The rich club coefficient

The rich club coefficient in networks can be described as, for a given degree k, the tendency of nodes with degree higher than k to be more densely connected to themselves than to nodes with degree lower than k [10]. It is characterized when the hubs, nodes with higher degrees are, on average, more intensely interconnected than the nodes with smaller degrees. More precisely, it happens when the nodes with degree larger than k tend to be more densely connected among themselves than the nodes with degree smaller than k, for any significant range of degrees in the network.

Formally, it is described as follows: consider a graph G with N nodes and M edges representing a complex network. Let N_k be the number of nodes with degree larger than k, and M_k be the number of edges between such nodes. The so-called rich-club coefficient $\phi(k)$ for a given degree k is given by

$$\phi(k) = \frac{2|M|_{>k}}{|N|_{>k}(|N|_{>k} - 1)} \tag{1.11}$$

However, nodes with higher degrees are naturally more likely to be more interconnected simply because they have more incident edges [12]. Indeed, even in the case of the ER graph an increasing rich-club coefficient with k can be found. This implies that the increase of k is a natural consequence of the fact that nodes with large degree have a larger probability of sharing edges than low degree vertices. This feature is therefore imposed by construction and does not represent a signature of any particular organizing principle or structure, as is clear in the ER case. The simple inspection of the k trend is therefore potentially misleading in the discrimination of the rich-club phenomenon [12].

Then, for the proper evaluation of this property, the rich club coefficient should be normalized by its corresponding value in a random graph which follows the same (probably highly skewed) degree distribution. Such a random graph can be generated, for example, by the following procedure described in [45]: take two edges of the empirical

network and switch one of their endpoints randomly. If sufficient iterations of this process are carried out, thus the procedure shuffles the edge structure of the network but conserves its degree structure. Then the rich-club coefficient is computed for the resulting maximally random network, $\phi_{ran}(k)$, and it is used to find the normalized rich-club coefficient as follows

$$\rho(k) = \frac{\phi(k)}{\phi_{ran}(k)} \tag{1.12}$$

While $\phi(k)$ gives the rich-club coefficient with respect to an ideal uncorrelated graph, $\rho(k)$ is a realistic normalized measure that takes into account the structure and finiteness of the network. Figure 1.13 presents the normalized version of the rich club coefficient described in [10] for the LCC (largest connected component) of C and figure 1.14 for the LCC of D_2 (network formed by board members holding at least two board positions). It can be seen a strong indication of the rich club phenomena over all range of k.

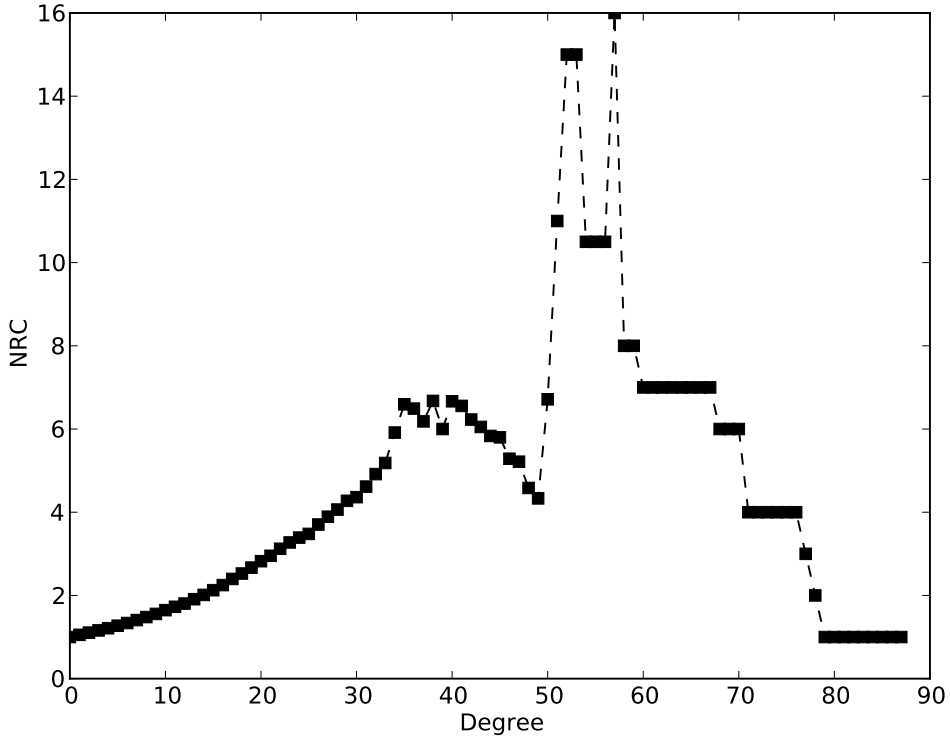

FIGURE 1.13: Normalized Rich Club Coefficients for varying degrees for the LCC of C. It can be seen a strong indication of the rich club phenomena over the full range of k.

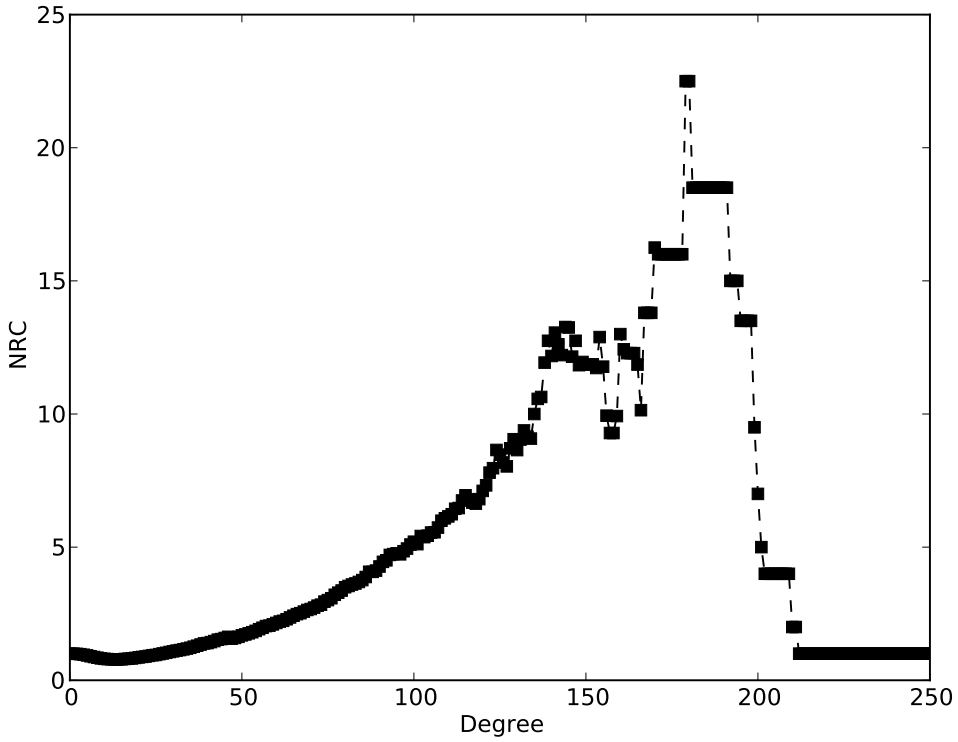

FIGURE 1.14: Normalized Rich Club Coefficients for varying degrees for the *LCC* of D_2. It can be seen a strong indication of the rich club phenomena over the full range of k.

1.7.4 Coreness

The *coreness* measure as defined in [46] was applied to this dataset. Ideally, one can think of a core as a set of nodes that are tightly connected to themselves, and a periphery as a set of nodes which are not connected to themselves but connected to the core. This ideal network would have an adjacency matrix full of ones in the intra-core block, and full of zeros in the intra-periphery block. Then a statistic for the existence of a core is a measure of distance between the empirical adjacency matrix and this ideal perfect core-periphery structure. Finally, the problem reduces to finding the partition of a matrix which yields the smallest distance to the ideal structure.

The present section is thus concerned with the existence of significant cores in the national networks formed by board members. In the terms presented by [46], here the discrete model of core periphery is investigated, that is, the problem of finding a single

partition (thus dividing the nodes in two sub graphs) that maximizes the person correlation coefficient between the partitioned empirical graph and the ideal core-periphery structure.

According to [47], in order to find such non empty subgraph (the optimal partition) it suffices to minimize the following statistic:

$$Z(S_1) = \sum_{(i \leq j) \in S_1} \Pi_{A_{ij}=0} + \sum_{(i \leq j) \notin S_1} \Pi_{A_{ij}=1} \tag{1.13}$$

where S is a graph $S = 1, ..., n$ with n nodes, S_1 is the subset of S ($S_1 \in S$) presumed to be the core of the graph, A is the binary adjacency matrix indicating whether two nodes are connected or not, and Π is an indicator function Π_P, which is equal to 1 if P is true, and equal to 0 otherwise. Note that the Z measures increases when it finds two nodes at the core which are not connected (first term of right hand side), and also when it finds two nodes of the periphery which are connected (second term of the left hand side).

This same author also shows that it is possible to minimize the Z statistic, and thus to find the optimal partition, in $O(n^2)$ time without relying on heavy and non exact optimization procedures, such as linear optimization and genetic algorithms. The algorithm proposed by [47] is able to outperform its alternatives to such a great extent because it is rooted in the finding that the members of the optimal core will necessarily be the nodes with the highest degrees (for a proof, see [47]). When one considers this fact, finding the core is just a matter of sorting nodes by degree, forming the possible cores by sequentially adding nodes with high degrees and computing the correspondent Z statistic. The procedure halts when the addition of a new node to the core increases the Z statistic.

Table 1.11 presents the size of the core and the correspondent fitness measure to the ideal core/periphery model for selected countries as described in [46], and using the algorithm developed by [47]. More specifically, here the national networks of board members (directors) are considered. No significant evidence of a core can be found for the majority of the countries, arguably because the networks are not composed by single one-dimensionally layered core-periphery structure as it might be the case for other networks such as inter-banking networks [48].

1.8 Conclusion

In this chapter, several features of the networks formed by interlocking directorates were presented as stylized facts, meaning that the existence of such features is widespread over a large and diverse set of economies. For instance, it could be seen that the accumulation of board positions by single individuals cannot be described by a simple random allocation of positions to directors, and thus that other forces might drive its dynamics.

It was also shown that interlocking networks present a large connected component, although this is not totally unexpected if a random graph is used as a benchmark. Afterwards, the dichotomy between order and randomness presented in the WS small world graphs was shown to account for the small world phenomena presented in empirical networks, and the preferential attachment process from the BA models able to account for the highly skewed degree distributions.

In addition, it could also be seen that some countries engage in the global network of board members differently from the others. For instance, it was observed that a great deal of the absolute number of board directors, and the majority of the most central actors, are based in North Atlantic countries. With respect to the profile of the firms engaging in international interlocks, the lower country assortativity levels observed in companies with high degrees indicate that very well connected firms are the responsible for sustaining a connected global network, while smaller and less connected firms usually engage in domestic interlocking. The special role of financial institutions could also be observed, mainly by means of their higher average centrality. Financial institutions also possess a much larger board on average (up to 40% larger), meaning that for them it might be more worthwhile to engage in interlocks than for non financial institutions.

Finally, evidence was shown supporting that the rich club phenomena is also a stylized fact of board membership networks, which is not accounted for by any of the random models described here. As in the case of the accumulation of board positions by individuals not being explained by a simple chance process, the higher level of intra-hub connectivity (the rich club phenomena) cannot be explained by the traditional BA models of preferential attachment, and thus, other factors might have influence on them.

The *rich-gets-richer* effect was used as an explanation for the existence of a very well connected core in the networks of interlocking directorates [49]. It was argued that it is just a natural consequence of adding nodes at random and attaching them to already well connected nodes. The main contribution of this investigation is to show that the high levels of intra hub connectivity (the rich-club phenomena) presented in real world interlocking networks cannot plausibly be seen as an outcome of chance (at least not from the preferential attachment scheme), and thus proper explanation for the phenomena is still required.

Appendix A. The Topology of the Global Interlocking Directorates

TABLE 1.7: Number of positions, directors, and companies for the top 50 countries by the number of directors. The last two columns show the average number of board positions per director and the average board size in number of positions.

Country	Positions (1)	Directors (2)	Companies (3)	(1)/(2)	(1)/(3)
United States	62090	51892	8864	1.20	7.00
Canada	21303	14590	3428	1.46	6.21
India	12351	9755	1443	1.27	8.56
United Kingdom	9410	7656	1412	1.23	6.66
Australia	7758	5966	1485	1.30	5.22
South Korea	6977	6734	1345	1.04	5.19
China	6764	6396	1119	1.06	6.04
Germany	5544	4850	774	1.14	7.16
Thailand	5311	4391	507	1.21	10.48
France	4574	3728	643	1.23	7.11
Italy	4064	3362	267	1.21	15.22
Singapore	3615	2751	489	1.31	7.39
South Africa	3099	2431	318	1.27	9.75
Poland	3063	2727	503	1.12	6.09
Pakistan	3025	2314	382	1.31	7.92
Sweden	2850	2270	405	1.26	7.04
Philippines	2302	1564	228	1.47	10.10
Russia	2178	1922	214	1.13	10.18
Israel	2138	1660	359	1.29	5.96
Switzerland	2120	1659	287	1.28	7.39
Sri Lanka	2074	1305	249	1.59	8.33
Norway	1994	1728	171	1.15	11.66
Jordan	1962	1810	218	1.08	9.00
Indonesia	1683	1449	337	1.16	4.99
Malaysia	1670	1523	242	1.10	6.90
Vietnam	1646	1600	473	1.03	3.48
Greece	1620	1473	203	1.10	7.98
Spain	1609	1373	150	1.17	10.73
Mexico	1581	1226	108	1.29	14.64
Bangladesh	1556	1368	143	1.14	10.88
Nigeria	1442	1277	161	1.13	8.96
Turkey	1264	1024	177	1.23	7.14
Brazil	1175	990	145	1.19	8.10

Continued on next page

Table 1.7 – *Continued from previous page*

Country	Positions (1)	Directors (2)	Companies (3)	(1)/(2)	(1)/(3)
Belgium	1161	948	130	1.22	8.93
Denmark	1111	972	147	1.14	7.56
Kuwait	1076	973	167	1.11	6.44
Netherlands	1034	777	148	1.33	6.99
Finland	1014	837	120	1.21	8.45
Oman	793	663	107	1.20	7.41
Austria	773	647	81	1.19	9.54
Hong Kong	772	656	130	1.18	5.94
New Zealand	754	627	127	1.20	5.94
Ireland	751	594	80	1.26	9.39
Cyprus	739	609	102	1.21	7.25
United Arab Emirates	734	649	100	1.13	7.34
Argentina	712	611	61	1.17	11.67
Bermuda	623	481	75	1.30	8.31
Portugal	573	502	48	1.14	11.94
Channel Islands	547	430	86	1.27	6.36
Egypt	498	462	88	1.08	5.66

TABLE 1.8: Number of positions, directors, and companies by sectors of economic activity. The last two columns show the average number of board positions per director and the average board size in number of positions.

Sector	Positions (1)	Directors (2)	Companies (3)	(1)/(2)	(1)/(3)
Banks and Thrifts	20217	18662	1759	1.08	11.49
Metals and Mining	18407	12764	3178	1.44	5.79
Financial Services	13932	11200	2035	1.24	6.85
Energy	13327	10087	2129	1.32	6.26
Software and Technology	12623	10769	2208	1.17	5.72
Pharmaceuticals and Biotechnology	10874	8991	1289	1.21	8.44
Food and Beverages	9270	7713	1262	1.20	7.35
Computers and Electronic	8665	7437	1474	1.17	5.88
Real Estate	8226	6734	1237	1.22	6.65
Media	6219	5112	905	1.22	6.87
Heavy Machinery	5977	4997	880	1.20	6.79
Chemicals	5907	4889	851	1.21	6.94
Commercial Services and Supplies	5844	4916	965	1.19	6.06
Utilities	5833	4712	630	1.24	9.26
Restaurants and Leisure	5602	4512	818	1.24	6.85
Insurance	5536	4581	546	1.21	10.14
Retail	5345	4325	729	1.24	7.33
Building and Construction	4717	3901	659	1.21	7.16
Clothing Textiles	4601	3798	673	1.21	6.84

Continued on next page

Table 1.8 – *Continued from previous page*

Sector	Positions (1)	Directors (2)	Companies (3)	(1)/(2)	(1)/(3)
Construction Services	4405	3720	650	1.18	6.78
Healthcare Equipment/Supplies	3829	3243	522	1.18	7.34
Communication Services	3072	2388	404	1.29	7.60
Electrical Equipment	3020	2564	485	1.18	6.23
Healthcare Services	2925	2492	411	1.17	7.12
Wholesale and Distribution	2924	2431	456	1.20	6.41
Auto Parts	2913	2475	417	1.18	6.99
Semiconductors	2673	2278	413	1.17	6.47
Appliances and Furniture	1776	1525	260	1.16	6.83
Misc. Consumer Products	1769	1489	263	1.19	6.73
Conglomerates	1510	1098	167	1.38	9.04
Paper and Forest Products	1490	1210	201	1.23	7.41
Aerospace and Defense	1475	1178	191	1.25	7.72
Packaging and Containers	1406	1146	214	1.23	6.57
Transportation Infrastructure	1225	1049	138	1.17	8.88
Diversified Services	1208	1054	187	1.15	6.46
Railroads and Trucking Services	937	738	135	1.27	6.94
Sea Transportation	930	785	139	1.18	6.69
Airlines	823	664	82	1.24	10.04
Automobiles	818	603	93	1.36	8.80
Air Freight	704	584	106	1.21	6.64
Tobacco	319	250	46	1.28	6.93

Table 1.9: Eigenvector centrality (first column) and connections diversity (second column) by sector of economic activity. While the eigenvector centrality shows which are the most central sectors of activity in the network, the diversity of its connections indicate whether the sector influences just a few other related sectors or a large part of the network. The diversity of the connections is defined as the Shannon Entropy of the weighted connections. That means it will be close to 0 when the sector basically connects to one or just a few other sectors (like Metals and Mining, for example), and it will be close to 1 if the sector connects more or less equally to all other sectors (like Financial Services, for example).

Sector	Eigenvector	Entropy
Miscellaneous Financial Services	0.385	0.849
Software and Technology Services	0.376	0.666
Metals and Mining	0.299	0.484
Miscellaneous Commercial Services and Supplies	0.280	0.887
Energy	0.274	0.638
Computers and Electronic Equipment	0.248	0.811
Media	0.212	0.781
Real Estate	0.190	0.837
Banks and Thrifts	0.182	0.830
Food and Beverages	0.177	0.845

Continued on next page

Table 1.9 – *Continued from previous page*

Sector	Eigenvector	Entropy
Restaurants and Leisure	0.167	0.833
Retail	0.161	0.854
Pharmaceuticals and Biotechnology	0.159	0.599
Heavy Machinery	0.156	0.880
Chemicals	0.138	0.885
Utilities	0.135	0.785
Engineering and Construction Services	0.115	0.877
Insurance	0.113	0.760
Communication Services	0.112	0.827
Wholesale and Distribution	0.108	0.889
Building Products and Construction Materials	0.099	0.891
Healthcare Equipment/Supplies	0.099	0.707
Healthcare Services	0.094	0.778
Clothing, Textiles and Accessories	0.091	0.854
Electrical Equipment	0.075	0.904
Semiconductors	0.073	0.731
Auto Parts	0.061	0.875
Conglomerates	0.054	0.910
Aerospace and Defense	0.046	0.856
Appliances and Furniture	0.043	0.915
Diversified Services	0.042	0.876
Misc. Consumer Products	0.040	0.894
Packaging and Containers	0.037	0.906
Paper and Forest Products	0.037	0.901
Railroads and Trucking Services	0.035	0.873
Transportation Infrastructure	0.033	0.888
Automobiles	0.028	0.908
Air Freight	0.026	0.913
Sea Transportation	0.024	0.859
Airlines	0.024	0.901
Tobacco	0.008	0.885

Table 1.10: Most important board members. The list presents the 19 most important board members according to betweenness and eigenvector centrality (the top-10 members according to each definition, with an overlap of one member)

Name	Positions	Degree	Companies
Dieter Zetsche	3	61	Daimler AG
			Deutsche Bank AG

Continued on next page

Table 1.10 – *Continued from previous page*

Name	Positions	Degree	Companies
			RWE AG
Henning Kagermann	6	72	Bayerische Motoren Werke AG
			Deutsche Bank AG
			Deutsche Post AG
			Münchener Rückversicherungs-Gesellschaft AG
			Nokia Corporation
			Wipro
Clemens Borsig	5	73	Bayer AG
			Daimler AG
			Deutsche Bank AG
			Fraport AG
			The Linde Group
Deepak Parekh	12	85	DP World
			Exide Industries
			GlaxoSmithKline Pharmaceuticals
			HDFC Bank
			Housing Development Finance Corp.
			Indian Hotels Co.
			Infrastructure Development Finance Co.
			Lafarge S.A.
			Mahindra and Mahindra
			Siemens
			WNS (Holdings)
			Zodiac Clothing Company
Peter Crossgrove	8	44	Barrick Gold Corporation
			Detour Gold Corporation
			Dundee REIT
			Excellon Resources Inc.
			Lake Shore Gold Corp.
			Pelangio Exploration Inc.
			QLT Inc.
			Standard Gold Inc.
Karl-Ludwig Kley	4	71	Bayerische Motoren Werke AG
			Deutsche Bank AG
			HSBC Trinkaus and Burkhardt AG
			Merck KGaA
Maurice Lévy	3	65	Deutsche Bank AG
			Publicis Groupe SA

Continued on next page

Table 1.10 – *Continued from previous page*

Name	Positions	Degree	Companies
			The Blackstone Group LP
Paul Achleitner	4	69	Bayer AG
			Daimler AG
			Deutsche Bank AG
			RWE AG
Roland Berger	8	95	Deutsche Bank AG
			Fiat S.p.A.
			Fresenius SE and Co KGaA
			Italy1 Investment S.A.
			Prime Office REIT-AG
			RCS MediaGroup S.p.A
			The Blackstone Group LP
			3W Power SA
Keki Dadiseth	8	70	Britannia Industries
			Godrej Properties
			Indian Hotels Co.
			Marsh and McLennan Companies Inc.
			Omnicom Group Inc.
			Piramal Healthcare
			Prudential plc
			Siemens
Charles Powell	7	72	Barrick Gold Corporation
			Caterpillar Inc.
			Hongkong Land Holdings
			Mandarin Oriental International
			Rolls Royce Holdings plc
			Schindler Holding AG
			Textron Inc.
Josef Ackermann	4	75	Deutsche Bank AG
			Royal Dutch Shell plc
			Siemens AG
			Zurich Insurance Group AG
Ratan Tata	12	97	Alcoa Inc.
			Fiat S.p.A.
			Indian Hotels Co.
			Nelco
			Rolls Royce Holdings plc
			Tata Chemicals

Continued on next page

Table 1.10 – *Continued from previous page*

Name	Positions	Degree	Companies
			Tata Consultancy Services
			Tata Global Beverages
			Tata Motors
			Tata Power Co.
			Tata Steel
			Bombay Dyeing and Manufacturing
Subramaniam Ramadorai	9	85	Asian Paints
			CMC
			Deutsche Bank AG
			Hindustan Unilever
			Piramal Healthcare
			Tata Communications
			Tata Consultancy Services
			Tata Elxsi
			Tata Teleservices (Maharashtra)
Alexei Mordashov	3	71	Deutsche Bank AG
			Joint Stock Company Severstal
			Lafarge S.A.
Nasser Munjee	12	69	ABB
			Ambuja Cements
			Britannia Industries
			Cummins India
			Development Credit Bank
			Housing Development Finance Corp.
			Repro India
			Shipping Corp. of India
			Tata Chemicals
			Tata Motors
			Unichem Laboratories
			Voltas
Ian Smith	6	29	Bolero Resources Corp.
			Euro Ressources SA
			Max Resource Corp.
			Santa Fe Metals Corp.
			Transurban Group
			Yellowhead Mining Inc.
Wazir Khoja	8	35	Askari Bank
			Bank Al Habib

Continued on next page

Table 1.10 – *Continued from previous page*

Name	Positions	Degree	Companies
			Fauji Fertilizer Co.
			KSB Pumps (Pakistan)
			Packages
			Pak Suzuki Motor Co.
			Sui Northern Gas Pipelines
			Thatta Cement Company
Kenichi Ayukawa	2	8	Maruti Suzuki India
			Pak Suzuki Motor Co.

TABLE 1.11: Size of the core and the correspondent fitness measure (correlation) to the ideal core/periphery model for selected countries. More specifically, here the national networks of board members (directors) are considered. No significant detection of a core can be observed for the majority of the countries, arguably because the networks are not composed by single one-dimensionally layered core-periphery structure as it might be the case for other networks such as interbanking networks.

Country	Nodes	Density	Core size	Correlation
All	50320	0.0001	45	0.0043
United States	14078	0.0003	27	0.0075
Canada	4235	0.0017	29	0.0176
India	2388	0.0029	32	0.0369
Australia	1660	0.0025	14	0.0182
United Kingdom	1632	0.0022	14	0.0174
Japan	1248	0.0025	14	0.0287
Germany	1056	0.0037	18	0.0628
Malaysia	1052	0.0053	19	0.0369
Hong Kong	950	0.0065	23	0.0544
Sweden	939	0.0049	16	0.0371
China	767	0.0041	12	0.0390
France	675	0.0070	19	0.0694
Singapore	640	0.0074	15	0.0488
Israel	583	0.0089	18	0.0608
Thailand	553	0.0101	17	0.0622
Italy	505	0.0105	18	0.0818
South Africa	448	0.0113	16	0.0718

Continued on next page

Table 1.11 – *Continued from previous page*

Country	Nodes	Density	Core size	Correlation
Norway	425	0.0092	11	0.0589
Poland	351	0.0092	9	0.0468
Russia	329	0.0144	15	0.1035
Finland	317	0.0120	10	0.0566
Philippines	317	0.0259	21	0.1345
Switzerland	308	0.0110	10	0.0609
Sri Lanka	286	0.0358	22	0.1079
Denmark	286	0.0144	11	0.0619
New Zealand	275	0.0136	9	0.0623
Pakistan	275	0.0175	11	0.0716
Spain	245	0.0155	11	0.1045
Netherlands	197	0.0189	10	0.0903
Belgium	189	0.0183	9	0.1033
Brazil	186	0.0237	11	0.1138
Taiwan	143	0.0221	8	0.1066
Mexico	132	0.0630	19	0.2072
Austria	129	0.0359	11	0.1100
Bangladesh	126	0.0309	8	0.1027
Indonesia	109	0.0321	8	0.1136
United Arab Emirates	107	0.0319	7	0.1264
Nigeria	103	0.0333	7	0.0906
Oman	98	0.0347	7	0.1070
Saudi Arabia	94	0.0336	6	0.1106
Jordan	87	0.0369	6	0.0979
South Korea	72	0.0376	5	0.0966
Greece	63	0.0573	7	0.1581
Kuwait	61	0.0404	5	0.1312
Kenya	56	0.0838	10	0.1583
Zimbabwe	48	0.0718	5	0.1190
Ireland	47	0.0611	5	0.1494
Peru	46	0.0889	7	0.1119

Continued on next page

Table 1.11 – *Continued from previous page*

Country	Nodes	Density	Core size	Correlation
Argentina	42	0.1022	7	0.2308
Bahrain	41	0.1110	7	0.1942
Portugal	40	0.0744	6	0.2144
Qatar	38	0.0711	4	0.1365
Turkey	33	0.2045	9	0.1453
Cyprus	32	0.0907	4	0.1532
Egypt	28	0.0873	4	0.1709
Mauritius	28	0.2196	7	0.2972
Chile	22	0.2121	6	0.2640
Hungary	22	0.1342	4	0.3634
Slovenia	22	0.1039	3	0.2189
Luxembourg	20	0.1737	5	0.2860

Chapter 2

Interlocking Directorates in Spain: Evidence from a Comprehensive Data Set

Introduction

In the previous chapter, it was shown that several properties appear consistently as stylized facts among a diverse set of board membership networks. More specifically, it could be seen that (a) binomial random benchmark models are not able to explain the accumulation of board positions presented in real world data; (b) there is a large connected component comprising the majority of the nodes in the networks, regardless if one takes into account individual countries or aggregated data at the global level; (c) all the networks are of the small-world type, that is, they present very short diameters with respect to the total number of nodes together with high clustering coefficients; (d) the empirical degree distribution of all networks is highly skewed, and can, thus, not be explained by the WS random rewiring models; and (e) they present an excessive rich club coefficient, indicating there is high level of intra-hub connectivity which is not explained by the BA preferential attachment models.

The present chapter is organized as follows. The first section confirms the findings

from the first chapter in the light of a richer dataset concerning Spanish board networks, comprising seven years from 2004 to 2010. These findings add to the growing literature stressing the fundamental similarities between interlocking networks from a diverse set of countries.

The second section highlights the most influential nodes, companies, and sectors of activity, to stress the high participation of financial institutions in the social network of board members, in agreement with extensive literature (see [37] in general, and [50] for the specific case of Spain). Although the idea that banks in the twentieth century Spain formed a cartel through interlocking directorates was ruled out by [51], it is clear that financial institutions were very important actors in the networks.

The third section investigates the relation between network centrality and performance measures. A significant inverse relation between centrality and leverage of non-financial institutions could be observed during the period, suggesting that board linkages might have generated some kind of special conditions for lending that would not exist if based on economic criteria only. This finding adds evidence to the discussion presented by [52]. In addition, no significant relation between centrality and economic performance was found, differently from [17], but in agreement to [53].

Additionally, the role of the highly capitalized Ibex companies in the network, gender differences, and the participation of politicians in company boards are investigated in the fourth section. It could be seen, for instance, (a) that more than half of the directors holding two or more board positions serve in at least one Ibex board, (b) that women's participation is increasing, although they still have smaller average centrality then men, and (c) that politicians are more likely to get a second position than non politicians.

In this chapter, data from three different sources are used: the first section presents data collected from the CNMV (*Comissión Nacional del Mercado de Valores*) with respect to board affiliation from which all centrality measures are calculated. The third section introduces firm level data collected from the SABI (*Iberian Balance Sheet Analysis System*) dataset [54] which will be used to check whether network measures have

an explicit impact on firms' performance metrics. Finally, the fourth section uses politicians' lists from the Spanish national congress.

2.1 Network stylized facts

Following the approach described in the previous chapter, information from the database was represented by incidence matrices, which allow the calculation of network measures both in terms of connected companies and connected directors. This section explores the stylized facts found in the previous chapter with respect to the richer data set composed of Spanish companies over seven years, from 2004 to 2010.

2.1.1 Data description

The data were collected from the CNMV website `http://www.cnmv.es` (*Comissión Nacional del Mercado de Valores*) in October 2012. More specifically, in the index page of the website there is a link to *Entidades emisoras: Información regulada y otra* under the *Consultas a registros oficiales* section. Then, there is the link *Información sobre Gobierno Corporativo* which leads to a document search environment. The names of the board directors are presented in the type of document called *Informe anual del gobierno corporativo*, which is available in a standard and complete format from 2004 to 2010. There are three different kinds of reports which classify companies as: (a) Listed Companies (*Sociedades Anónimas Cotizadas*); (b) Savings Banks (*Cajas de Ahorro*); or (c) Other Issuers (*Otras Entidades Emisoras*). Tables 2.1-2.3 show some descriptive statistics.

TABLE 2.1: Number of companies.

Year	Listed Companies	Other Issuers	Savings Banks	Total
2004	183	17	38	238
2005	177	20	39	236
2006	173	20	42	235
2007	169	21	42	232
2008	167	23	42	232
2009	158	22	39	219
2010	154	25	32	211

TABLE 2.2: Number of board positions.

Year	Listed Companies	Other Issuers	Savings Banks	Total
2004	1694	190	649	2533
2005	1678	223	670	2571
2006	1677	218	720	2615
2007	1646	236	733	2615
2008	1687	247	735	2669
2009	1611	245	679	2535
2010	1568	278	602	2448

TABLE 2.3: Number of board members.

Year	Listed Companies	Other Issuers	Savings Banks	All
2004	1407	179	649	2179
2005	1375	213	670	2190
2006	1394	208	720	2255
2007	1357	223	733	2245
2008	1420	237	735	2315
2009	1374	236	679	2224
2010	1356	267	602	2154

Table 2.4 depicts the accumulation of multiple board positions. It can be seen a consistent reduction in the number of multiple board memberships from 2008 to 2010, a fact that is most likely due to the financial crisis of 2008.

TABLE 2.4: Number of directors holding at least 2-6 positions.

Directors holding at least N positions	N=2	N=3	N=4	N=5	N=6
2004	179	51	15	4	2
2005	177	62	13	5	1
2006	184	49	15	5	1
2007	178	47	19	9	1
2008	174	39	20	8	2
2009	173	32	15	4	2
2010	171	32	11	5	1

Savings Banks boards are different from the others. Tables 2.5 and 2.6 show that their average sizes are around 70% higher, and that there are no interlocks among themselves.

2.1.2 Binomial benchmark for the accumulation of board positions

Following the approach described in [27], figure 2.1 compares, for 2010, the relative frequency of multiple board memberships to a random benchmark given by the probability of observing multiple board membership in an independent sequence of $k = 293$ (*number*

TABLE 2.5: Average number of members per board.

Year	Listed Companies	Other Issuers	Savings Banks	Total
2004	9.26	11.18	17.08	10.64
2005	9.48	11.15	17.18	10.89
2006	9.69	10.90	17.14	11.13
2007	9.74	11.24	17.45	11.27
2008	10.10	10.74	17.50	11.50
2009	10.20	11.14	17.41	11.58
2010	10.18	11.12	18.81	11.60

TABLE 2.6: Ratio number of board members/number of board positions.

Year	Listed Companies	Other Issuers	Savings Banks	Total
2004	83.1%	94.2%	100.0%	88.2%
2005	81.9%	95.5%	100.0%	87.8%
2006	83.1%	95.4%	100.0%	88.8%
2007	82.4%	94.5%	100.0%	88.5%
2008	84.2%	96.0%	100.0%	89.6%
2009	85.3%	96.3%	100.0%	90.3%
2010	86.5%	96.0%	100.0%	90.9%

of board positions - number of directors) Bernoulli trials with probability $p = 1/2154$ *(1/number of directors)* of success. It can be seen that the chances of accumulating board positions at random are several orders of magnitude lower than what is observed in the empirical data.

2.1.3 Existence of a Large Connected Component

A large connected component (LCC) could be observed during the entire time spam (2004 to 2010), confirming that earlier findings for German data [22] are also valid for the Spanish case. Table 2.7 depicts the size of the LCC, which encompasses around 70% of the nodes and links in the network of directors, while table 2.8 shows that the LCC consists of about 65% of the nodes and almost all the links in the companies' network.

2.1.4 Persistence of the Large Connected Component

This Large Connected Component persists over the period, regardless of personal turnover. Table 2.9 presents the rate of survival of directors and companies in the LCC, both with respect to the previous year and to the first year (2004). It could be seen that nearly 70-80% of the directors remain in the largest connected component in the subsequent

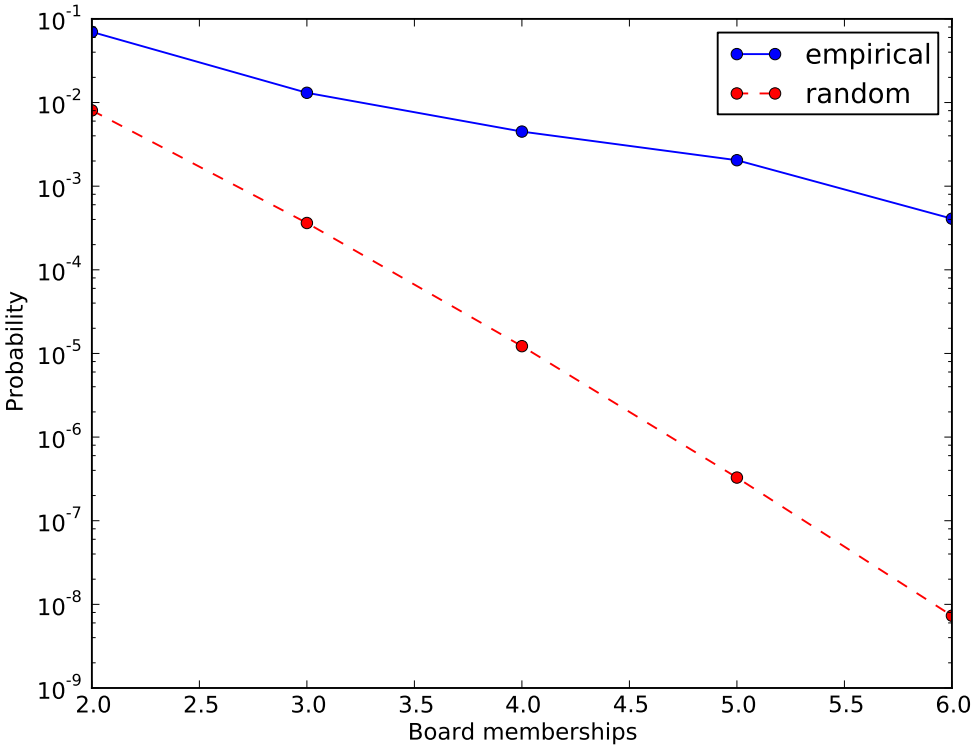

FIGURE 2.1: Relative frequency of empirical multiple board membership (red circles) and the random binomial benchmark (blue x's), for the year 2010.

TABLE 2.7: Nodes and edges of the networks of directors.

Year	Directors	Links	In LCC	Links	Nodes Ratio	Links Ratio
2004	2179	15173	1421	11017	65.2%	72.6%
2005	2190	15491	1450	11435	66.2%	73.8%
2006	2255	15964	1528	12005	67.8%	75.2%
2007	2245	16367	1520	12160	67.7%	74.3%
2008	2315	16940	1553	12522	67.1%	73.9%
2009	2224	15795	1486	11501	66.8%	72.8%
2010	2154	15683	1485	11732	68.9%	74.8%

TABLE 2.8: Nodes and edges of the networks of companies.

Year	Companies	Links	In LCC	Links	Nodes Ratio	Links Ratio
2004	238	381	152	377	63.9%	99.0%
2005	236	388	152	386	64.4%	99.5%
2006	235	393	156	392	66.4%	99.7%
2007	232	400	159	398	68.5%	99.5%
2008	232	392	155	391	66.8%	99.7%
2009	219	343	144	341	65.8%	99.4%
2010	211	325	143	322	67.8%	99.1%

year, and that this figure is higher for companies, being around 85-90%. As pointed out in [22], the LCC seems to be persistent independently of the individuals holding the board positions. For instance, only 32% of the directors in 2010 were present in the LCC in 2004, while 60% of the companies remained the same over the period.

TABLE 2.9: Rate of survival of nodes. The Large Connected Component persists over the period, regardless of personal turnover.

Year	Directors (2004)	Companies (2004)	Directors (last)	Companies (last)
2005	77%	91%	77%	91%
2006	63%	81%	74%	88%
2007	50%	75%	69%	88%
2008	43%	71%	77%	86%
2009	38%	67%	77%	85%
2010	32%	60%	79%	86%

2.1.5 Small world

A peculiar feature of the network of board members is the existence of node communities by construction (the boards), forming complete subgraphs in which all the nodes (the board members) are connected to each other. These communities can be seen in figure 2.2, illustrating the largest connected component of the network of directors in 2010.

This feature may impact some specific statistical measures. For example, the existence of such communities produces trivially high average clustering coefficients. In addition, the degree of a board member will depend on the total number of seats on the boards in which he has a position. Hence, two directors in equally connected but differently sized boards have different degree centralities. In this sense, figure 2.3 shows the network composed only by the directors holding at least two positions. This resulting network keeps all important information with regard to information flow in the entire network, but removes the noise from disproportionality between board sizes.

From this point on, we refer only to the LCC of the network of companies, and to the LCC of the network formed by directors holding at least two board positions. Tables 2.10 and 2.11 present the density, radius, diameter, and average clustering coefficient for the network of companies and for the network of directors, respectively.

As it can be seen in tables 2.10 and 2.11, both networks present both relatively short radius and high clustering coefficient, suggesting they are small world networks. In

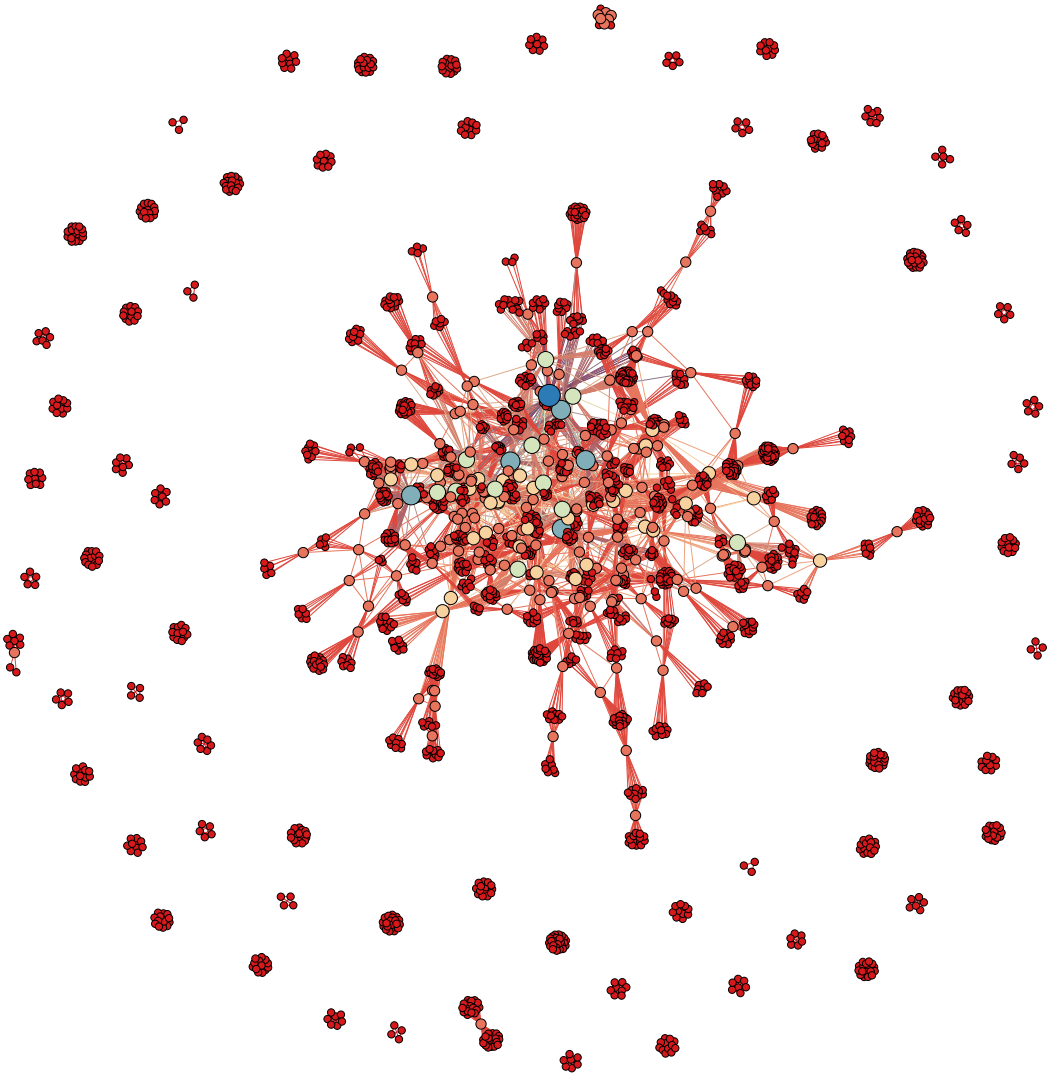

FIGURE 2.2: Network of all board members (2010). Nodes are colored and sized by number of board positions.

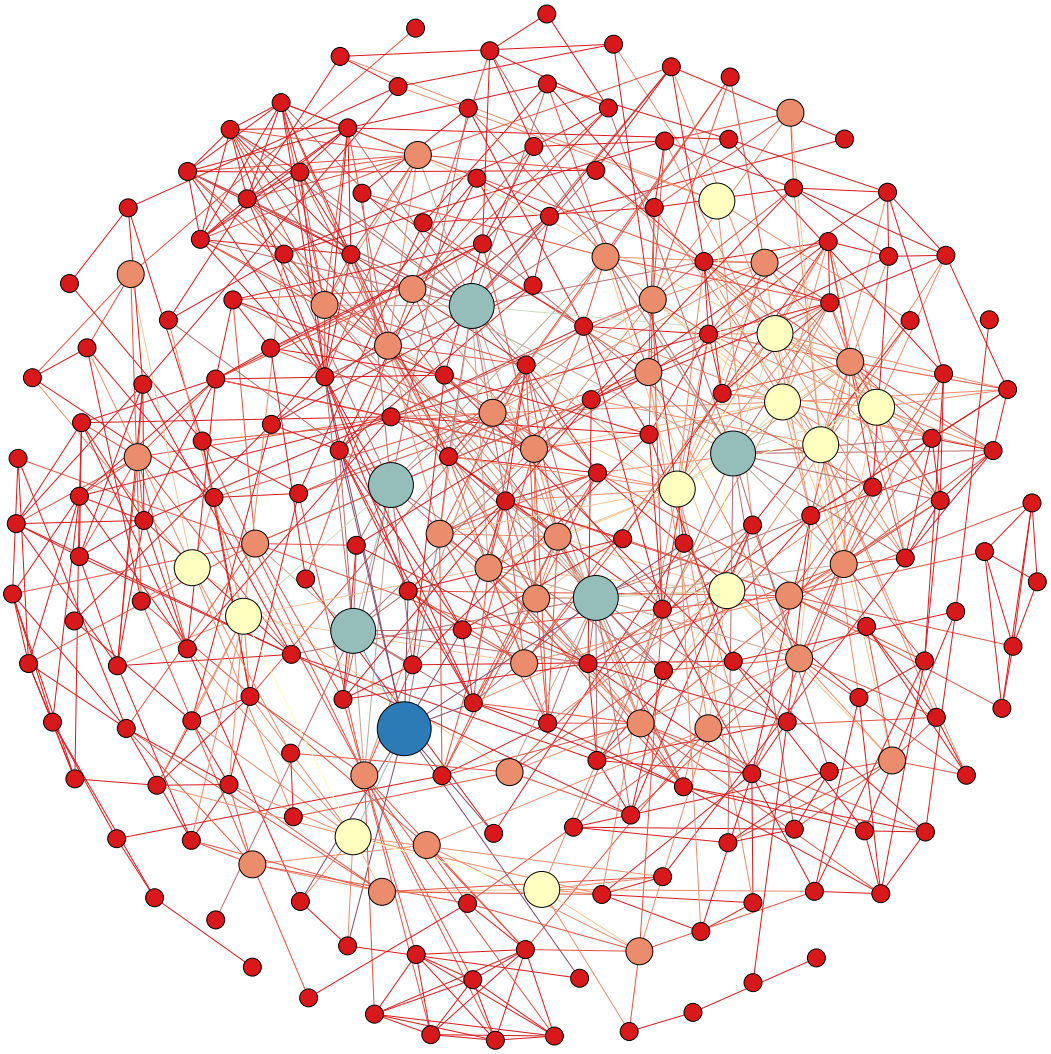

FIGURE 2.3: Network of board members holding at least two board positions (2010). Nodes are colored and sized by number of board positions.

TABLE 2.10: Network statistics for companies in the LCC.

Year	Density	Radius	Diameter	Avg. Clustering	Avg. Shortest Path Length
2004	0.54%	6	11	0.70	4.39
2005	0.55%	5	9	0.65	4.39
2006	0.48%	5	9	0.64	4.51
2007	0.50%	6	10	0.63	4.41
2008	0.48%	6	11	0.66	4.58
2009	0.47%	6	11	0.67	4.66
2010	0.47%	6	11	0.69	4.65

TABLE 2.11: Network statistics for directors in the LCC and holding more than one position.

Year	Density	Radius	Diameter	Avg. Clustering	Avg. Shortest Path Length
2004	3.29%	5	10	0.34	3.82
2005	3.36%	5	8	0.33	3.62
2006	3.24%	5	8	0.31	3.66
2007	3.17%	5	9	0.31	3.61
2008	3.28%	5	10	0.32	3.72
2009	3.31%	5	10	0.27	3.80
2010	3.17%	6	10	0.29	3.82

practice, this kind of network presents hubs (nodes with degrees much higher than the average) and communities (strongly interconnected sub graphs which are connected to each other through the hubs), which combined form the so-called small world phenomena.

2.1.6 Heavy-tailedness of the Degree Distribution

Although WS random rewiring models can reproduce the relative short average path lengths present in the Spanish interlocking network data, it cannot account for the heavy tails in the distribution of the degrees. Figure 2.4 shows the degree distribution for the network of directors in 2010. Visual inspection by itself suggests non normality, which is confirmed by the Anderson-Darling tests [55]. In addition, exponential and logistic distributions could also be ruled out at the 1% significance level. Table 2.12 presents the test statistics and its correspondent critical value at 1% for the exponential, normal, and logistic distributions.

TABLE 2.12: Anderson-Darling test statistic and its correspondent critical value at 1% for data coming from selected distributions. It can be seen that normal, exponential, and logistic distributions can be ruled out at 1% significance level

Distribution	Test statistic	Critical at 1%
Exponential	253.845	1.956
Normal	50.045	1.09
Logistic	23.232	0.906

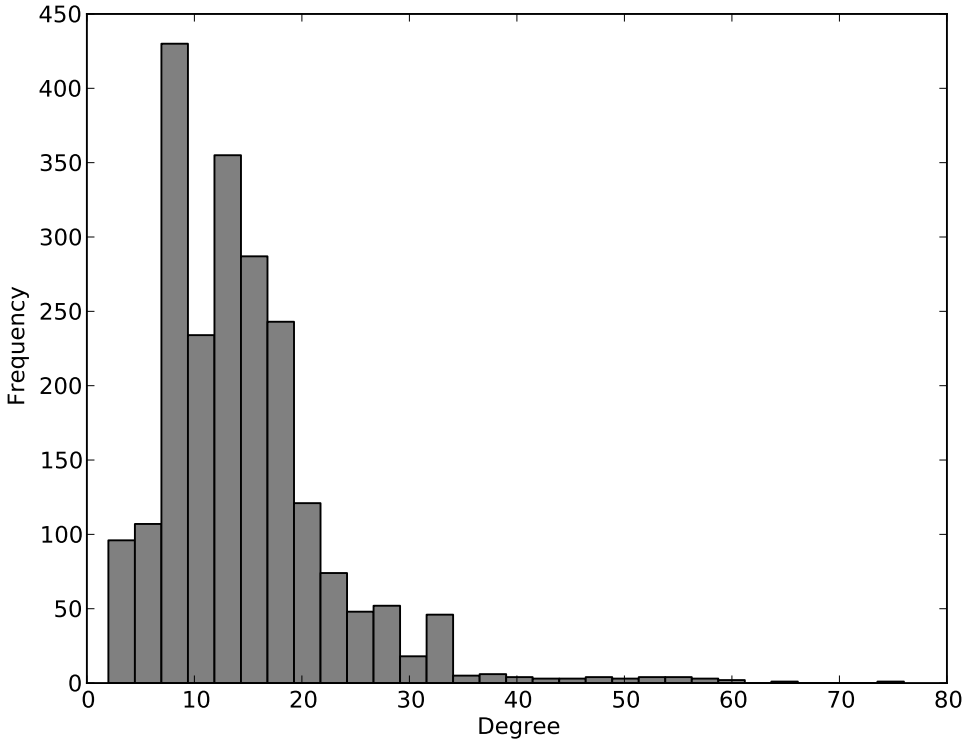

FIGURE 2.4: Degree distribution for the network formed by directors, 2010.

2.1.7 Network core

The *coreness* measure as defined in [46] was applied to this dataset. Ideally, one can think of a core as a set of nodes that are tightly connected to themselves, and a periphery as a set of nodes which are not connected to themselves, but connected to the core. This ideal network would have an adjacency matrix full of ones in the intra-core block, and full of zeros in the intra-periphery block. Then a statistic for the existence of a core is a measure of distance between the empirical adjacency matrix and this ideal perfect core-periphery structure.

The present section is thus concerned with the existence of significant cores in the

national networks formed by board members. In the terms presented by [46], here the discrete model of core periphery is investigated, that is, the problem of finding a single partition (thus dividing the nodes in two sub graphs) that maximizes the Pearson correlation coefficient between the partitioned empirical graph and the ideal core-periphery structure.

According to [47], in order to find such non empty subgraph (the optimal partition) it suffices to minimize the following statistic:

$$Z(S_1) = \sum_{(i \leq j) \in S_1} \Pi_{A_{ij}=0} + \sum_{(i \leq j) \notin S_1} \Pi_{A_{ij}=1} \tag{2.1}$$

where S is a graph $S = 1, ..., n$ with n nodes, S_1 is the subset of S ($S_1 \in S$) presumed to be the core of the graph, A is the binary adjacency matrix indicating whether two nodes are connected or not, and Π is an indicator function Π_P, which is equal to 1 if P is true, and equal to 0 otherwise. Note that the Z measures increases when it finds two nodes at the core which are not connected (first term of right hand side), and also when it finds two nodes of the periphery which are connected (second term of the left hand side).

This same author also shows that it is possible to minimize the Z statistic, and thus to find the optimal partition, in $O(n^2)$ time without relying on heavy and non exact optimization procedures, such as linear optimization and genetic algorithms. The algorithm proposed by [47] is able to outperform its alternatives to such a great extent because it is rooted in the finding that the members of the optimal core will necessarily be the nodes with the highest degrees (for a proof, see [47]). When one considers this fact, finding the core is just a matter of sorting nodes by degree, forming the possible cores by sequentially adding nodes with high degrees and computing the correspondent Z statistic. The procedure halts when the addition of a new node to the core increases the Z statistic.

Table 2.13 presents the fitness measure (defined as the Pearson correlation coefficient applied to matrices) to the ideal core/periphery model both for the networks of directors and of companies, as described in [46], and using the algorithm developed by [47]. It can be seen only small evidence of a core in both the networks (given by the close to

0 correlation coefficients), arguably because the networks are not composed by a single one-dimensionally layered core-periphery structure as it might be the case for other networks such as inter-banking lending networks [48].

TABLE 2.13: Fitness measure (defined as the Pearson correlation coefficient applied to matrices) to the ideal core/periphery model both for the networks of directors and of companies. It can be seen only small evidence of a core of the network of companies, arguably because the networks are not composed by a single one-dimensionally layered core-periphery structure as it might be the case for other networks such as inter-banking lending networks.

year	companies	directors
2004	0.1237	0.0357
2005	0.1196	0.0331
2006	0.1136	0.0318
2007	0.1144	0.0357
2008	0.1121	0.0361
2009	0.1015	0.0349
2010	0.0956	0.0349

2.1.8 Rich Club Phenomenon

The rich club phenomenon in networks can be described as, for a given degree k, the tendency of nodes with degree higher than k to be more densely connected themselves than to nodes with degree lower than k [10]. Table 2.14 presents the normalized version of the rich club coefficient described in [56] for the network formed by listed companies. The threshold 1 indicates that the probability of two nodes being connected does not depend on their degrees, while values above 1 are evidence of the existence of the rich club phenomenon.

Table 2.14 also shows an almost nonexistent (close to zero) degree assortativity [34], which is defined by the Person's correlation coefficient for degrees of nodes at either end of an edge, thus ruling out the possibility that the nodes with high degree are strongly connected to each other just because they have more connections. The close to 0 degree assortativity shows that there is no preference of nodes to attach to nodes of similar degree, while the above 1 normalized rich club coefficient shows nodes with high degrees are more connected to themselves than to nodes of smaller degree. Table 2.15 presents even higher values of the rich-club coefficient for the network of directors, and low values of degree assortativity, indicating the existence of a tightly inter-connected core of directors.

TABLE 2.14: Rich club coefficient for companies as a function of degree threshold.

Degree	2004	2005	2006	2007	2008	2009	2010
2	1.020	1.006	1.003	1.015	1.006	1.007	1.012
3	1.050	1.022	1.043	1.029	1.026	1.041	1.020
4	1.094	1.051	1.084	1.031	1.057	1.094	1.012
5	1.063	1.055	1.036	1.089	1.102	1.132	1.018
6	1.040	1.105	1.008	1.196	1.160	1.134	1.036
7	1.038	1.083	1.033	1.231	1.250	1.179	0.965
8	1.114	1.064	1.074	1.255	1.266	1.085	1.088
9	1.172	1.100	1.133	1.269	1.357	1.300	0.950
10	1.095	1.353	1.154	1.316	1.440	1.214	1.400
11	0.750	1.400	1.154	1.167	1.353	1.286	1.250
12	0.800	1.800	1.222	1.111	1.600	1.286	1.000
Assortativity	0.009	-0.030	0.023	0.015	0.014	-0.010	-0.001

TABLE 2.15: Rich club coefficient for directors as a function of degree threshold.

Degree	2004	2005	2006	2007	2008	2009	2010	
2	1.001	1.002	1.000	1.001	1.001	1.001	1.001	1.001
3	1.009	1.004	1.007	1.005	1.003	1.005	1.007	1.005
4	1.017	1.006	1.011	1.013	1.010	1.018	1.016	1.029
5	1.034	1.027	1.029	1.030	1.033	1.029	1.039	1.060
6	1.057	1.059	1.061	1.048	1.061	1.052	1.064	1.122
7	1.086	1.088	1.092	1.070	1.097	1.098	1.122	1.160
8	1.101	1.120	1.148	1.100	1.136	1.167	1.234	1.188
9	1.192	1.169	1.218	1.126	1.208	1.209	1.300	1.254
10	1.217	1.221	1.287	1.170	1.252	1.318	1.378	1.290
11	1.292	1.236	1.414	1.238	1.308	1.443	1.467	1.378
12	1.355	1.372	1.433	1.288	1.420	1.458	1.364	1.546
13	1.418	1.484	1.575	1.366	1.524	1.549	1.400	1.681
14	1.428	1.629	1.669	1.476	1.541	1.524	1.292	1.592
15	1.486	1.576	1.906	1.611	1.613	1.667	1.204	1.486
16	1.496	1.701	1.899	1.658	1.523	1.794	1.769	1.483
17	1.333	1.857	1.988	1.826	1.556	1.448	1.769	1.538
18	1.379	2.014	2.110	1.885	1.621	1.048	1.455	1.333
19	1.269	2.172	2.270	1.950	1.885	1.333	1.833	1.222
20	1.340	2.236	2.200	2.000	1.859	1.071	1.833	1.500
21	1.341	2.356	2.259	2.076	1.767	1.071	2.000	2.000
22	1.171	2.600	1.951	2.068	2.000	0.778	1.000	1.000
23	1.174	2.343	1.714	2.135	1.667	0.200	1.000	1.000
24	1.235	2.226	1.917	2.414	1.690	0.200	1.000	1.000
25	1.444	1.944	1.833	2.529	1.947	0.333	1.000	1.000
Assortativity	0.069	0.070	0.049	0.051	0.054	0.060	0.050	0.043

2.2 Most Important Players

2.2.1 Most Important Directors

Table 2.25 presents the list of the 30 most import directors (and the board they serve in), ordered according to eigenvector centrality for the year 2010.

2.2.2 Most Important Companies

Table 2.26 presents the list of the 30 most import companies (and their respective sectors), ordered according to eigenvector centrality for the year 2010.

2.2.3 Network of Sectors

This section considers sectors as the nodes of the network, instead of using companies or directors. Hence, a weighted graph can be created, considering edge weight as the number of board members two sectors share. Table 2.27 presents the number of companies, directors, and board positions by sector for the year of 2010. The last column, called *Intra connectivity*, presents the ratio between the number of positions in that sector and the number of unique directors. It can be seen a high level of interlocking among companies of the *"APARCAMIENTO Y AUTOPISTAS"* sector.

Assortativity is defined as the tendency of nodes to attach to other nodes with whom they share a specific attribute. As an example, degree assortativity is the tendency of nodes to attach to other nodes with similar levels of degree. In this way, sector assortativity is the tendency of nodes to attach to other nodes of the same sector. If sector assortativity is positive, it is more likely for a node to attach to another node from the same sector than from another sector. Table 2.28 shows some basic network measures. It is worthwhile to note the downward intra sector assortativity trend from 2004 to 2010, from positive to negative values, indicating that the practice of serving simultaneously on two boards of the same sector is being reduced over the period.

Figure 2.5 shows that financial institutions (comprised by the nodes labeled as *FINANCIACIÓN Y SEGUROS*) have a special place in the Spanish interlocking networks,

followed by the construction (*CONSTRUCIÓN*) and the real estate sectors (*INMOBILIARIAS*). The special role of financial institutions will be further addressed in forthcoming sections.

2.2.4 The Banking System

The argument of financial hegemony presented by [37] is based on the observation that banks play a central role in unifying the network of corporations linked through shared directors. The idea is that banks can benefit more from the *business scan* than other companies because they have money invested across the economy, and thus for them it is worth to recruit top level directors from non financial institutions [35].

Considering the Spanish case during the time period from 2004 to 2010, it can be seen not only that the boards of financial institutions are significantly larger when compared to non financial institutions. For instance, table 2.16 shows that banks present on average board sizes 40% to 50% larger than non financial institutions. This is in agreement with [35].

TABLE 2.16: Average board size for financial and non financial corporations

year	financial	non financial	difference
2004	13.250	9.407	40.85%
2005	13.513	9.500	42.24%
2006	14.000	9.694	44.42%
2007	14.397	9.836	46.37%
2008	14.763	9.917	48.87%
2009	14.986	9.919	51.08%
2010	15.354	9.925	54.70%

Assortativity is the general preference of nodes to attach to others that are similar with regard to some attribute [34]. The classic example is the degree assortativity, given by the Person correlation coefficient between the degrees of nodes at either end of the edges. As a correlation coefficient, it ranges from -1 (perfect dissortativity) to 1 (perfect assortativity). In the specific case, the network of sectors presents degree assortativity very close to zero, in the sense that on the average, companies are equally likely to attach to a second company independently of the number of connection this company has. Analogously, a positive (negative) sector assortativity means that it is more (less) likely to a company of a given sector to attach to another company of the same sector.

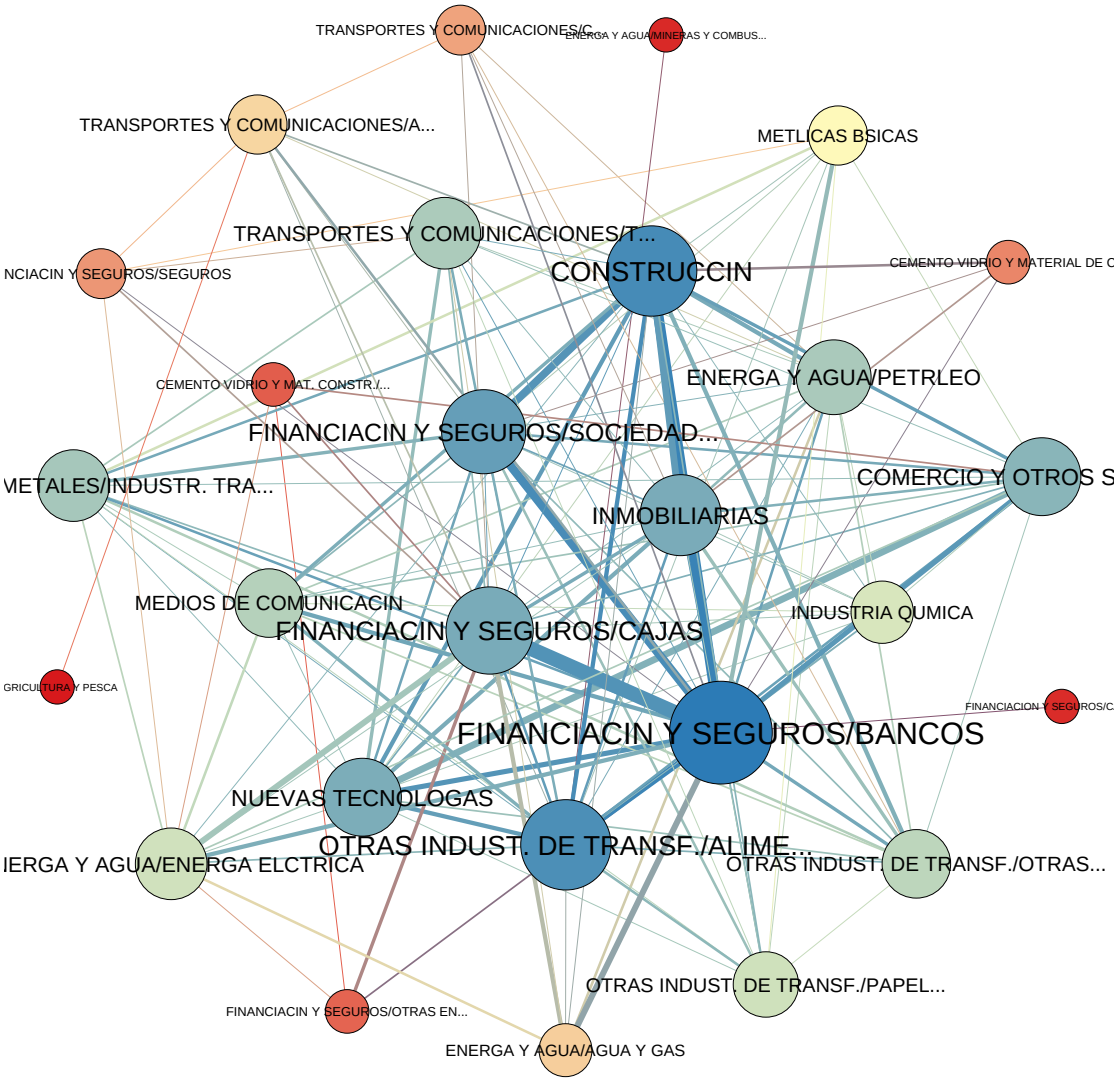

FIGURE 2.5: Weighted Network of Sectors, 2010. Nodes are colored by eigenvector centrality, and sized by degree. Edges are sized by the number of directors serving in both sectors.

Figure 2.6 shows the special role of banks in the network of directors, 2010. Although the banking system remains as the most important sector of the network, table 2.17 shows that there was a significant reduction in the number of intra-banking interlocks during the period. This can be seen by the significant change in the intra-sector assortativity for banks from 0.194 in 2004 to -0.123 in 2010.

TABLE 2.17: Participation of the Banking System - Companies.

Year	Other	Banks	Share	Bank-to-Bank Assortativity	Degree Assortativity
2004	218	20	9.17%	0.194	0.009
2005	215	21	9.77%	0.170	-0.030
2006	214	21	9.81%	0.198	0.023
2007	211	21	9.95%	0.132	0.015
2008	213	19	8.92%	-0.071	0.014
2009	201	18	8.96%	-0.108	-0.010
2010	192	19	9.90%	-0.123	-0.001

This finding is in agreement with vast literature (see [37] in general). Although the idea that banks in the twentieth century Spain formed a cartel through interlocking directorates was ruled out by [51], it is clear that financial institutions were very important actors in the networks. Particularly considering the case of Spain in 1993, [50] presents two findings which could be confirmed using updated data. The first is concerned with the special positions banks have on the network, and the second states that inter-sector interlocks are found more often than intra-sector interlocks.

2.3 Network position impact on firm level data

The purpose of this section is to contrast firm level data to the network related measures calculated from the dataset described in the previous subsection. It is inspired by the discussions in [53] presenting evidence of weak corporate governance associated with busy boards, and in [35] by comparing the distinct effects that interlocks to banks might have on different economies. Evidence presented here supports that (a) there seems to exist no relationship between network centrality and profitability, and (b) an inverse relationship between network centrality and leverage could be observed in Spain during the time period. In addition, the social network of directors is also investigated in the light of [17] to check whether the *busyness* level of the board of directors (and not the centrality

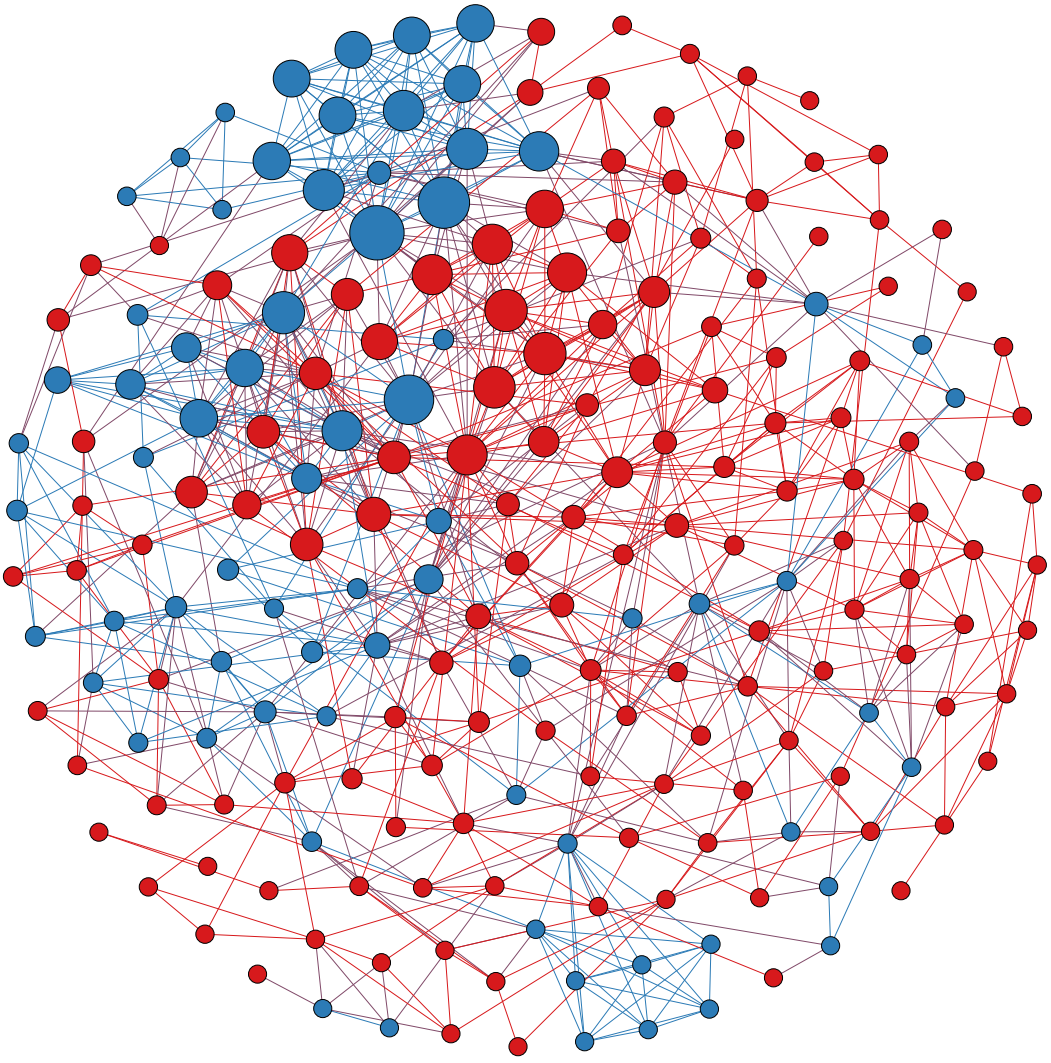

FIGURE 2.6: Nodes are sized by eigenvector centrality. Blue nodes denote directors holding at least one board position in a bank, 2010

of the whole board in the network of companies) might have effects on firm performance.

Specifically, here the *eigenvector* centrality is used as a measure of node importance in the network, both for directors and for companies. Traditionally, the *degree* and *betweenness* definitions of centrality are used in the literature. The former ranks the nodes according only to its number of direct connections, while the former does this according only the length of its shortest paths to other nodes. Eigenvector centrality is based on the idea that the rank of a node is also influenced by the rank of its connections, and thus that two connections may increase a given node centrality differently, depending on their own connection. With respect to the definition of the *busyness* level of a director, here it is considered the traditional definition using the number of positions as it also is the average centrality of the directors in a board as a measure of how *busy* it is [17].

In order to check for possible effects of network related measures on firm level data, here the same approach in [17] is used. Specifically, firm fixed-effects models were estimated using economic profitability or leverage as the dependent variable. Firm specific data considered here was collected from the SABI (*Iberian Balance sheet Analysis System*) database [54], and consists of a measure of economic profitability, defined as

$$economic\ \ profitability = \frac{net\ income}{total\ assets} \tag{2.2}$$

and a measure of leverage, which is considered in order to check whether the specific position of a firm in the network could possibly influence its financing profile, defined as:

$$leverage = \frac{equity}{total\ assets} * 100 \tag{2.3}$$

It is important to note that, since the interest is mainly focused on different financing profiles depending on a firm's network position, in the following only data from non financial institutions is considered. This is important in order to being able to analyze the relationship between interlocks and bank lending. Considering that the bank system is composed by several of the most central actors in the network, it is of interest here to check whether proximity to the most central actors (which is translated to centrality,

given the transitive nature of the eigenvector definition of centrality) improves or not some performance indicators.

Additionally to the original centrality variables, their rank-transformed versions were also tested. Since any measure of centrality calculated from graph theory is by definition determined by the combination of all other nodes in the networks and their own connections, their absolute values are of no practical meaning (a given level of centrality is said to be *high* only in comparison to some other *low* level). Moreover, this procedure corrects for the fat tail presented in the distribution of centrality scores. Figures 2.9 to 2.16 present scatter plots and histograms for selected pairs of variables.

As suggested by visual inspection, an inverse relation between leverage and network centrality rank could be observed, in agreement to previous findings for [53], suggesting that board linkages might have generated some kind of special conditions for lending that would not exist if based on economic criteria only. No significant relation between economic performance and centrality could be observed, regardless of being measured according to [17] or not. The next two subsections provide more details on both topics.

2.3.1 Relationship between centrality and performance

There is an extense and open debate about the possible impact of network centrality on firm level performance indicators (for a comprehensive survey, see [9]). In addition to a measure of economic profitability, here the leverage conditions of the companies were also target of investigation. Inspired by the finding presented in [36] of a negative impact of bank connections on performance measures, here it is hypothesized that bank interlocks could have guaranteed via personal connections special financial conditions which would not occur under normal circumstances. Finally, this would have reflected on the leverage conditions of the most central non financial companies.

Although a board linkage may provide the benefit of better information flows between a borrower and lender, a person on the board of both a bank and a borrowing firm may face a conflict of interest: the person has a fiduciary duty to both the bank and the firm and these interests may diverge [35]. A practical concern is that such connections could lead banks to treat connected firms specially, and, therefore, might expose depositors

and eventually taxpayers to non justifiable losses. In this sense, [35] presents a trade-off resulting from board linkages to financial institutions by investigating whether connections affect lending and borrowing behavior. From the positive side, board linkages may reduce the costs of information both for lenders and borrowers. According to [57], firms in Japan connected to their bank were insulated from cash flow shocks that could distort investment choices. Such advantages of interlocking to banks are also presented in [35], considering US companies in 1992.

Considering the negative side of the trade-off, bank interlocks may generate pressure for special treatment of a borrower not normally justifiable on economic terms. In this direction, other studies suggest that such kinds of conflicts of interests with respect to lending are important reasons for the fragility of financial systems. For example, [58] argue that the Asian crisis of 1997 was in great extent due to lenders continuing to provide credit to not well performing connected borrowers. Similar findings are also reported in [35] for Russia and Mexico. These are examples of cases where the connections have been misused.

In order to investigate whether centrality had impact on performance variables for the specific case of Spain, here the approach presented in [17] was followed by estimating firm fixed-effects models using performance as the explained variable. Table 2.29 supports the use of year dummies, while 2.30 suggests a better fit is achieved using rank-transformation of centrality. By considering the rank-transformed models (2) and (4) of table 2.30, it can be seen that a significant inverse relation between centrality and leverage can be found. A coefficient of -0.003 relating the rank-transformed centrality and leverage is to be interpreted as: each step a company goes to the top of the most central companies reduces its leverage by 0.3%. This finding adds evidence to the list of situations where interlocks might have been misused presented by [35].

2.3.2 Investigation on the value of busy directors

In a related study, [59] use methods of social network analysis to investigate whether directors' social networks provide valuable resources to their firms, find them to be rewarded for their connectedness, and their connectedness to be positively related to future firm performance.

In a slightly more specific context, [17] are interested in whether the presence of *busy* directors is correlated with poor performance indicators, due to the lack of time and/or focus from these directors in working for the boards they sit on. While a great deal of the literature finds no relation between busyness and performance [53], [17] suggest that a negative relation emerges when one uses a proper definition of *busy*. Traditionally, the *busyness* of a director has been measured as the number of positions he/she holds. This is arguably to misrepresent the true value of *busyness* of a director because the time-consuming activities can vary wildly from one board to another. As an alternative to the traditional *busyness* definition, they suggest that the *busyness* of a director should be measured by the degree of embeddedness of this director in the network, and they define embeddedness as the director's eigenvector centrality in the network of directors. Finally, the average level of director-busyness of a company can be assessed by the average eigenvector centrality of its directors.

The same methodology was applied here to find no evidence of impact of the number of positions and measures of economic performance, as shown in the first two columns of table 2.31. This finding indicates that the number of board appointments a director holds does not seem to influence profitability in Spain, according to previous findings for Germany [17]. However, an inverse relation between leverage of a company and the average eigenvector centrality of its directors can be observed, exactly as described in the last subsection when considering the eigenvector of the company itself. Results shown in table 2.32. This is in agreement with [17], who argues that the raw number of positions is not as powerful as social networks methods to find out patterns in interlocking boards networks.

2.4 Ibex, gender differences, and politicians

This section collects some other findings related to the centrality level of individual directors. More specifically, it begins by presenting in the first subsection the reach of the highly capitalized Ibex companies in the network. It can be seen that the number of directors holding at least one position in an Ibex company represent more than half of the total directors holding more than one position.

Then, inspired by the *Ley de Igualdad* established in 2007, the second subsection deals with gender equality by investigating both quantitatively and qualitatively women participation in the boards of management. Although a reduction in inequality could be seen since the new regulation, women keep being under represented both in absolute terms and with respect to centrality measures.

Finally, the third subsection defines a politician as a director who is presented at any of the previous years national congressmen. Then, it is argued that politicians are much more engaged in multiple board positions than non politicians, but also that this effect disappears when only directors holding at least two board positions are considered.

2.4.1 Ibex boards

Table 2.18 presents the share of directors serving on at least one Ibex company both for the network of all directors and for the network composed only by those holding two or more board positions (D_2). It can be seen that 54.1% of the directors holding two or more board positions serve on the board of an Ibex company. If this figure is compared to the total share of positions in Ibex boards of only 16.3%, there is clear evidence that the practice of multiple board memberships is largely centered on the most highly capitalized companies of the Spanish economy forming the Ibex. Such results are in agreement with the literature [60].

This observation highlighted above can also be demonstrated by means of a simple Z-test of difference in proportions. In 2010, considering that there are 433 directors serving in at least one Ibex company, and that 126 of them hold two or more board positions, it is observed that around 30% of the directors serving in at least an Ibex company hold two or more board positions. On the other hand, there are 1721 directors who do not serve in any Ibex boards, and only 86 of them hold two or more board positions, yielding a ratio of around 5%. The two-tailed Z-score for the test of difference in proportions is around 15, which results in a statistically significant difference at 1% significance level, with respect to the different patterns of board positions accumulations by directors holding or not at least one position in an Ibex company.

Figure 2.7 depicts this fact by coloring directors according to the participation in Ibex boards. In addition, figure 2.8 presents the comparison of the probabilities associated with the accumulation of a given number of board positions, both for directors serving in at least one Ibex company (solid blue) and for directors not serving the board of any Ibex company (dashed red).

TABLE 2.18: Share of directors serving on at least one Ibex company both for the network of all directors and for the network composed only by those holding two or more board positions (D_2). It can be seen that 54.1% of the directors holding two or more board positions serve on the board of an Ibex company. If this figure is compared to the total share of positions in Ibex boards of only 16.3%, there is clear evidence that the practice of multiple board memberships is largely centered on the most highly capitalized companies of the Spanish economy forming the Ibex.

Year	Other (all)	Ibex (all)	Share (all)	Other (2 bp)	Ibex (2 bp)	Share (2 bp)
2004	1823	356	16.34%	112	132	54.10%
2005	1797	393	17.95%	109	147	57.42%
2006	1849	406	18.00%	105	149	58.66%
2007	1884	361	16.08%	104	147	58.57%
2008	1891	424	18.32%	104	138	57.02%
2009	1805	419	18.84%	93	126	57.53%
2010	1721	433	20.10%	86	126	59.43%

2.4.2 Gender Differences

This section investigates differences in gender participation on company boards, specially in the light of the new regulation established in 2007 to promote gender equality. The Article 75 of the Constitutional Act 3/2007 of 22 March for effective equality between women and men (*"Ley Orgánica 3/2007, de 22 de marzo, para la igualdad efectiva de mujeres y hombres"*) it is stated that companies were obliged to include in their boards a number of women which allows for a balanced presence of men and women (*"incluir en su Consejo de Administración un número de mujeres que permita alcanzar una presencia equilibrada de mujeres y hombres"*).

It was found that, although there still nothing like a balanced presence, women participation increased during the time period, with a special help from a step in 2008. Moreover, it was also found that a great deal of this improvement in gender equality was achieved by the highly capitalized Ibex companies. It could also be seen a significant increase in average centrality when comparing the periods before and after the Act, despite the absolute increase in the number of women in the boards. These findings

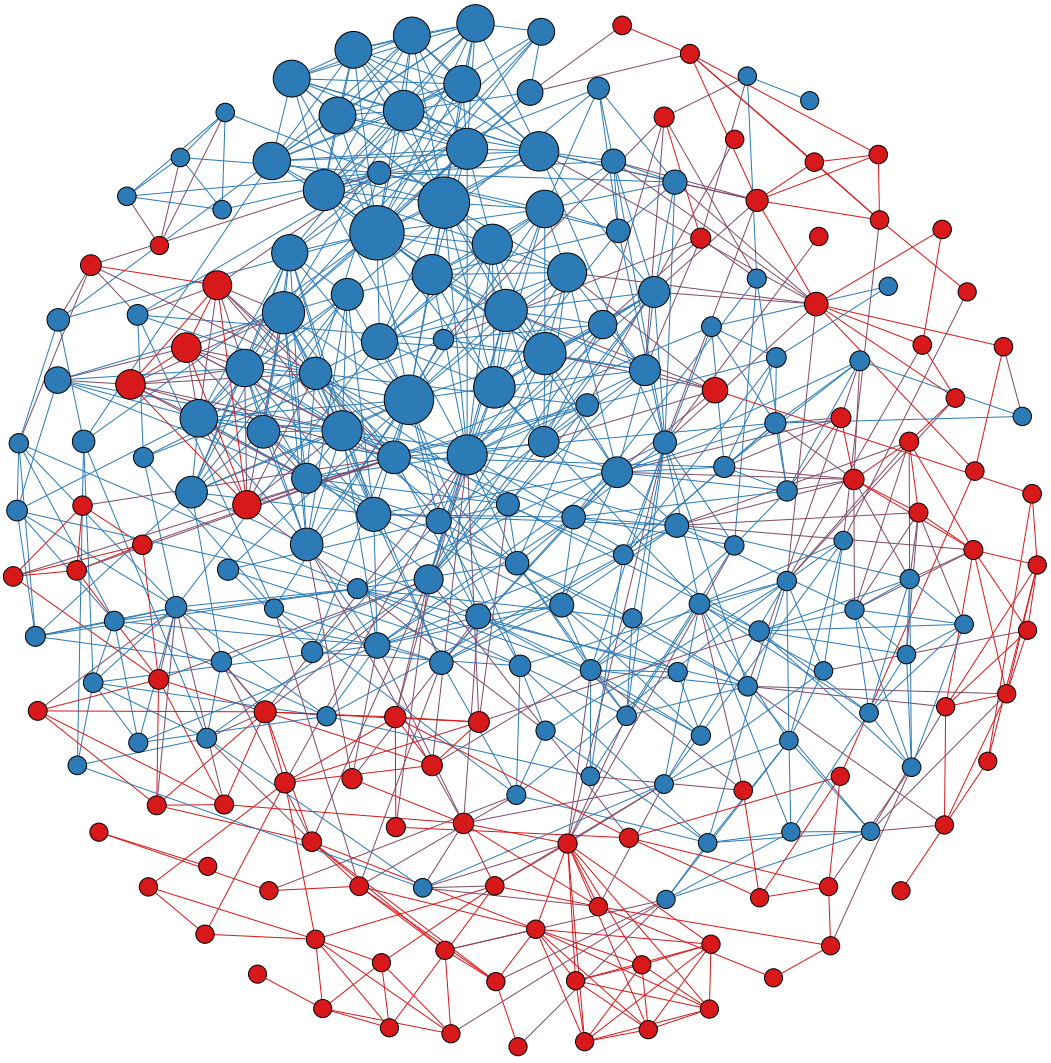

FIGURE 2.7: Nodes are sized by eigenvector centrality. Blue nodes indicate directors holding at least one board position in an Ibex company, 2010

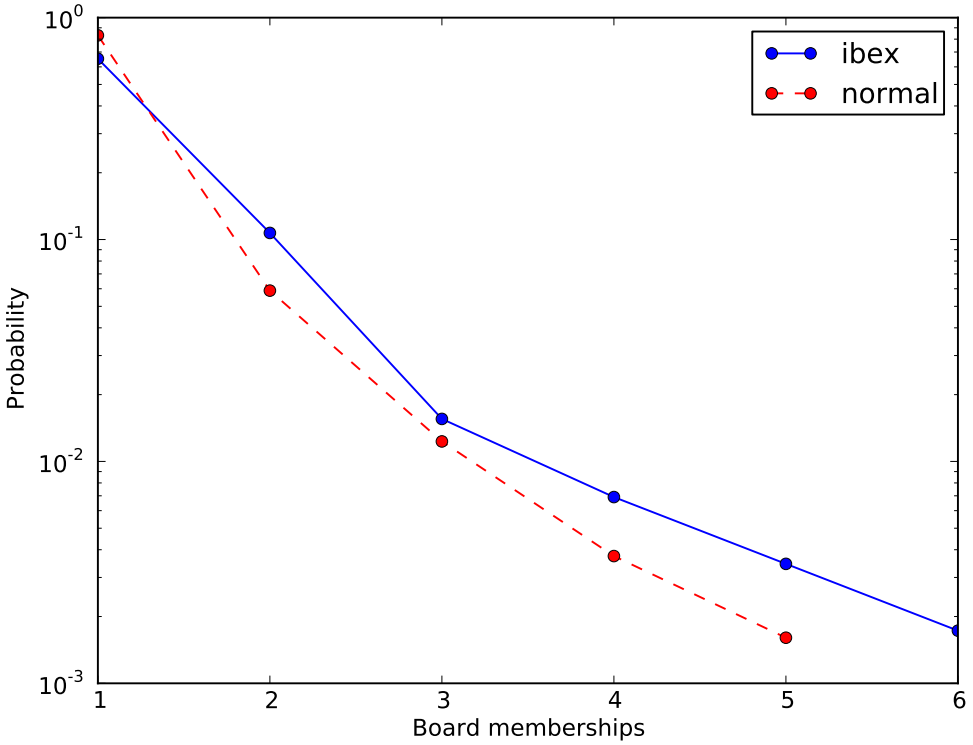

FIGURE 2.8: Comparison of the probabilities associated with the accumulation of a given number of board positions in 2010, both for directors serving in at least one Ibex company (solid blue) and for directors not serving the board of any Ibex company (dashed red).

suggest a positive effect of the Act with regard to its purposes. On the other hand, it is still clear that women are under represented in the networks (if one assumes a *balanced presence* to mean equal proportions), and that they have average centralities still significantly smaller than men.

TABLE 2.19: Consistent increasing participation of women in the network, from 8.7% of the directors in 2004 to 12.3% in 2010. However, table shows that it is still more unlikely to find women than men in the Ibex boards, fact shown by the negative (although increasing) log odd likelihood ratio between women serving in Ibex companies and serving in companies in general.

Year	Men	Women	Women Share
2004	2312	221	8.7%
2005	2343	228	8.9%
2006	2347	268	10.2%
2007	2340	275	10.5%
2008	2366	303	11.4%
2009	2225	310	12.2%
2010	2147	301	12.3%

Table 2.19 clearly shows a consistent increasing participation of women in the network, from 8.7% of the directors in 2004 to 12.3% in 2010. However, table 2.20 shows that it is still more unlikely to find women than men in the Ibex boards, fact shown by the negative (although increasing) log odd likelihood ratio between women serving in Ibex companies and serving in companies in general. Both tables support the idea that the participation of women in company boards increased during the entire period. As shown in table 2.20, there is a step in women participation in Ibex companies from 5.6% in 2007 (the last year before the Act) to 10.7% in 2010 (three years after the Act).

TABLE 2.20: Women participation increased during the time period, with a special help from a step in 2008. Moreover, it was also found that a great deal of this improvement in gender equality was achieved by the highly capitalized Ibex companies. It could also be seen a significant increase in average centrality when comparing the periods before and after the Act, despite the absolute increase in the number of women in the boards.

Year	p(W | I)	p(W)	p(I | W)	p(I)	Log odd ratio
2004	3.94%	8.72%	7.24%	16.03%	-0.345
2005	3.60%	8.87%	7.02%	17.27%	-0.391
2006	5.18%	10.25%	8.96%	17.71%	-0.296
2007	5.66%	10.52%	8.73%	16.21%	-0.269
2008	8.40%	11.35%	13.53%	18.28%	-0.131
2009	10.34%	12.23%	15.81%	18.70%	-0.073
2010	10.70%	12.30%	17.28%	19.85%	-0.060

In order to analyze structural changes brought by the Act, the sample was divided in two periods, namely before the Act (from 2004 to 2007) and after the Act (from 2008 to 2010). Table 2.21 shows that the relative average centrality of women with respect to men (that is, average centrality of women divided by average centrality of men) has increased. To support the structural change effect, table 2.21 also presents the test statistics and the p-value for the Mann-Whitney test comparing the distribution of centrality values between men and women. It is worthwhile to note that in the period before the Act, the null hypothesis that both samples came from the same distribution (with same parameters) can be rejected with 5% of significance, while this is no longer true for the period after the Act.

TABLE 2.21: In the period before the Act, the null hypothesis that both samples came from the same distribution (with same parameters) can be rejected with 5% of significance, while this is no longer true for the period after the Act.

year	rel. avg. centrality M/W	U	p-value
before Act	0.445	18090	0.023
after Act	0.531	13706	0.158

With respect to the patterns of accumulation of multiple board positions, gender inequalities are also found. Considering the year of 2010, there are 221 out of 2154 directors holding at least two board positions, yielding a ratio of 10.26%. If one looks only for male directors, there are 204 out of 2154 directors holding at least two board positions, yielding a ratio of 10.88%. For women, the ratio is significatively lower (Z-score of 1.8472 for a test of proportions, yielding a p-value of 0.032), only 6.09% because only 17 out of 279 female directors hold at least two board positions.

2.4.3 Political affiliation

It was possible to identify politicians among the directors by matching their names with the list provided by the Spanish National Congress available at `http://www.congresso.es`. More specifically, at the home page of the website there is a section called *Diputados*, which provides a link (*Listado completo de la composición de la Cámara*) to the full list of Congress members from 1977 to 2011. Directors are then considered *Politicians* if they were listed at least once in this full list of congress members, regardless of the year they served the Congress.

Table 2.22: Politician participation.

Year	Not Politician	Politician	Politician Share
2004	2481	52	2.1%
2005	2516	55	2.1%
2006	2558	57	2.2%
2007	2555	60	2.3%
2008	2603	66	2.5%
2009	2482	53	2.1%
2010	2385	63	2.6%

Table 2.22 presents the number of politicians which could be identified among the directors, and their respective participation share in the network. Table 2.23 presents decreasing (though positive) log likelihood ratios between the chances of finding a politician in he boards of Ibex companies and in all boards, indicating that the participation of politicians is more concentrated in the most capitalized companies.

In the exact opposite way of the findings regarding women participation from the previous subsection, if all directors are considered (and not only those in D_2 holding at least two board positions), there is clear evidence that directors who had served at least once in the national congress are characterized by a 50% higher centrality than directors who

TABLE 2.23: Politicians participation in Ibex companies.

Year	p(P | I)	p(P)	p(I | P)	p(I)	Log odd ratio
2004	3.45%	2.05%	26.92%	16.03%	0.225
2005	4.28%	2.14%	34.55%	17.27%	0.301
2006	3.89%	2.18%	31.58%	17.71%	0.251
2007	3.07%	2.29%	21.67%	16.21%	0.126
2008	3.48%	2.47%	25.76%	18.28%	0.149
2009	2.74%	2.09%	24.53%	18.70%	0.118
2010	3.50%	2.57%	26.98%	19.85%	0.133

had never. However, when only those directors in D_2 are considered, the centralities of politicians and non politicians can no longer be told apart. Relative average centralities and the results of Mann-Whitney test comparing the distribution of centrality between politicians and non politicians are presented in table 2.24. These results suggest that being a current or former congressman definitely helps directors to move from one to two positions only, but has no effects on the accumulation of further positions.

TABLE 2.24: Relative average centralities and the results of Mann-Whitney test comparing the distribution of centrality between politicians and non politicians. This results suggest that being a current or former congressman definitely help directors to move from one to two positions only, but has no effects on the accumulation of further positions.

	rel. avg. centrality P/N	U	p-value
all directors	1.553	2367366	0.000
directors in D_2	0.942	37480	0.796

With respect to the patterns of accumulation of multiple board positions, it can be seen that being a politician increases the chances of assuming two or more board positions, opposite to the results concerning gender differences. Considering the year of 2010, there are 221 out of 2154 directors holding at least two board positions, yielding a ratio of 10.26%. If one looks only for directors who had been a politician at least once in the past, there are 8 out of 53 directors holding at least two board positions, yielding a ratio of 15.09%. This is substantially higher than for women (only 6.09%), indicating that politicians are more likely to assume two or more board positions than women.

Conclusion

In the first section of this chapter it was shown that all stylized facts described in the first chapter (such as small worldness, the existence of a large connected component, and

rich club phenomena) still hold in the Spanish specific case, considering a wider time spam from 2004 to 2010. It was also shown that the core persists in time regardless of personal turnover, and that the accumulation patterns of board positions by individuals observed in empirical data cannot be explained by a simple random binomial procedure.

By using firm specific data on profitability and leverage, the third section highlights that no significant relation between network centrality and profitability could be observed, and that a negative significant relation existed between centrality and leverage, indicating that interlocks might have been misused to guarantee special lending conditions not justifiable only by economic circumstances, and that a high lending ratio required adjustment in the corporate governance structure.

The fourth section depicted the highly capitalized Ibex companies as prominent actors of the network, the effective but not sufficient impact of a new gender equality regulation, and finally the advantage politicians have to jump from one to two board positions.

Appendix B. Interlocking Directorates in Spain: Evidence from a Comprehensive Data Set

Table 2.25: Most important directors (according to 2010 figures)

Name	Companies
DON ISIDRO FAIN CASAS	CAIXABANK, S.A.
	ABERTIS INFRAESTRUCTURAS, S.A.
	TELEFONICA, S.A.
	CAJA DE AHORROS Y PENSIONES DE BARCELONA
	REPSOL, S.A
DON JUAN MARA NIN GNOVA	CAIXABANK, S.A.
	GAS NATURAL SDG, S.A.
	REPSOL, S.A
DON JAVIER ECHENIQUE LANDIRIBAR	ENCE ENERGIA Y CELULOSA, S.A.
	REPSOL, S.A
	BANCO DE SABADELL, S.A.
	ACS, ACTIVIDADES DE CONSTRUCCION Y SERVICIOS, S.A.
DON LUIS FERNANDO DEL RIVERO ASENSIO	SACYR VALLEHERMOSO, S.A.
	TESTA INMUEBLES EN RENTA, S.A.
	REPSOL, S.A
DON JOSE MANUEL LOUREDA MANTIN	SACYR VALLEHERMOSO, S.A.
	TESTA INMUEBLES EN RENTA, S.A.
	REPSOL, S.A
DON PABLO VALLBONA VADELL	ABERTIS INFRAESTRUCTURAS, S.A.
	ACS, ACTIVIDADES DE CONSTRUCCION Y SERVICIOS, S.A.
	BANCA MARCH, S.A.
	CORPORACION FINANCIERA ALBA, S.A.
JUAN ABELLO GALLO	SACYR VALLEHERMOSO, S.A.
	COMPANIA VINICOLA DEL NORTE DE ESPANA, S.A.
	REPSOL, S.A

Continued on next page

Table 2.25 – *Continued from previous page*

Name	Companies
DON JUAN ROSELL LASTORTRAS	CAIXABANK, S.A.
	GAS NATURAL SDG, S.A.
DON SALVADOR GABARR SERRA	CAIXABANK, S.A.
	CAJA DE AHORROS Y PENSIONES DE BARCELONA
	GAS NATURAL SDG, S.A.
DON LEOPOLDO RODS CASTA	ABERTIS INFRAESTRUCTURAS, S.A.
	CAJA DE AHORROS Y PENSIONES DE BARCELONA
	CAIXABANK, S.A.
DON LUIS SUAREZ DE LEZO MANTILLA	GAS NATURAL SDG, S.A.
	REPSOL, S.A
DON ANTONIO BRUFAU NIUBO	GAS NATURAL SDG, S.A.
	REPSOL, S.A
DON JUAN MARCH DE LA LASTRA	ACS, ACTIVIDADES DE CONSTRUCCION Y SERVICIOS, S.A.
	BANCA MARCH, S.A.
	INDRA SISTEMAS, S.A.
	CORPORACION FINANCIERA ALBA, S.A.
DON DEMETRIO CARCELLER ARCE	COMPANIA LOGISTICA DE HIDROCARBUROS CLH, S.A.
	EBRO FOODS, S.A.
	SOCIEDAD ANONIMA DAMM
	SACYR VALLEHERMOSO, S.A.
	GAS NATURAL SDG, S.A.
DON ALAIN MINC	CAIXABANK, S.A.
	PROMOTORA DE INFORMACIONES, S.A.
DON LUIS CARLOS CROISSIER BATISTA	TESTA INMUEBLES EN RENTA, S.A.
	ADOLFO DOMINGUEZ, S.A.
	REPSOL, S.A
DON SANTOS MARTINEZ CONDE GUTIERREZ BARQUIN	ACERINOX, S.A.

Continued on next page

Table 2.25 – *Continued from previous page*

Name	Companies
	ACS, ACTIVIDADES DE CONSTRUCCION Y SERVICIOS, S.A.
	BANCA MARCH, S.A.
	CORPORACION FINANCIERA ALBA, S.A.
DON ANGEL DURANDEZ ADEVA	MEDIASET ESPANA COMUNICACION, S.A.
	REPSOL, S.A
DON GONZALO GORTZAR ROTAECHE	CAIXABANK, S.A.
	VIDACAIXA, S.A. DE SEGUROS Y REASEGUROS
DON DAVID K. P. LI	CAIXABANK, S.A.
	TELEFONICA, S.A.
DON FRANCISCO SERVANDO VERDU PONS	ACS, ACTIVIDADES DE CONSTRUCCION Y SERVICIOS, S.A.
	BANCA MARCH, S.A.
	CORPORACION FINANCIERA ALBA, S.A.
DON JORGE MERCADER MIR	CAIXABANK, S.A.
	MIQUEL Y COSTAS & MIQUEL, S.A.
DON MIQUEL NOGUER PLANAS	CAIXABANK, S.A.
	CAJA DE AHORROS Y PENSIONES DE BARCELONA
DOA MARIA DOLORS LLOBET MARIA	CAIXABANK, S.A.
	CAJA DE AHORROS Y PENSIONES DE BARCELONA
DON JAVIER GOD MUNTAOLA	CAIXABANK, S.A.
	CAJA DE AHORROS Y PENSIONES DE BARCELONA
DOA IMMACULADA JUAN FRANCH	CAIXABANK, S.A.
	CAJA DE AHORROS Y PENSIONES DE BARCELONA
DON FLORENTINO PREZ RODRGUEZ	ABERTIS INFRAESTRUCTURAS, S.A.
	ACS, ACTIVIDADES DE CONSTRUCCION Y SERVICIOS, S.A.
DON CARMELO DE LAS MORENAS LOPEZ	FAES FARMA, S.A.
	REPSOL, S.A

Continued on next page

Table 2.25 – *Continued from previous page*

Name	Companies
DON JAVIER MONZON DE CACERES	ACS, ACTIVIDADES DE CONSTRUCCION Y SERVICIOS, S.A.
	INDRA SISTEMAS, S.A.
DON PEDRO JOSE LOPEZ JIMENEZ	ENCE ENERGIA Y CELULOSA, S.A.
	ACS, ACTIVIDADES DE CONSTRUCCION Y SERVICIOS, S.A.

TABLE 2.26: Most important companies (according to 2010 figures)

Company	Sector
REPSOL, S.A	ENERGA Y AGUA/PETRLEO
ACS, ACTIVIDADES DE CONSTRUCCION Y SERVICIOS, S.A.	CONSTRUCCIN
SACYR VALLEHERMOSO, S.A.	CONSTRUCCIN
CORPORACION FINANCIERA ALBA, S.A.	FINANCIACIN Y SEGUROS/SOCIEDADES DE CARTERA
PROMOTORA DE INFORMACIONES, S.A.	MEDIOS DE COMUNICACIN
EBRO FOODS, S.A.	OTRAS INDUST. DE TRANSF./ALIMENT. BEBIDAS Y TABACO
ENCE ENERGIA Y CELULOSA, S.A.	OTRAS INDUST. DE TRANSF./PAPEL Y ARTES GRFICAS
ABERTIS INFRAESTRUCTURAS, S.A.	TRANSPORTES Y COMUNICACIONES/APARCAMIENTO Y AUTOP.
INDRA SISTEMAS, S.A.	NUEVAS TECNOLOGAS
GAS NATURAL SDG, S.A.	ENERGA Y AGUA/AGUA Y GAS
FERROVIAL, S.A.	CONSTRUCCIN
COMPAIA LOGISTICA DE HIDROCARBUROS CLH, S.A.	TRANSPORTES Y COMUNICACIONES/TRANSPORTES
CAIXABANK, S.A.	FINANCIACIN Y SEGUROS/BANCOS
BANCA MARCH, S.A.	FINANCIACIN Y SEGUROS/BANCOS
GAMESA CORPORACION TECNOLOGICA, S.A.	OTRAS INDUST. DE TRANSF./OTRAS INDUST. MANUFACTUR.
DINAMIA CAPITAL PRIVADO, S.A., SCR	FINANCIACIN Y SEGUROS/SOCIEDADES DE CARTERA
BANCO DE SABADELL, S.A.	FINANCIACIN Y SEGUROS/BANCOS

Continued on next page

Table 2.26 – *Continued from previous page*

Company	Sector
CARTERA INDUSTRIAL REA, S.A.	FINANCIACIN Y SEGUROS/SOCIEDADES DE CARTERA
TESTA INMUEBLES EN RENTA, S.A.	INMOBILIARIAS
ADOLFO DOMINGUEZ, S.A.	OTRAS INDUST. DE TRANSF./OTRAS INDUST. MANUFACTUR.
COMPAIA VINICOLA DEL NORTE DE ESPAA, S.A.	OTRAS INDUST. DE TRANSF./ALIMENT. BEBIDAS Y TABACO
CAJA DE AHORROS Y PENSIONES DE BARCELONA	FINANCIACIN Y SEGUROS/CAJAS
VOCENTO, S.A.	MEDIOS DE COMUNICACIN
BANCO GALLEGO, S.A.	FINANCIACIN Y SEGUROS/BANCOS
TELEFONICA, S.A.	TRANSPORTES Y COMUNICACIONES/COMUNICACIONES
BANCO DE VALENCIA, S.A.	FINANCIACIN Y SEGUROS/BANCOS
MEDIASET ESPAA COMUNICACION, S.A.	MEDIOS DE COMUNICACIN
SOCIEDAD ANONIMA DAMM	OTRAS INDUST. DE TRANSF./ALIMENT. BEBIDAS Y TABACO
IBERIA LINEAS AEREAS DE ESPAA, S.A.	TRANSPORTES Y COMUNICACIONES/TRANSPORTES
PESCANOVA, S.A.	OTRAS INDUST. DE TRANSF./ALIMENT. BEBIDAS Y TABACO

TABLE 2.27: Numer of positions, companies, and directors by sector, 2010. The last column shows the sector intraconnectivity, which is defined as the number of intra sector connections divided by the total number of connections.

Sector	Positions	Companies	Avg Board Size	Directors	Intra connectivity
SEGUROS/CAJAS	602	32	18.81	602	0.0000
SEGUROS/BANCOS	252	19	13.26	249	0.0120
INMOBILIARIAS	185	25	7.40	184	0.0054
COMERCIO/SERVICIOS	151	15	10.07	150	0.0067
TRANSF./MANUFACTUR.	113	14	8.07	113	0.0000
NUEVAS TECNOLOGÍAS	113	11	10.27	113	0.0000
CONSTRUCCIÓN	106	8	13.25	106	0.0000
ALIMENT. BEB./TABACO	101	11	9.18	98	0.0306
TRANSF.DE METALES	95	10	9.50	94	0.0106
ENERGÍA ELÉCTRICA	76	7	10.86	75	0.0133
SEGUROS/CARTERA	74	9	8.22	74	0.0000
SEGUROS/CAJAS RURALES	59	4	14.75	59	0.0000
MEDIOS DE COMUNIC.	57	4	14.25	55	0.0364
PAPEL Y ARTES GRÁFICAS	51	5	10.20	51	0.0000
METÁLICAS BÁSICAS	50	4	12.50	50	0.0000
APARCAMIENTO Y AUTOP.	46	5	9.20	39	0.1795
TRANSPORTES	45	3	15.00	44	0.0227
ENERGÍA ELÉCTRICA	45	3	15.00	45	0.0000
SEGUROS/SEGUROS	43	3	14.33	43	0.0000
INDUSTRIA QUÍMICA	32	4	8.00	32	0.0000
PETRÓLEO	29	2	14.50	29	0.0000
SEGUROS/OTRAS	28	2	14.00	28	0.0000
VIDRIO Y MAT.CONST.	25	3	8.33	25	0.0000
CEMENTO	22	2	11.00	22	0.0000
COMUNICACIONES	17	1	17.00	17	0.0000
AGRICULTURA Y PESCA	16	3	5.33	16	0.0000

TABLE 2.28: Basic measures for the network of sectors

Year	Density	Radius	Diameter	Avg. Clustering	Avg. Shortest Path Length	Assortativity
2004	51.85%	2	3	0.66	1.60	0.035
2005	54.77%	2	3	0.69	1.55	0.035
2006	52.92%	2	3	0.68	1.60	0.028
2007	56.00%	2	3	0.71	1.56	0.015
2008	59.33%	2	3	0.70	1.53	0.001
2009	49.29%	2	4	0.64	1.66	-0.016
2010	49.29%	2	3	0.65	1.66	-0.029

TABLE 2.29: Fixed effects models. The first two models use profitability as the dependent variable, while the last two use leverage. Models (2) and (4) also include dummy years in addition to the firm specific fixed effects.

	Dependent variable:			
	economic profitability		leverage	
	(1)	(2)	(3)	(4)
centrality	9.996	10.866	−11.103*	−12.062*
	(7.384)	(7.400)	(6.623)	(6.606)
2005		2.325		−0.850
		(1.720)		(1.522)
2006		3.797**		−2.390
		(1.790)		(1.549)
2007		2.538		−2.133
		(1.788)		(1.568)
2008		1.958		−4.093***
		(1.793)		(1.568)
2009		−0.788		−5.390***
		(1.820)		(1.590)
2010		1.408		−4.383***
		(1.887)		(1.605)
Observations	879	879	867	867
R^2	0.003	0.018	0.004	0.033
Adjusted R^2	0.002	0.014	0.003	0.027
F Statistic	1.832 (df = 1; 661)	1.535 (df = 8; 654)	2.810* (df = 1; 706)	2.997*** (df = 8; 699)
Note:				*p<0.1; **p<0.05; ***p<0.01

TABLE 2.30: Fixed effects models. The first two models use profitability as the dependent variable, while the last two use leverage. Models (1) and (3) are based on the original centrality measures, and models (2) and (4) are based on their rank transformed versions.

	Dependent variable:			
	economic profitability		leverage	
	(1)	(2)	(3)	(4)
centrality	10.866		−12.062*	
	(7.400)		(6.606)	
rank(centrality)		0.003*		−0.003***
		(0.001)		(0.001)
2005	2.325	2.375	−0.850	−0.897
	(1.720)	(1.719)	(1.522)	(1.519)
2006	3.797**	3.922**	−2.390	−2.509
	(1.790)	(1.790)	(1.549)	(1.546)
2007	2.538	2.644	−2.133	−2.138
	(1.788)	(1.785)	(1.568)	(1.563)
2008	1.958	2.041	−4.093***	−4.123***
	(1.793)	(1.791)	(1.568)	(1.564)
2009	−0.788	−0.716	−5.390***	−5.435***
	(1.820)	(1.818)	(1.590)	(1.586)
2010	1.408	1.452	−4.383***	−4.436***
	(1.887)	(1.885)	(1.605)	(1.601)
Observations	879	879	867	867
R^2	0.018	0.021	0.033	0.038
Adjusted R^2	0.014	0.015	0.027	0.031
F Statistic	1.535 (df = 8; 654)	1.728* (df = 8; 654)	2.997*** (df = 8; 699)	3.438*** (df = 8; 699)
Note:				*p<0.1; **p<0.05; ***p<0.01

TABLE 2.31: Fixed effects models. The first two models use profitability as the dependent variable, while the last two use leverage. Models (1) and (3) are based on the tradicional busyness measures, and models (2) and (4) are based on their rank transformed versions.

	Dependent variable:			
	economic profitability		leverage	
	(1)	(2)	(3)	(4)
busyness_tradicional	−0.782		37.300	
	(41.856)		(34.155)	
rank(busyness_tradicional)		0.0003		−0.003
		(0.002)		(0.002)
2005	2.294	2.308	−0.769	−0.954
	(1.724)	(1.726)	(1.526)	(1.525)
2006	3.679**	3.715**	−2.194	−2.619*
	(1.793)	(1.808)	(1.554)	(1.561)
2007	2.592	2.625	−2.215	−2.640*
	(1.791)	(1.804)	(1.570)	(1.580)
2008	1.960	2.005	−4.058**	−4.573***
	(1.797)	(1.821)	(1.573)	(1.590)
2009	−0.803	−0.770	−5.397***	−5.645***
	(1.823)	(1.838)	(1.592)	(1.598)
2010	1.292	1.323	−4.318***	−4.528***
	(1.889)	(1.902)	(1.607)	(1.611)
Observations	879	879	867	867
R^2	0.015	0.015	0.030	0.032
Adjusted R^2	0.011	0.011	0.024	0.026
F Statistic	1.262 (df = 8; 654)	1.264 (df = 8; 654)	2.721*** (df = 8; 699)	2.890*** (df = 8; 699)
Note:				*p<0.1; **p<0.05; ***p<0.01

TABLE 2.32: Fixed effects models. The first two models use profitability as the dependent variable, while the last two use leverage. Models (1) and (3) are based on the original busyness measures, and models (2) and (4) are based on their rank transformed versions.

	Dependent variable:			
	economic profitability		leverage	
	(1)	(2)	(3)	(4)
busyness	−1.753		−1.399	
	(1.722)		(1.339)	
rank(busyness)		−0.001		−0.005**
		(0.003)		(0.002)
2005	2.305	2.304	−0.813	−0.788
	(1.722)	(1.723)	(1.525)	(1.521)
2006	3.753**	3.693**	−2.192	−2.139
	(1.791)	(1.791)	(1.554)	(1.549)
2007	2.668	2.615	−2.242	−2.248
	(1.790)	(1.791)	(1.569)	(1.564)
2008	2.005	1.975	−4.117***	−4.100***
	(1.795)	(1.796)	(1.571)	(1.567)
2009	−0.845	−0.806	−5.418***	−5.414***
	(1.822)	(1.823)	(1.593)	(1.589)
2010	1.151	1.254	−4.392***	−4.480***
	(1.892)	(1.891)	(1.609)	(1.605)
Observations	879	879	867	867
R^2	0.017	0.015	0.030	0.034
Adjusted R^2	0.012	0.011	0.024	0.028
F Statistic	1.393 (df = 8; 654)	1.275 (df = 8; 654)	2.708*** (df = 8; 699)	3.117*** (df = 8; 699)
Note:				*p<0.1; **p<0.05; ***p<0.01

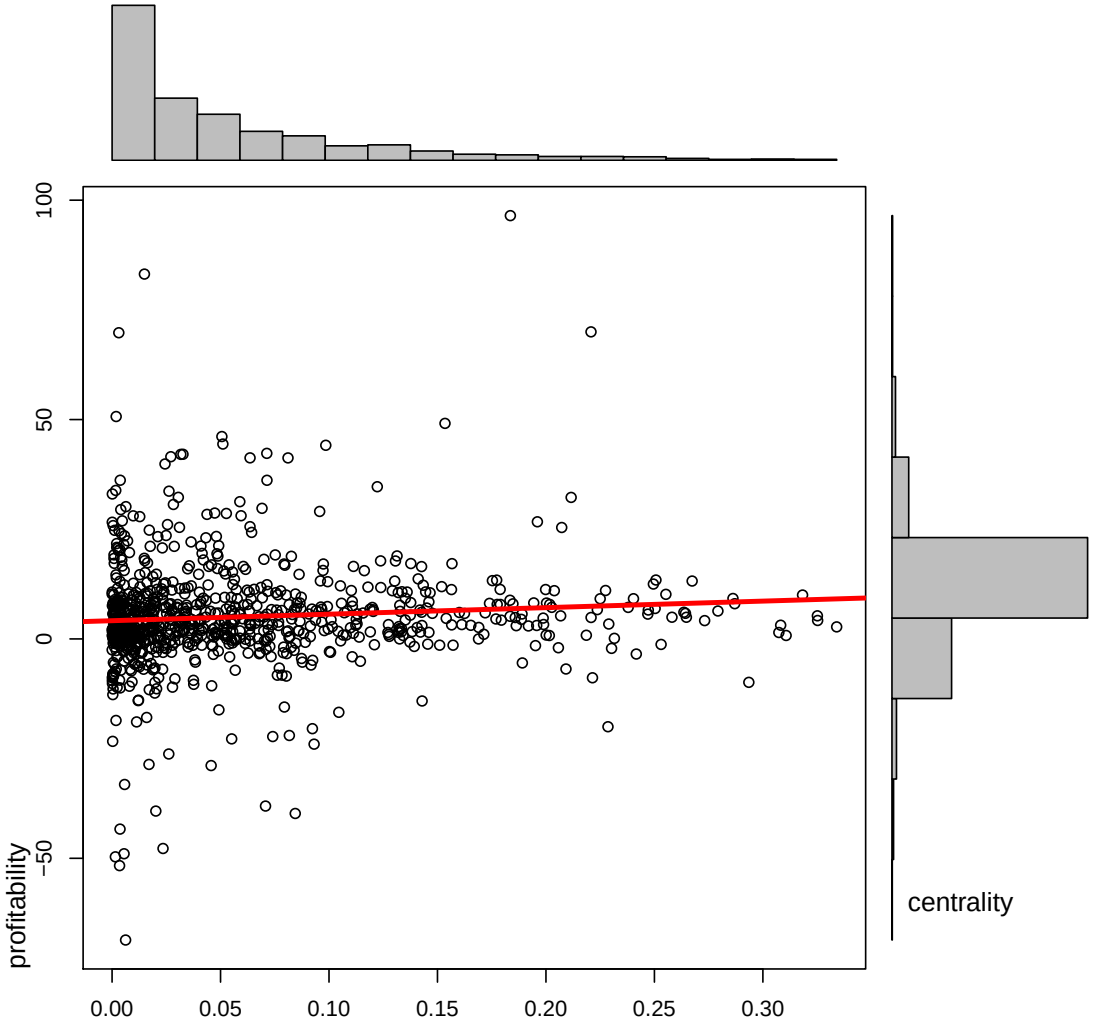

FIGURE 2.9: Scatter plot and histograms for profitability and centrality

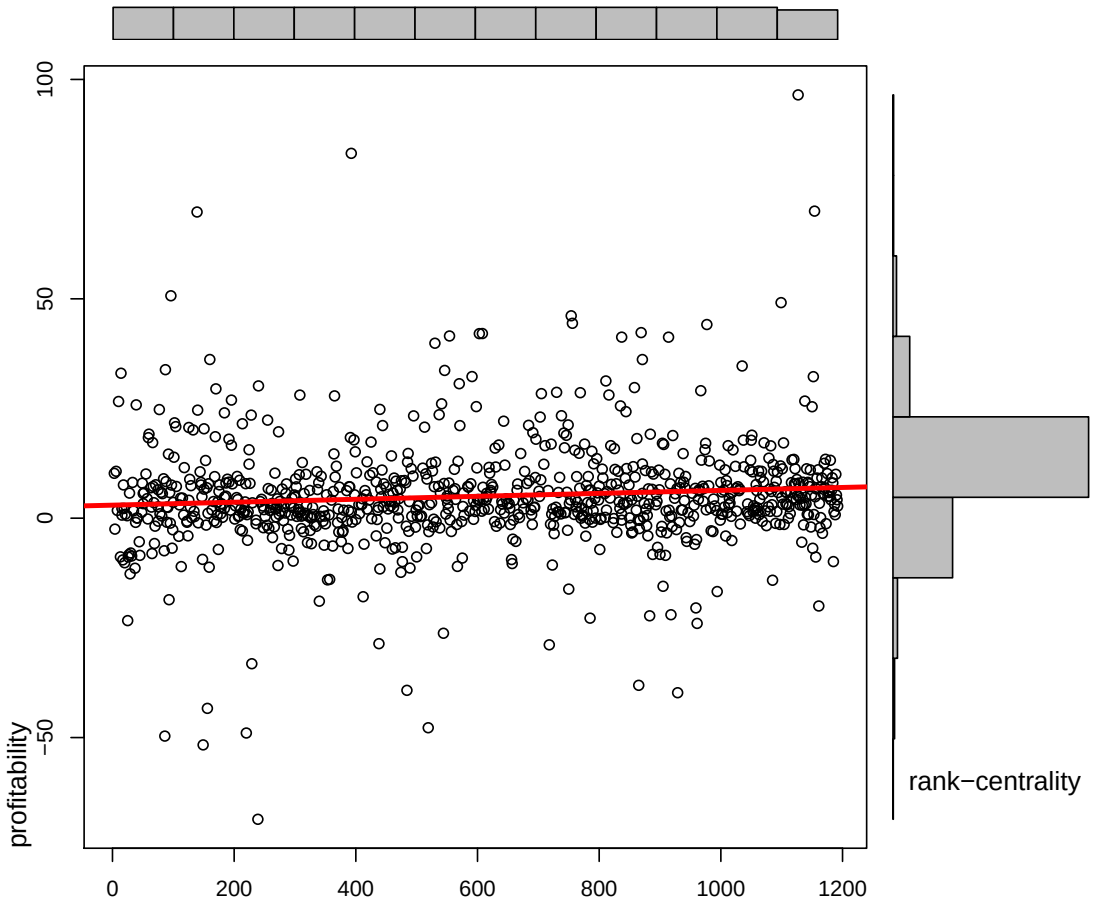

FIGURE 2.10: Scatter plot and histograms for profitability and rank-transformed centrality

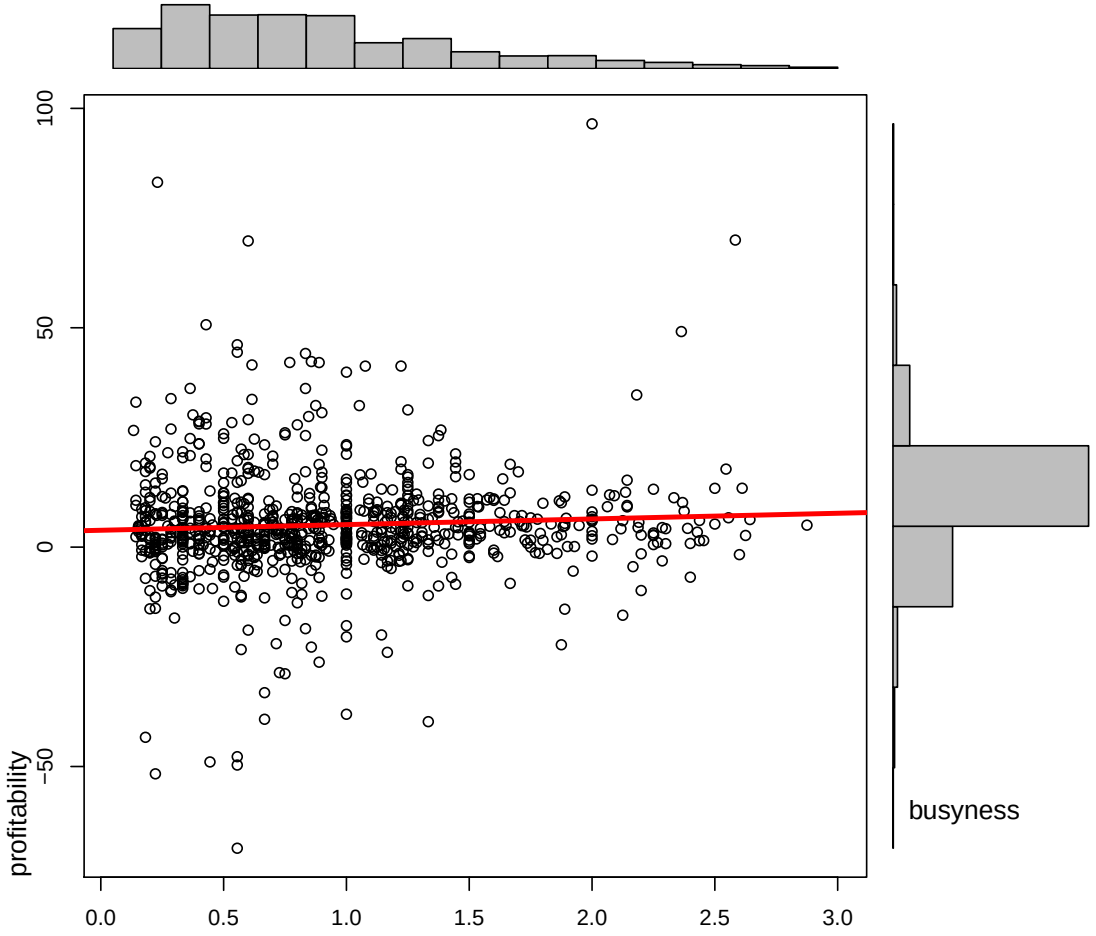

FIGURE 2.11: Scatter plot and histograms for profitability and busyness

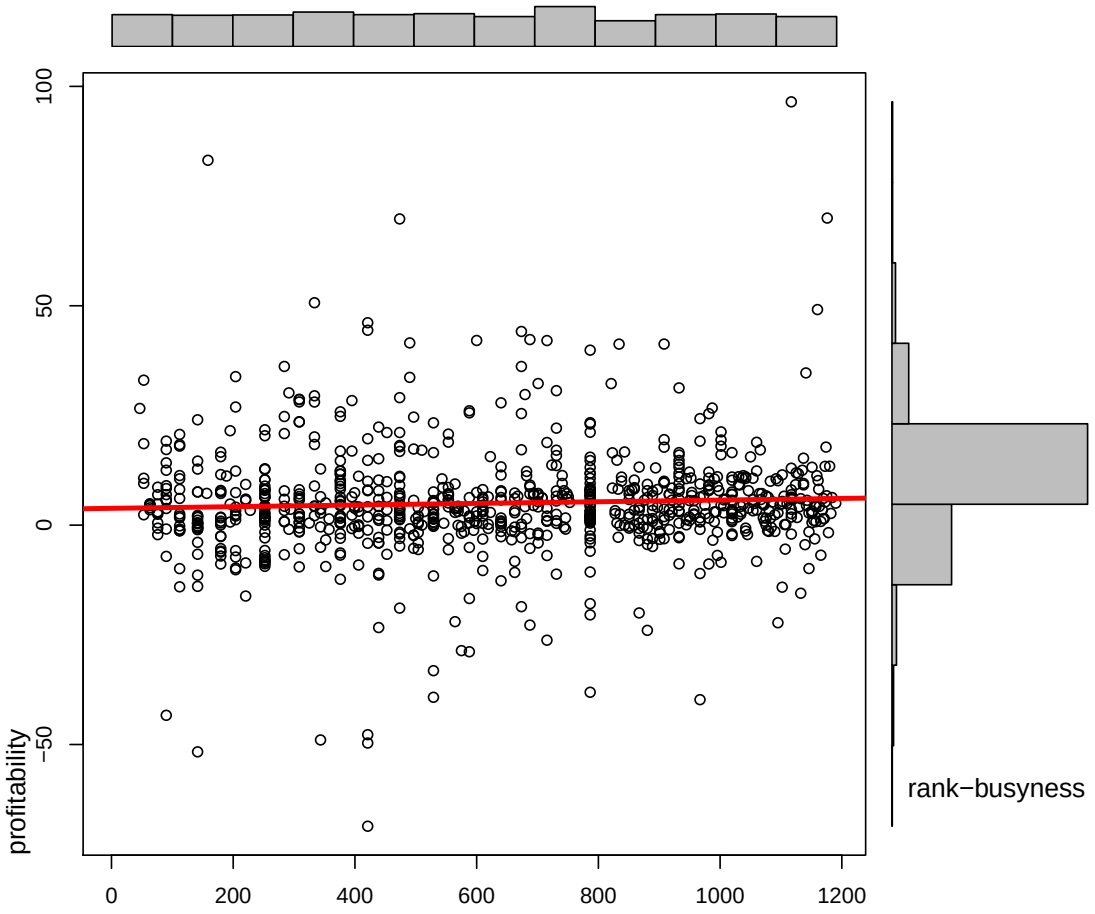

FIGURE 2.12: Scatter plot and histograms for profitability and rank business

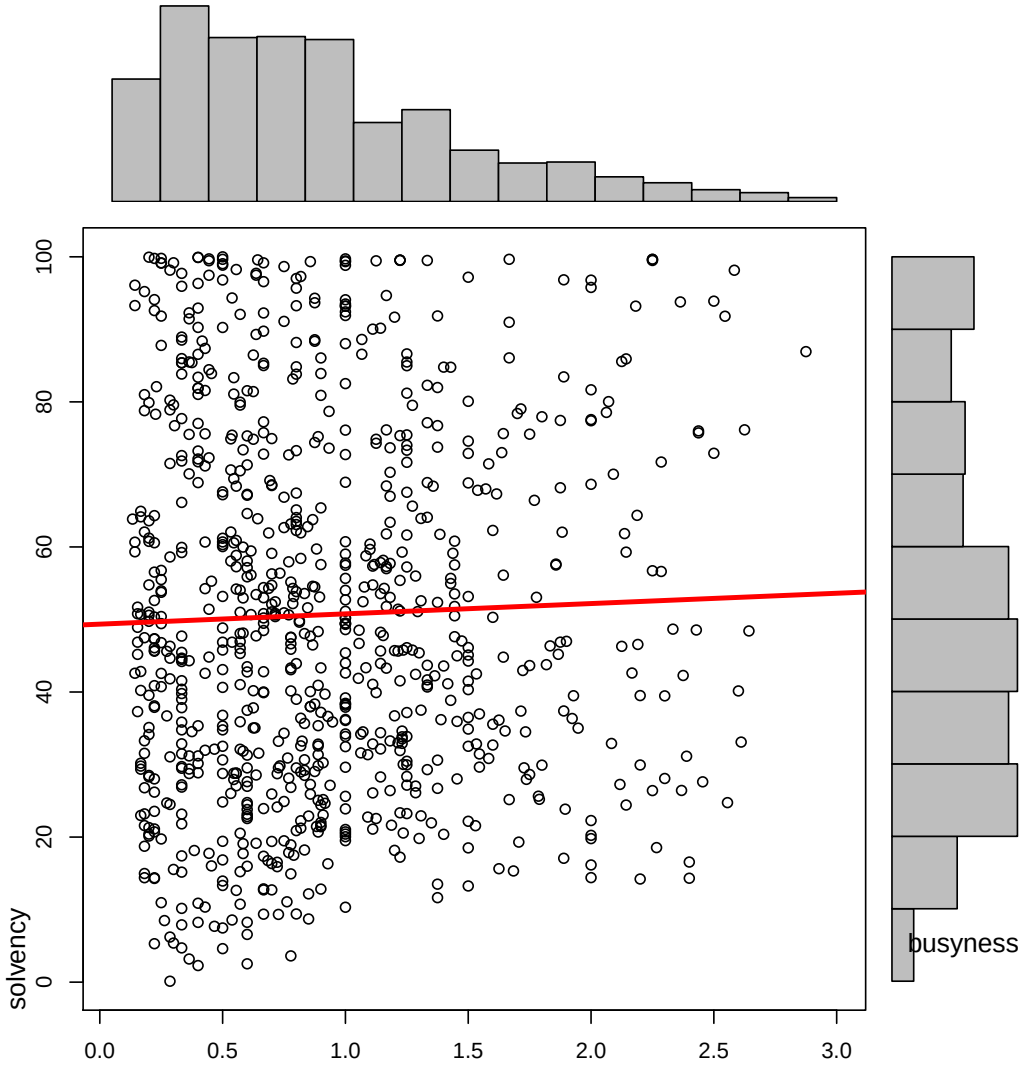

FIGURE 2.13: Scatter plot and histograms for leverage and busyness

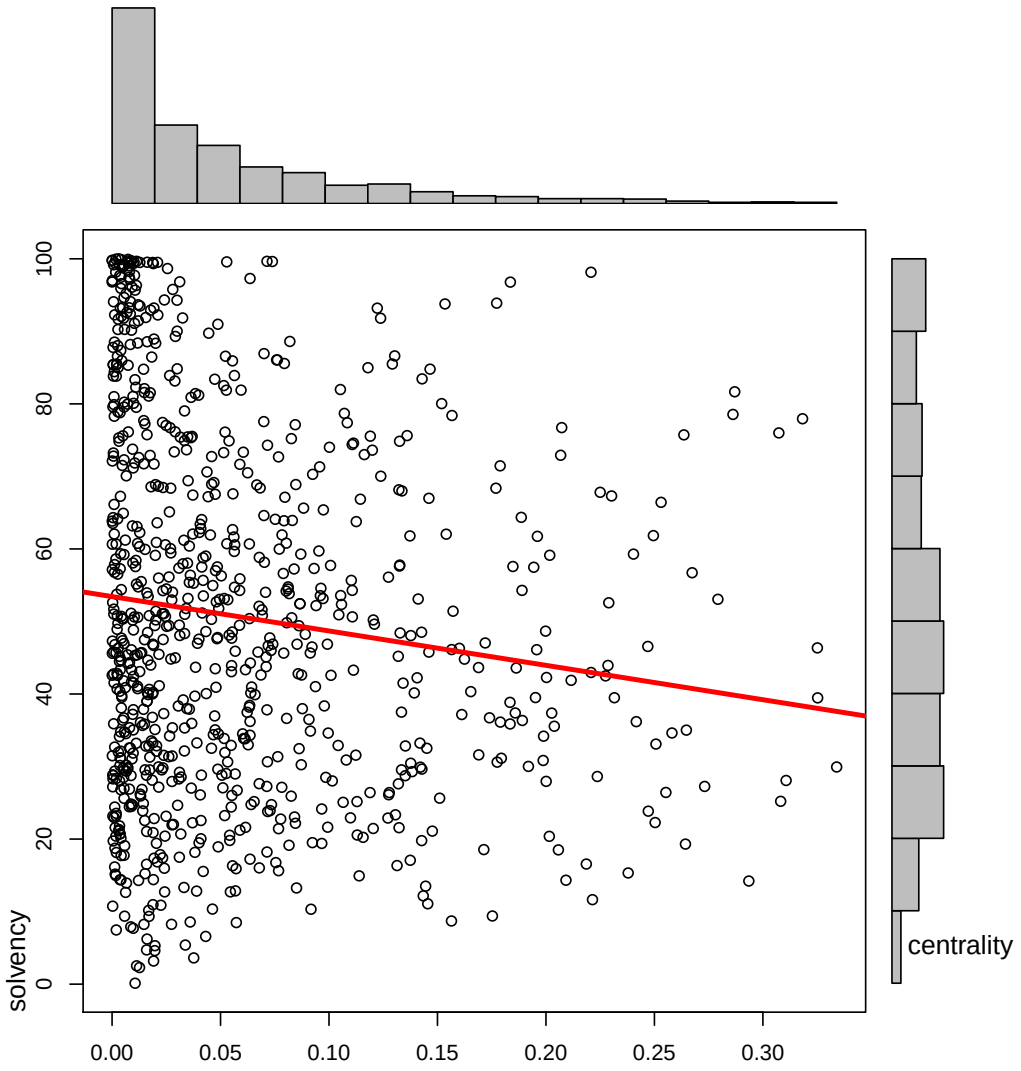

FIGURE 2.14: Scatter plot and histograms for leverage and centrality

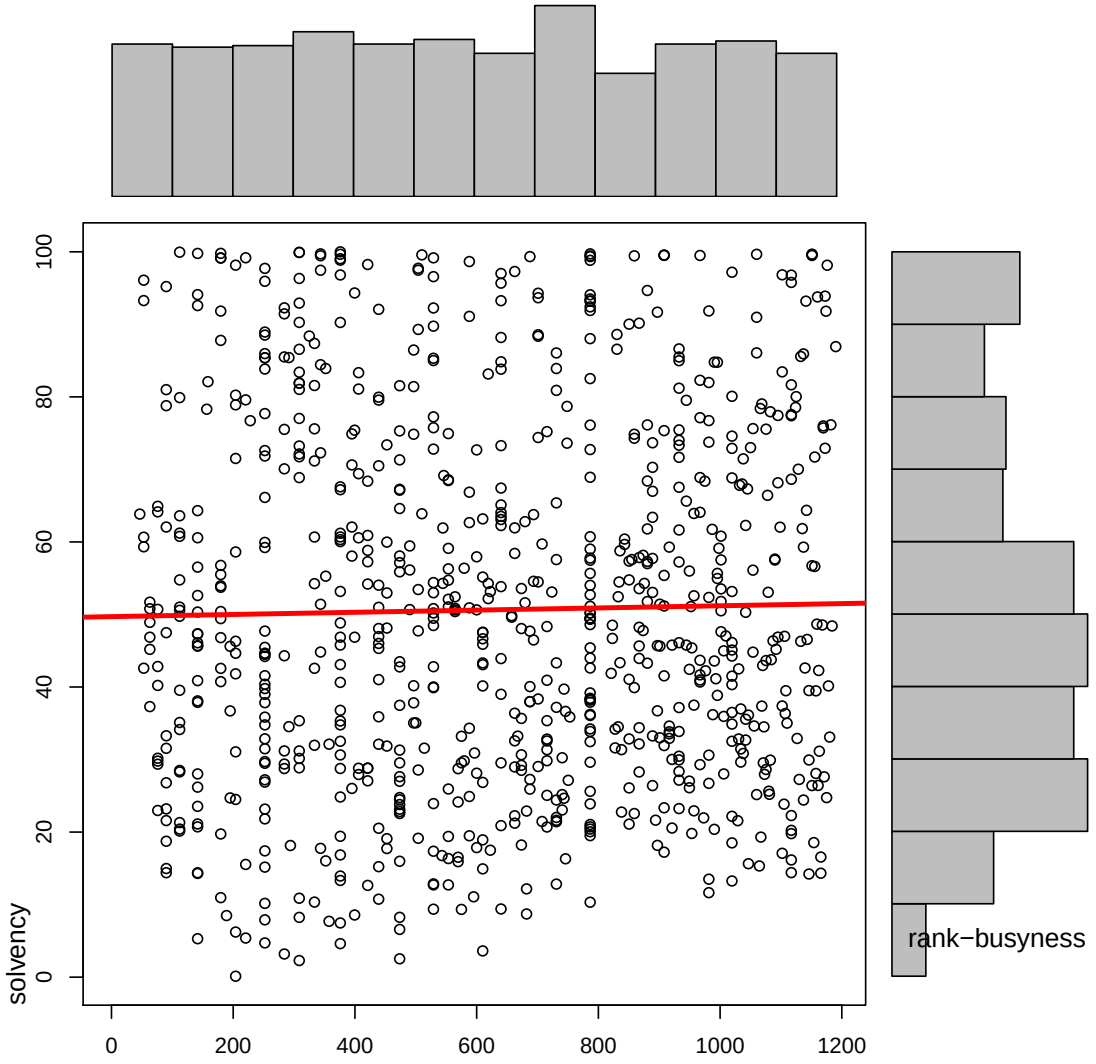

FIGURE 2.15: Scatter plot and histograms for leverage and rank-busyness

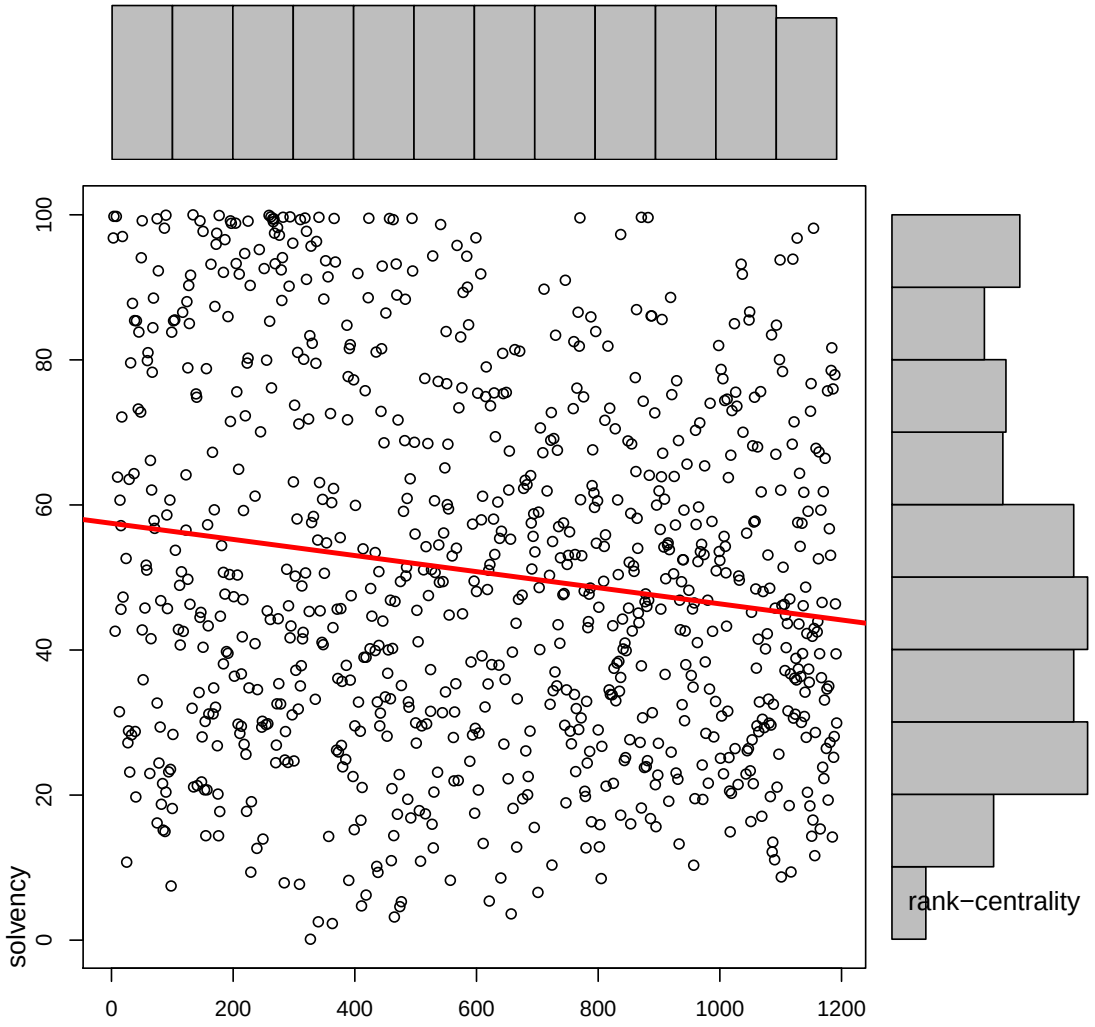

FIGURE 2.16: Scatter plot and histograms for leverage and rank-centrality

Chapter 3

Investigation on the Simulation Horizon Requirement for Estimation of Agent Based Models

Introduction

Agent Based Modeling (ABM) is a modern methodology for modeling systems composed of several agents who interact with each other independently. In complex systems as modern economies, this interaction may generate aggregate behavior that cannot be derived only by means of the study of the individual [61]. This characteristic is present in complex systems and is called emergent properties, i.e., there are observed properties resulting from the interaction between agents that cannot be studied simply by summing up individual behavior or by means of a representative agent.

It can be said that ABM is the third scientific method after deduction and induction. In this sense, several hypotheses are formulated on the behavior of agents and on their forms of organization, precisely like deduction [62]. However, the main objective is not to prove general theorems, but to generate artificial data for evaluation by means of induction. Agent-based models have been widely applied in several scientific areas in

order to study problems such as supply chains, consumer markets, and the Insurance industry in economics; transportation and electric power markets in engineering, population dynamics, and ecological networks in biology.

Although some earlier uses can be found, according to [63] it was only in the late nineties that these microscopic (agent-based) models became popular in both economics and physics literature. Within economics, the ABM methodology is mostly applied in the field of finance. [64] underscores several reasons that make financial markets rich environments for agent based modeling, such as the persisting debate on market efficiency and the existence of some mysterious puzzles regarding financial time series.

Such puzzles are the so-called stylized facts: some statistical properties that appear consistently in a large variety of financial time series, regardless if one looks at data from different markets (e.g., shares, exchange) or different national economies. As an illustration, [63] suggests that, recently, the majority of the researches in the field agree that the cumulative distribution of the returns follows a power law with exponent around 3. This is not necessarily in agreement with the Efficient Market Hypothesis literature, seen that it postulates that prices should fluctuate randomly, and hence not following any kind of scaling rule. There is an extensive list of other stylized facts presented by [65] which are also not accounted for by the Efficient Market Hypothesis. The next section of this investigation details a selected group of them.

According to [63], the agent based model ability to reproduce the stylized facts is its principal achievement, and also its source of scientific validation. In fact, these authors argue that some of these models can reproduce several stylized facts at the same time to an impressive quantitative extent. According to [4], normally these models have their parameters calibrated manually in order to match at least in order of magnitude a selected number summary of statistics, and thus being considered as validated. Although such procedure can distinguish the *bad* from the *good* models, the same authors points out the need of a less informal method for goodness-of-fit comparisons than manual calibration when the aim is to distinguish between the *good* and the *very good* models.

In this sense, one is not concerned with the calibration of the parameters of a given model, but with the precise estimation of them instead. There are different ways the

optimal set of parameters of a model can be found, but here the Method of Simulated Moments (MSM) is considered. The idea is that the distance between some empirical reference and synthetic time series generated by a run of a model using a given set of parameters can be measured, at least with respect to a previously defined set of summary statistics (or moments) of interest. Despite being a natural way of thinking about the degree of goodness-of-fit of a model, the MSM is specially helpful when exact solutions are too complicated to obtain analytically [4].

Considering this broad perspective, that is, the estimation of agent based models and the comparison between different models in terms of goodness of fit, this investigation is concerned with two problems. First, it is considered that the accurate estimation of Agent Based Models (ABM) by the method of simulated moments is possibly affected by the simulation horizon one allows the model to run due to sample variability. Then, the first objective of this essay is to investigate the effects of this kind of variability on the distribution of the values of the objective function subject to optimization.

As a working hypothesis, the following statement is considered: if the simulation horizon is not sufficiently large, the resulting distribution may present frequent extreme points, which can lead to inaccurate results when one tries to compare different models. In an attempt to answer to this question, a model contest is carried out using different simulation horizons to assess the difference in goodness of fit when inactive traders are introduced in one of the Structural Stochastic Volatility models proposed by [5].

Using this same experiment, a second question is considered in this investigation concerning the improvements in goodness of fit brought by the inclusion of these inactive traders in the Structural Stochastic Volatility (SSV) model. The idea is to assess which model is *better* at reproducing some of the stylized facts. This answers the second question. In addition, to answer the first question, it is checked if this difference is influenced somehow by the simulation horizon one allows the models to run in order to compute the moments of the generated time series.

The rest of this investigation is organized as follows. The first section presents some selected stylized facts which will be used in the estimation of the models. The second section of the investigation briefly provides an overview of the Agent Based Model

(ABM) methodology, which is claimed to take into account the so-called stylized facts to a great extent, and, thus, could be viewed as an alternative to the Efficient Market Hypothesis theoretical background [66]. In doing so, selected recent empirical findings are highlighted, and a brief taxonomy for ABMs is presented. Then, in the next section specific ABMs are discussed in greater detail while focusing on their ability to explain some of the stylized facts. The last two sections section deal explicitly with the estimation of ABMs by the method of simulated moments and present an investigation on the simulation horizon requirements by means of an example of model contest assessing the difference in goodness of fit of allowing inactive traders in one of the Structural Stochastic Volatility models proposed by [5].

3.1 Stylized Facts

Apart from the theoretical critiques developed by [67], the Efficient Market Hypothesis (EMH) seems to be misaligned with some empirical features of financial markets. This debate is presented by [66] by portraying how various lines of research refer to these empirical findings, each in its own different way. On the EMH side, these findings were referred to as anomalies, that is, there should be at least a few strange empirical results in disagreement with the established theoretical foundation. On the other hand, recent studies have referred to these empirical results as *stylized facts*, meaning that they can be found quite regularly in financial markets and, thus, they deserve proper theoretical explanation.

An extensive list of these stylized facts is presented by [65] concerning several data formats (such as returns and trading volume) and frequencies (ranging from tick-by-tick order book data to annual seasonality). Here, attention is only focused on some of those data concerning daily price returns, namely the absence of autocorrelation in raw returns, fat tails of absolute returns, and volatility clustering. According to [4] these are the stylized facts that have received more attention in the literature.

The absence of autocorrelation in raw returns has never been referred to as an anomaly, because it is an empirical finding in total agreement with the EMH theoretical background. It is related to the martingale property [68], which states that markets behave

similar to a random walk. According to [66], this is the EMH's most important empirical finding, but the author also points out that a lot of attention was paid to it, thus neglecting in consequence other relevant stylized facts.

With regard to the tails of returns distributions, it is expected by the EMH that they would behave normally due to the arrival of purely random information. However, even old empirical findings [68] suggested that the normal distribution is not well suited to financial returns, because it has probability mass more concentrated on its mean and extreme values than is expected in a normally distributed process.

Since it is seen that kurtosis is not well suited for evaluating such a statistical property, it is then common to deal with the Hill estimator of tail index α, calculated as follows: first, absolute daily returns are sorted in a descending order so that a threshold value which defines a tail v^p can be calculated as the correspondent first p (here $p = 5\%$) returns, and m is defined as the number of returns labeled as belonging to the tail. Finally, the Hill estimator is given by the equation 3.1.

$$\alpha = \frac{m}{\sum_{k=1}^{m} [ln(v_k) - ln(v^p)]} \tag{3.1}$$

Finally, volatility clustering deals with the fact that directions of returns are hard to predict, but not their magnitude. There seem to exist alternate moments of financial fury and relaxation, printing clusters of high and low volatility on empirical data that are not at all accounted for by the EMH background. As pointed out by [66], even though a great deal of research on econometrics is focused on modeling this fact (the ARCH methodology), very little research has been done to explain it.

3.2 Taxonomy

According to an extensive survey conducted on the topic dealt with by [65], during the 1990s, the first attempts were made to explain some observed regularities in financial data by means of ABM. The main concern of these early works was to artificially reproduce some of the so-called stylized facts observed in real financial data. Hence, the objective of the authors just mentioned was to simulate and calibrate parameters of an

artificial financial market by ABM, and then to apply standard econometric techniques to evaluate how much of the stylized facts (both quantitatively and qualitatively) could be reproduced by their artificial generated data.

Even though these early works share the goal of matching stylized facts, their ABM formulations may vary dramatically. For this reason, taxonomy was developed by [65] in an attempt to classify recent work on ABM with regard to specific aspects, namely agent heterogeneity, learning, and interactions.

With regard to heterogeneity, agents can basically be divided into two groups: N-types and autonomous agents. In the former, all possible types of behavior are pre-defined in some sense by the designer; whereas in the latter, new strategies (that is, agent types) can emerge autonomously. We can consider the model by [6] as an example of N-type design, in which agents can be fundamentalists (that is, their demands respond proportionally to the current deviation from fundamental price) or chartists (who try to extrapolate the last trend observed). Chartists' strategy is also determined by a sentiment index (pessimism or optimism) that determines whether chartists believe that the last trend observed will be maintained or reversed. On the other hand, we can consider the Santa Fe Artificial Stock Market [69] as an example of autonomous agent design. In this context, agents are allowed to autonomously search for profitable strategies that were usually not pre-defined by the designer by means of genetic search algorithms.

With regard to learning, [66] points to a branch of literature called *Adaptive Belief Systems* (ABS), which, unlike some of the other less flexible models, allows agents to dynamically switch between different strategies. With regard to the N-type models, this feature is most commonly introduced by means of two approaches, namely transition probabilities and discrete choice. Following the transition probability approach, a *majority index* is defined as representing how much one group dominates (or is dominated by) the other. Each agent switches from one group to the other according to time-varying transition probabilities π_t^{fc} and π_t^{cf}, which are functions of the current state of the system, which is generally defined here as a_t.

According to [5], it can be demonstrated under some assumptions, that at the macroscopic level, population shares are depicted by

$$n_t^f = n_{t-1}^f + n_{t-1}^c \pi_{t-1}^{cf}(a_{t-1}) - n_{t-1}^f \pi_{t-1}^{fc}(a_{t-1}) \tag{3.2a}$$

$$n_t^c = 1 - n_t^f \tag{3.2b}$$

whereas the transition probabilities are given by

$$\pi_{t-1}^{cf}(a_{t-1}) = min(1, ve^{a_{t-1}}) \tag{3.3a}$$

$$\pi_{t-1}^{fc}(a_{t-1}) = min(1, ve^{-a_{t-1}}) \tag{3.3b}$$

where v can be viewed as a flexibility parameter.

On the other hand, there is the discrete-choice approach proposed by [70], in which the adjustment happens directly on the population shares (and not on its rate of change) according to the following equation

$$n_t^{f,c} = \frac{e^{\beta a_{t-1}^{f,c}}}{e^{\beta a_{t-1}^f} + e^{\beta a_{t-1}^c}} \tag{3.4}$$

where β is the intensity of choice, and the state of the system is allowed to be different for each group. The way the state of the system influences agent choice significantly varies in literature. As examples, one can consider the specification of a herding $a_t = \alpha_n(n_t^f - n_t^c)$ or a misalignment component $a_t = \alpha_p(p_t - p^*)$ where p^* is the fundamental price. This will be pursued in greater detail in the next section.

Finally, the way agents interact defines the structure of the artificial financial market and its price determination. When considering N-type models, it is common to sum up demand of both groups and to assume a market maker who holds a sufficiently large inventory to supply any excess of demand and to absorb any excess of supply. Then, this market maker adjusts the price in the next period to reflect this excess demand or supply. However, as stated by [71], this is not a very realistic assumption in the way that no actual market clearing is taking place. In addition, a true market clearing mechanism would be easier to be implemented in an autonomous agent design by means of direct numerical clearing.

3.3 Agent Based Model Implementation

In the remaining part of the section, two specific agent-based models are described in greater detail, namely the trading inactivity model proposed by [72] and the structural stochastic volatility model proposed by [5]. The idea is to present some practical issues concerning the development of an agent-based model, and also to introduce the task of estimating its parameters that is the objective of the next section.

3.3.1 Trading Inactivity Model

In an attempt to use simple agent based models to illustrate the potential effects of regulatory policies on financial markets, [72] introduces a modification on the chartists-fundamentalists traditional scheme by allowing agents also to be absent from markets, that is, they can be inactive. This innovation may imprint models with more reality and also is important for using agent based models in the analyses of regulatory and taxing policies. This section outlines this model by focusing on this new device of trading inactivity and also on the model's power to reproduce some of the stylized facts.

As it is common practice, the demands of chartists and fundamentalists are respectively given by

$$D_t^C = b(p_t - p_{t-1}) + \beta_t \tag{3.5a}$$

$$D_t^F = c(F_t - p_t) + \gamma_t \tag{3.5b}$$

where D stands for demand, the superscripts C and F represents chartists and fundamentalists respectively, t is the time unit, p is the log of price, F is the log of fundamental price, b and c are positive reaction parameters for chartists and fundamentalists respectively, β and γ are IID random normal process with zero mean and σ^β and σ^γ are standard deviations that capture intra-group heterogeneity for chartists and fundamentalists, respectively.

In this context, price formation is given by the following price impact function

$$p_{t+1} = p_t + a(W_t^C D_t^C + W_t^F D_t^F) + \alpha_t \tag{3.6}$$

where W denote population shares, a is a positive price adjustment coefficient and α is an IID random normal process with zero mean and standard deviation σ^α.

The determination of W, that is, the choice between the three available strategies, depends on past performance and is given by the following equations in the spirit of the discrete choice approach:

$$A_t^C = (e^{p_t} - e^{p_{t-1}})D_{t-2}^C + dA_{t-1}^C - tax(e^{p_t} - e^{p_{t-1}})D_{t-2}^C \tag{3.7a}$$

$$A_t^F = (e^{p_t} - e^{p_{t-1}})D_{t-2}^F + dA_{t-1}^F - tax(e^{p_t} - e^{p_{t-1}})D_{t-2}^F \tag{3.7b}$$

$$A_t^O = 0 \tag{3.7c}$$

where the superscript O stands for inactivity, A denotes each strategy attractiveness and is composed by the sum of a short run capital gain term and an accumulated profits term which is weighted by the memory parameter d. tax is a percentage tax applied both when buying and selling the asset. Finally, defining β as the so called intensity of choice, population shares are represented by

$$W_t^C = \frac{e^{\beta A_t^C}}{e^{\beta A_t^C} + e^{\beta A_t^F} + 1} \tag{3.8a}$$

$$W_t^F = \frac{e^{\beta A_t^F}}{e^{\beta A_t^C} + e^{\beta A_t^F} + 1} \tag{3.8b}$$

$$W_t^C = \frac{1}{e^{\beta A_t^C} + e^{\beta A_t^F} + 1} \tag{3.8c}$$

Even though the author does not carry on a systematic estimation procedure, a set of benchmark input parameters are presented and thus the calibrated model is claimed to reproduce some of the stylized facts (mainly volatility clustering and fat tails) when no tax is applied. Figure 3.1 presents a single simulation of the model with the following set of input parameters presented by the author ($a = 1$, $b = 0.04$, $c = 0.04$, $d = 0.975$, $\beta = 300$, $\sigma^\alpha = 0.01$, $\sigma^\beta = 0.05$, and $\sigma^\gamma = 0.01$).

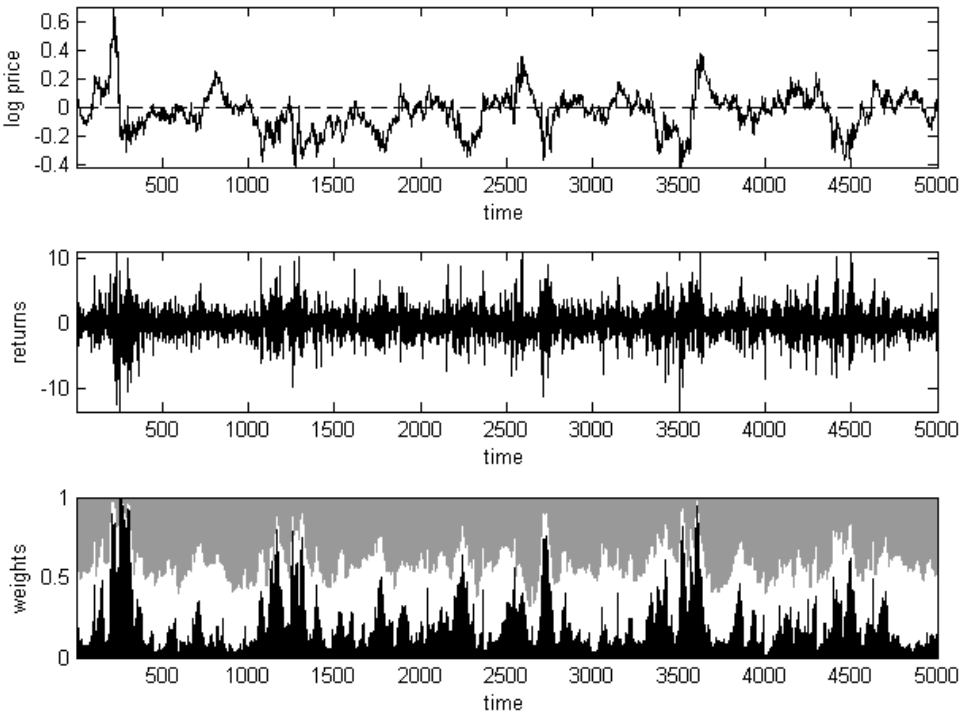

FIGURE 3.1: Upper panel shows the log of price, middle panel its percentage returns, and lower panel the shares of fundamentalists (gray), chartists (black) and inactive (white) traders.

3.3.2 Structural Stochastic Volatility Model

With regard to agent design, this is a two-group model where agents can be fundamentalists or chartists. The main difference is that fundamentalists respond to deviations from fundamental price, and chartists extrapolate the returns they just observed in the previous period. Thus, their demand functions $d_t^{f,c}$ are given by

$$d_t^f = \phi(p^* - p_t) + \varepsilon_t^f \quad \varepsilon_t^f \sim N(0, \sigma_f^2), \;\; \phi > 0 \tag{3.9a}$$

$$d_t^c = \chi(p_t - p_{t-1}) + \varepsilon_t^c \quad \varepsilon_t^c \sim N(0, \sigma_c^2), \;\; \chi \geq 0 \tag{3.9b}$$

where the superscripts f and c denote agent affiliation (fundamentalists and chartists, respectively); the subscript t represents time unit; p is the log of the price; p^* is the log of the (fixed) fundamental price; $\varepsilon^{f,c}$ are group-specific random terms (with zero mean and $\sigma_{f,c}$ standard deviations) that account for intra-group heterogeneity; ϕ corresponds to the responsiveness of the fundamentalists to the deviation from fundamental

price; and χ corresponds to the responsiveness of the chartists to the last trend observed.

However, this model also accounts for learning, in the sense that agents can dynamically change their minds and move to the other group. Therefore, the shares of each group in the total population are allowed to vary over time. Considering that $n_t^{f,c}$ denotes their respective population shares, total excess demand can be written as $n_t^f d_t^f + n_t^c d_t^c$. Seen that this equation may not balance, a market maker is assumed to hold a sufficiently large inventory for supplying any excess of demand and for absorbing any excess of supply. This is done by adjusting the price in the next period by a fixed coefficient that is inversely related to market liquidity. Considering these specifications, price determination at each time unit is given by

$$P_{t+1} = P_t + \mu[n_t^f \phi(p^* - p_t) + n_t^c \chi(p_t - p_{t-1}) + \varepsilon_t] \tag{3.10}$$

where

$$\varepsilon_t \sim N(0, \sigma_t^2), \quad \sigma_t^2 = (n_t^f)^2 \sigma_c^2 + (n_t^c)^2 \sigma_c^2 \tag{3.11}$$

summarizes what the authors coined as *Stochastic Structural Volatility* (SSV), and can be viewed as a structural modeling approach to time-varying variance.

What remains to be explained is the learning mechanism that yields the dynamics of the population shares. Even though the authors presented two different technical approaches for this, namely transition probabilities and discrete choice, only the latter will be considered here, given its best performance in a comparative study conducted by the same authors [4]. It is worth beginning with the definition of a switching index s_t, which attempts to measure the relative attractiveness of the fundamentalist's strategy in comparison to that of the chartist, given by

$$s_t = \alpha_0 + \alpha_x x_t + \alpha_d (p_t - p^*)^2 \tag{3.12}$$

where α_0 is a predisposition parameter to switch to fundamentalism; $\alpha_x x_t$ captures the idea of herding behavior; x_t is equal to $n_t^f - n_t^c$ in order to capture the relative presence

of the two groups; and α_d can be understood as a measure of the influence of price misalignment (that is, the larger the gap, the higher the attractiveness of switching to fundamentalism). Thus, in the spirit of the discrete-choice approach, the shares of the total population in each group can be written as $n_t^f = 1/[1 + e^{-\beta s_{t-1}}]$ and $n_t^c = 1 - n_t^f$, where β is the intensity of choice. Figure 3.2 compares outputs from a single run of the model with returns of S&P500 as a benchmark.

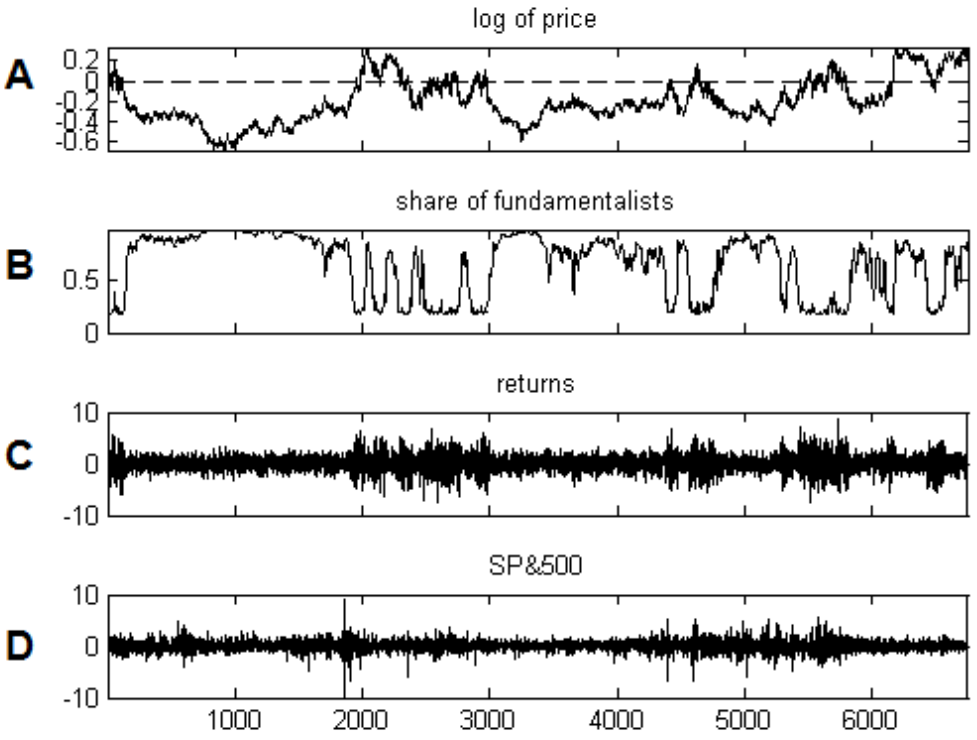

FIGURE 3.2: $T = 6750$ observations of (A) log of price, (B) share of fundamentalists, and (C) returns from a simple run of the model and (D) daily returns from S&P500 from January 1980 to March 2007. Inputs to the model are as follows: $\phi = 0.0728$, $\chi = 0.0896$, $\mu = 0.01$, $\alpha_0 = -0.327$, $\alpha_x = 1.815$, $\alpha_d = 9.6511$, $\sigma_f = 1.0557$, $\sigma_c = 2.9526$, $p^* = 0$, and $\beta = 1$.

3.3.3 Introducing Inactivity to SSV Models

This section described the exact same model from last section, but augmented to allow agents to be absent (inactive) from the market. Hence, it is now a three-group model (fundamentalists, chartists, and inactive), with demand functions $d_t^{f,c,i}$ given by

$$d_t^f = \phi(p^* - p_t) + \varepsilon_t^f \quad \varepsilon_t^f \sim N(0, \sigma_f^2), \quad \phi > 0 \tag{3.13a}$$

$$d_t^c = \chi(p_t - p_{t-1}) + \varepsilon_t^c \quad \varepsilon_t^c \sim N(0, \sigma_c^2), \quad \chi \geq 0 \tag{3.13b}$$

$$d_t^i = 0 \tag{3.13c}$$

where the subscript i denotes the inactive group, and all the other variables remain the same from equation 3.9. Another modification required from the two-group model described in the last section concerns the shares of the total population in each of the three groups, which is now described as

$$n_t^f = \frac{(1-\omega)\exp(\beta a_{t-1}^f)}{(1-\omega)[\exp(\beta a_{t-1}^f) + \exp(\beta a_{t-1}^c)] + \omega} \tag{3.14a}$$

$$n_t^c = \frac{(1-\omega)\exp(\beta a_{t-1}^c)}{(1-\omega)[\exp(\beta a_{t-1}^f) + \exp(\beta a_{t-1}^c)] + \omega} \tag{3.14b}$$

$$n_t^i = 1 - n_t^f - n_t^c \tag{3.14c}$$

where the parameter ω represents the share of the population which is inactive from the market.

3.4 Estimation

In this section, the Method of Simulated Moments is applied to the model (SSV augmented with inactive traders) just described. In order to follow this method of estimation, one has to first select the moments of interest. Following the approach developed by the authors just mentioned [4], only four stylized facts that have received more attention in the literature are considered here, namely the absence of autocorrelation in raw returns, fat tails of returns distribution, volatility clustering, and long memory. Therefore, it is argued that the following set of nine moments is enough to account for these four stylized facts, namely the Hill estimator of tail index of absolute returns $H(v)$, mean of the absolute returns $\bar{v}$, first-order autocorrelation of the raw returns $ac_1(r)$, and six different lags from the autocorrelation function of the absolute returns $ac_1(v)$, $ac_5(v)$, $ac_{10}(v)$, $ac_{25}(v)$, $ac_{50}(v)$, and $ac_{100}(v)$. Each single run of the model will then be compared with a specific empirical data set with regard to this vector of selected moments.

The distance between the moments vector m generated by a single run of the model (with set of inputs θ, sample size S, and random seed c) and the vector of empirical moments m^{emp} is defined by a weighted quadratic loss function in the following form

$$J = J[m(\theta, S, c)] = (m(\theta, S, c) - m^{emp})' W (m(\theta, S, c) - m^{emp}) \tag{3.15}$$

where W is a weighting matrix that intends to capture both correlation between individual moments and sampling variability.

Among several options for choosing a proper weighting matrix W, here the inverse of the estimated variance-covariance matrix of the moments $\hat{\Sigma}$ is used. In order to estimate such a matrix, the following bootstrapping method was applied. For the first and second moments ($H(v)$ and $\bar{v}$), $B = 10^6$ random resamples with replacement were constructed from the original series, and the respective moments were calculated. However, since the other moments deal with autocorrelations, such a procedure would be inadequate due to the destruction of long-term dependencies by the sampling procedure. Therefore, for these moments, an index-bootstrapping method was used by randomly selecting (with replacement) B set of time indexes $I^b = t_1^b, t_2^b, \ldots, t_1^T$ from indexes and then calculating the correlation coefficient regarding time lag h as $\gamma^b(h) = (1/T) \sum_{te I^b} (v_t - \bar{v})(v_{t-h} - \bar{v})$, where $\bar{v}$ is the mean value of v_t over T, T is the length of the original time series, and $v_{t-h} = \bar{v}$ if $t - h \leq 0$.

Considering m^b as the vector of moments of each of these bootstrapped resamples and $\bar{m}$ as the vector of their moment specific means, the variance-covariance matrix was, thus, estimated as $\hat{\Sigma} := (1/B) \sum_{b=1}^{B} (m^b - \bar{m})(m^b - \bar{m})'$, and finally $W = \hat{\Sigma}^{-1}$. Finally, the minimization problem $J[m(\theta, S, c)] = \min_{\theta}!$ was performed by the Nelder-Mead simplex algorithm to estimate the set of parameters θ that minimizes the loss function J. Here, only seven parameters (as defined in subsections 3.3.2 and 3.3.3) were allowed to vary, namely ϕ, χ, α_x, α_d, σ_f, σ_c, and ω where the remaining were fixed at $p^* = 0$, $\mu = 0.01$, $\alpha_0 = -0.327$, and $\beta = 1$. μ and β are just a matter of scale, and the starting value for α_0 (the predisposition parameter to switch to fundamentalism) results from manual calibration.

Starting from an initial set of parameters θ_i, the algorithm returns an estimated set of parameters θ and a value for the objective function J. To reduce the chances of getting trapped in a local minima, this obtained set of estimated parameters θ was re-introduced in the algorithm here as the initial set of parameters (that is, $\theta_i = \theta$), and this procedure was carried out as many times it was necessary until no improvement higher than 0.001 was achieved in the objective function.

3.5 Experiment on Simulation Horizon Requirements

In order to reduce sample variability, [4] points that a model simulation horizon S ten times bigger than the empirical size T (that is, $S = 10T$) was considered sufficient for their model comparison purposes. The main objective of this study is to assess how such results change when one increases simulation horizon beyond this value. For doing so, first it will be described in more detail how a model specific p-value is calculated by means of Monte Carlos runs, and then the comparison of these p-values calculated using both $S = 10T$ and $S = 100T$ will be presented. The same empirical reference time series presented in figure 3.2 will be used in this section.

3.5.1 Definition of a model specific p-value

Apart from providing the variance-covariance matrix, the bootstrap procedure of empirical data described in the previous section can also be used to assess the fit of different model simulations to real data. This idea, presented in [4], consists of calculating the value of the objective function J for each of the vector of moments m^e obtained by bootstrapping empirical data $E = 5000$ times, and then finding a critical value J_{critic} which represents the 95% quantile of the distribution of the objective function values. This critical value was found to be $J_{0.95} = 17.228$. In this sense, if a simulation run from a given model presents a value of the objective function higher than $J_{0.95}$, this run cannot be said to have a good fit to empirical data. Finally, the p-value of a model is given by the proportion of Monte Carlo runs which lies below this critical value. Figure 3.3 presents the distribution of objective function values obtained by bootstrapping empirical data, and its correspondent critical value.

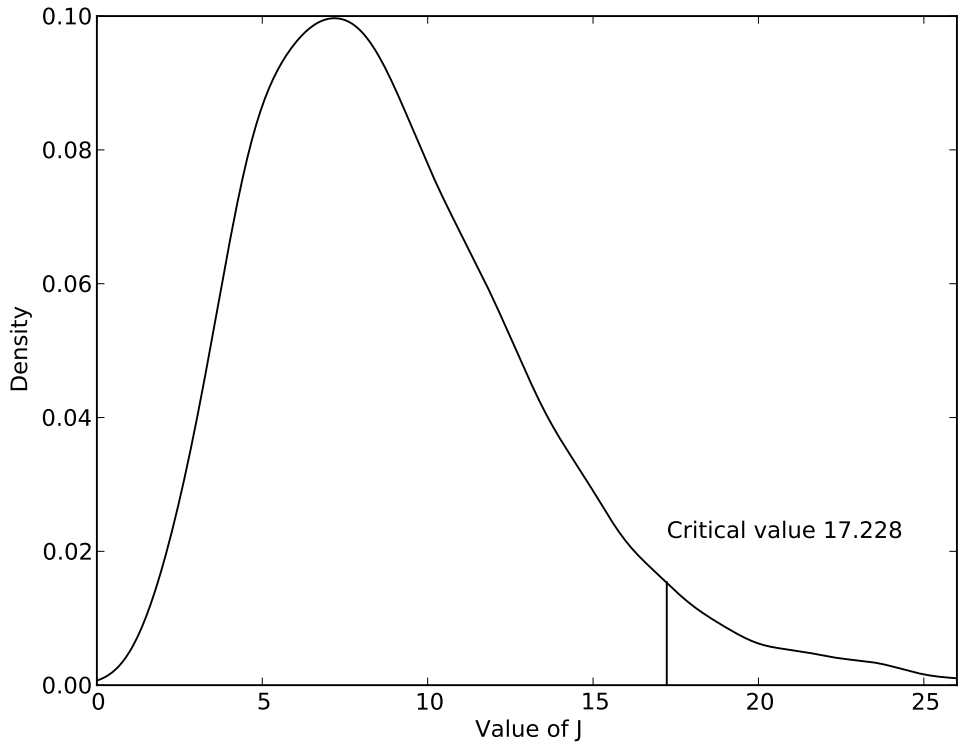

FIGURE 3.3: Distribution of objective function values obtained by bootstrapping empirical data, and its correspondent critical value.

3.5.2 Model fit for different simulation horizons

To begin with, table 3.1 shows, for a given random seed, and considering the simulation horizon of $S = 10T$, the set of optimal parameters obtained by a single run of the model, and their correspondent value of J. Table 3.2 shows the moments obtained with this optimized set of parameters in this specific run of the model, and compares them with the empirical moments for S&P500 and their bootstrapped statistics. It can be seen that, at least with regard to this specific random seed, the moments obtained with the optimal set of inputs is found inside the bands provided by bootstrapping empirical data.

TABLE 3.1: Estimated parameters for a given random seed, considering a simulation horizon of $S = 10T$.

J	ϕ	χ	α_x	α_d	σ_f	σ_c	ω
11.744	0.914	2.077	0.992	0.890	1.359	2.049	0.548

In order to check whether these results depend on the given pseudo-random number sequence, a similar estimation procedure to the one just described was carried on while

TABLE 3.2: Moments obtained with optimized parameters for $S = 10T$, the empirical moments for S&P500 and their bootstrapped quantiles.

	$H(v)$	$\bar{v}$	$ac_1(r)$	$ac_1(v)$	$ac_5(v)$	$ac_{10}(v)$	$ac_{25}(v)$	$ac_{50}(v)$	$ac_{100}(v)$
run	3.448	0.706	0.006	0.154	0.184	0.166	0.142	0.126	0.089
2.5	3.155	0.690	-0.018	0.128	0.163	0.148	0.125	0.107	0.075
mean	3.484	0.706	0.006	0.154	0.184	0.166	0.143	0.126	0.090
9.75	3.891	0.723	0.030	0.182	0.205	0.185	0.161	0.147	0.106

considering 1,000 different random seeds. Table 3.3 summarizes this Monte Carlo experiment by presenting the average and 5% bounds for the obtained optimized parameters and values of the objective function J. The p-value for this model (with inactive traders) and simulation horizon ($S = 10T$), calculated as described previously, is 0.290.

TABLE 3.3: Mean and bound values for parameters estimated for 1,000 different random seeds, considering a simulation horizon of $S = 10T$.

	J	ϕ	χ	α_x	α_d	σ_f	σ_c	ω
2.5	6.210	0.750	1.795	0.988	0.711	1.212	1.885	0.491
mean	18.833	0.948	1.962	0.993	0.964	1.328	2.075	0.538
97.5	62.944	1.160	2.184	0.998	1.098	1.538	2.178	0.597

Similarly, table 3.4 presents the same statistics as table 3.3, but now considering a longer simulation horizon of $S = 100T$. It can be seen that, although there is a larger variability for some of the estimated parameters, the resulting distribution of the values of the objective function presents much less extreme values. Figure 3.4 depicts this result, by showing the distribution of J both for a simulation horizon of $S = 10T$ (solid) and of $S = 100T$ (dashed). The obtained p-value for the longer case is 0.021, which is significantly smaller than for the shorter.

TABLE 3.4: Mean and bound values for parameters estimated for 1,000 different random seeds, considering a simulation horizon of $S = 100T$.

	J	ϕ	χ	α_x	α_d	σ_f	σ_c	ω
2.5	7.595	0.597	1.559	0.990	0.669	1.166	1.871	0.474
mean	10.702	0.961	1.952	0.991	0.928	1.379	2.030	0.546
97.5	16.268	1.301	2.217	0.992	1.184	1.642	2.218	0.609

The smaller values of the objective function J suggest that longer simulation horizons increase the ability of the model in reproducing the stylized facts. Table 3.5 presents two versions of a model contest, one for each simulation horizon $S = 10T$ and $S = 100T$. Figure 3.5 depicts this result, by showing the distribution of J for each pair of model-horizon. Although a significant reduction of sample variability is obtained by using larger simulation horizons, it can be seen that the central tendencies of each distribution of

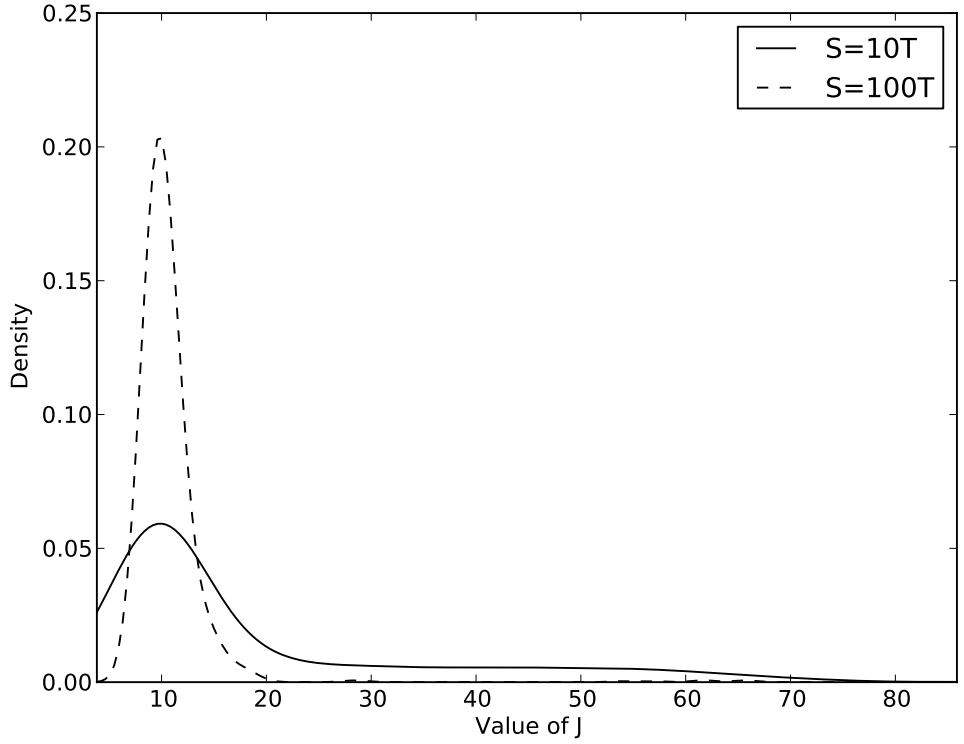

FIGURE 3.4: Comparison of the distributions of objective function values for simulation horizons of $S = 10T$ and $S = 100T$.

J do not change wildly with respect to S. In addition to that, there seems to be no improvements in parameter specification (facts shown by the larger width of the confidence intervals of parameters estimated with $S = 100T$). Hence, it is argued that, according to what was assumed in [4], $S = 10T$ is sufficient for these specific cases presented here.

3.5.3 Assessing the incorporation of inactive traders

The second objective of this investigation is to check for differences in goodness of fit of allowing inactive traders in one of the Structural Stochastic Volatility models proposed by [5]. It can be seen that the introduction of inactive traders improves the goodness of fit in both versions. It could be argued that the introduction of this more realistic feature indeed produces time series which are closer to the empirical reference from actual markets with respect to some selected stylized facts, regardless of the simulation horizon the model was allowed to run.

TABLE 3.5: Model contest to asses the improvement in goodness of fit when allowing inactive traders in SSV models using different simulation horizons. Although a significant reduction of sample variability is obtained by using larger simulation horizons, it can be seen that the central tendencies of each distribution of J do not change wildly with respect to S. In addition to that, there seems to be no improvements in parameter specification (facts shown by the larger width of the confidence intervals of parameters estimated with $S = 100T$). Hence, it is argued that, according to what was assumed in [4], $S = 10T$ is sufficient for these specific cases presented here.

	J	ϕ	χ	α_x	α_d	σ_f	σ_c	ω
DCA ($S = 10T$)	pvalue	0.349						
2.5	10.175	0.952	1.067	0.988	1.487	0.555	1.567	–
mean	16.451	1.063	1.222	0.991	1.613	0.607	1.643	–
97.5	27.151	1.191	1.338	0.993	1.725	0.655	1.732	–
DCA ($S = 100T$)	pvalue	0.051						
2.5	13.362	0.939	1.085	0.990	1.448	0.584	1.602	–
mean	15.518	1.072	1.227	0.991	1.607	0.607	1.632	–
97.5	17.530	1.218	1.339	0.992	1.750	0.624	1.666	–
DCA-I ($S = 10T$)	pvalue	0.290						
2.5	6.210	0.750	1.795	0.988	0.711	1.212	1.885	0.491
mean	18.833	0.948	1.962	0.993	0.964	1.328	2.075	0.538
97.5	62.944	1.160	2.184	0.998	1.098	1.538	2.178	0.597
DCA-I ($S = 100T$)	pvalue	0.021						
2.5	7.595	0.597	1.559	0.990	0.669	1.166	1.871	0.474
mean	10.702	0.961	1.952	0.991	0.928	1.379	2.030	0.546
97.5	16.268	1.301	2.217	0.992	1.184	1.642	2.218	0.609

Conclusion

In this chapter, the possible effects of the simulation horizon one allows the model to run was subject of investigation. The main objective was to check the following statement: if the simulation horizon is not sufficiently large, the resulting distribution may present frequent extreme points, which can lead to inaccurate results when one tries to compare different models. In order to answer to this question, a model contest was carried out using different simulation horizons to assess the difference in goodness of fit when inactive traders are introduced in one of the Structural Stochastic Volatility models proposed by [5].

It can be seen in figure 3.5 and in table 3.5 that the smaller values of the objective function J suggest that longer simulation horizons increase the ability of the model in reproducing the stylized facts. However, such results also show that the centroids of the distributions do not change (that is, the mean locations remain the same) when the model is simulated for a longer time horizon. While observing that there is no bias

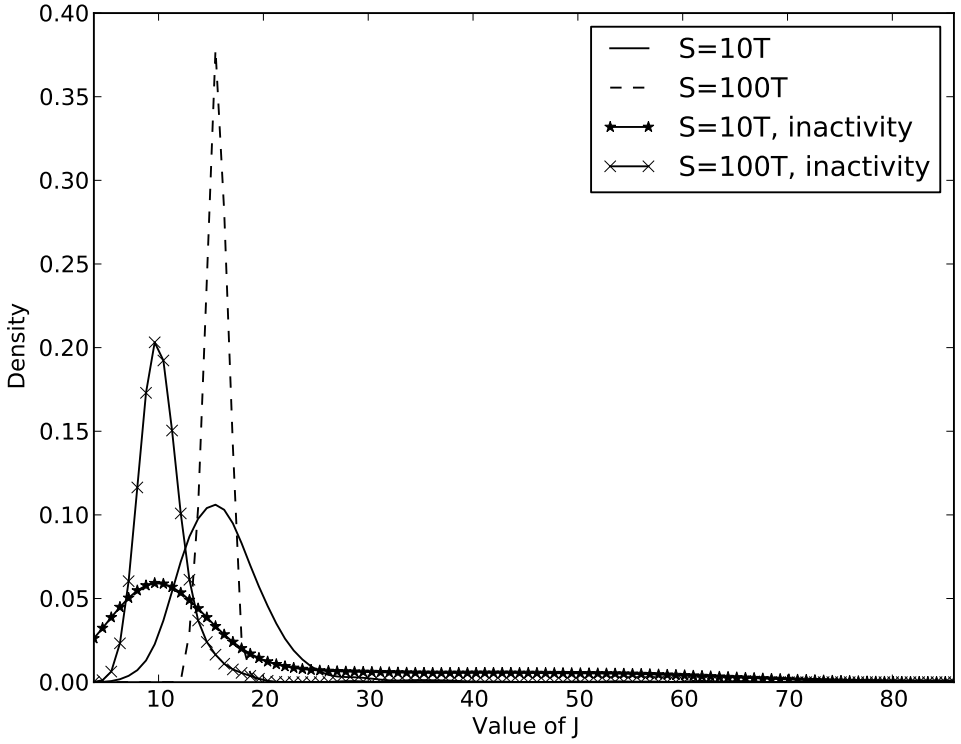

FIGURE 3.5: Comparison of the distributions of objective function values for simulation horizons of $S = 10T$ and $S = 100T$, and for inclusion/exclusion of inactive traders. The smaller values of the objective function J suggest that longer simulation horizons increase the ability of the model in reproducing the stylized facts.

introduced by reducing the simulation horizon from 100 to 10 times the empirical time horizon, it is then argued that, according to what is assumed in [5], simulating the model 10 times longer than the empirical time horizon is sufficient for the proposed model contest purposes.

The second objective of the investigation dealt with the improvements in goodness of fit brought by the inclusion of inactive traders in one of the Structural Stochastic Volatility (SSV) models proposed by [5]. By allowing agents also to hold their positions instead of going to the market every day, the model yields better goodness of fit when compared to the standard two agent types model, as can be seen by the smaller values of the objective function shown. By allowing agents to be inactive for some periods of time, the model gains a more realistic feature, and, hence, is able to better reproduce the stylized facts represented by the selected moments of interest.

With respect to the first objective, it is concluded that there is no bias in using smaller simulation horizons, although a smaller sample variability is achieved when the model is let to simulate for longer time horizons. Such results confirm the assumption made by [5], namely, to let the model run ten times longer then the reference empirical time series used in the process of estimation. Considering the second objective of this investigation, it can clearly be seen a significant improvement in terms of goodness-of-fit in allowing traders to be inactive for some periods of time. It seems that the incorporation of this realistic feature in the SSV models make them produce synthetic price time series which resemble more closely those observed in actual markets.

Chapter 4

Testing for non-linear structures in artificial financial data: A Recurrence Quantification Approach

Introduction

According to [3], early applications of empirical methods from chaos theory suggested the existence of low dimensional chaotic motion in empirical financial data. However, such results were questioned, and it is then believed that the search for low dimensional chaos in financial data was not successful. On the other hand, the independent and identically distributed (IID) hypotheses is often rejected, at the same time that raw returns present quite small degree of autocorrelation. These facts suggest that prices in financial markets do not behave completely at random, although their hidden structures seem more complex than those observed in low dimensional chaotic systems.

By considering artificial data generated from the Lux-Marchesi microscopic model [6], the aforementioned authors state that the resulting price dynamics appear less random than the pseudo-random numbers used as shocks to the fundamental price of the model. This is the case for the Lux-Marchesi model, and also for the Structural Stochastic

Volatility (SSV) model [4] discussed in the previous chapter. Such results are supported by the empirical chaos literature, where randomly reshuffled series usually lead to higher estimates of the so called correlation dimension.

Both models mentioned above are able to reproduce several of the stylized facts often observed in empirical financial data. For instance, the presence of a unit root in the price dynamics, the existence of heteroscedasticity (the so called volatility clustering) and the heavy tails in the distributions of returns, and the long term dependency of absolute returns. Along with all these structures usually found in empirical data is the very low autocorrelation of returns which makes the financial markets appear efficient, at least by considering the weak form of information efficiency from the Efficient Market Hypothesis.

Hence, the key result presented in [3] is that both simulated and empirical time series show traces of hidden structure, but apparently a more complicated one than that generated by low-dimensional deterministic dynamics. In order to check the significance of this behavior formally surrogate data tests are often applied [3]. The same path is followed in this chapter, but considering a different kind of non-linearity test based on the so called Recurrence Plot (RP) [73]. More specifically, the methodology described in [2] is applied to the time series generated by the Lux-Marchesi model as tested in [3] using BDS and Kaplan tests, and also to data generated by the Structural Stochastic Volatility (SSV) model proposed by [4] described in the previous chapter.

In the two next sections, simple chaotic systems (the logistic map and the Lorenz's attractor) are introduced in order to highlight the properties of the Recurrence Quantification Analysis (RQA) for detecting non-linearity or chaos in time series. RQA is a method of analyzing dynamical systems originally proposed by [74], and it is carried out by calculating some complexity measures on the Recurrence Plot (RP), which is a graphical representation of how often in time a trajectory visits the neighbor regions of its phase space. The last section of the essay presents the application of the surrogate tests for non-linearity or chaos based on the RQA complexity measures to synthetic data set generated from the two models mentioned above. The interest is comparing these results to those based on other tests for non-linearity or chaos presented by [3].

For instance, in the same way as pointed out by [3] and [2], the results presented here are unstable because both acceptance and rejection of linearity can be found in different realizations of the same model. However, different complexity measures generally agree within each subperiod of data, suggesting both that the two models are able to reproduce the empirically observed alternating periods of high and low volatility, and that the *RQA* measures are able to discriminate between these periods. In addition, it is also stressed that the hypothesis of chaos or linearity is rejected for the majority of the subsamples, indicating that, if there is a deterministic process ruling the data, it is more complicated than the dynamics from low dimensional chaotic systems.

4.1 Recurrence Quantification Analysis

Recurrence Quantification Analysis (*RQA*) is a nonlinear method of analyzing dynamical systems originally proposed by [74]. It is carried out by calculating some measures on the so-called Recurrence Plot (*RP*), which is a graphical representation of how often in time a trajectory visits the neighbor regions of its phase space.

This section is divided as follows: first, the Lorenz's attractor is used as an example for outlining the required procedures in the creation of a *RP*. Then, selected *RQA* measures are calculated to different parameters of the logistic map in order to illustrate their properties. The last part concludes by carrying out an *RQA*-based non-linearity test on artificial financial data generated by two different agent-based models.

4.1.1 Recurrence Plots

Recurrence plots (*RP*) were proposed by [73] as a tool for visualizing recurrences of dynamical systems. In order to build an *RP* for a given time series, one has to first reconstruct its phase-space trajectory. As stated by Takens' theorem [75], a topologically equivalent representation of the original high-dimension system can be reconstructed from a time sequence of observations of its states by means of the method of time delay. This procedure consists of generating, from the original time series X_t, the set of embedded vectors $X_t^m = X_t, X_{t+\tau}, X_{t+2\tau}, \cdots, X_{t+(m-1)\tau}$, where m is the underlying embedding dimension of the system, and τ is the time delay used in the reconstruction

of the phase space from a time series.

Among several methods for choosing an appropriate value for the embedding dimension m, [76] point that a heuristic approach is well suited when the final objective is to generate an RP. This approach consists of choosing a very high value for m ($m > 20$), and of sequentially decreasing its value until significant differences in the RP appear. Let m^* denote the value of m at this point. They state that this difference is due to the existence of false nearest neighbors, and, thus, a value of m a few dimensions higher than m^* should be enough for embedding.

Having reconstructed the phase space, the objective of an RP is to check for recurrence patterns, that is, to verify whether the system roughly returns to neighborhoods already visited in the past. To do so, how close two trajectories should be in order to be considered a recurrence has also to be defined. This is done by setting a critical value ϵ. Obviously, if ϵ is set to zero, then there would not be any recurrence at all and, on the other hand, if ϵ is sufficiently large, then every trajectory would be considered a recurrence.

Hence, an RP is a graphical representation of the square matrix of the distances between all paired time coordinates of the reconstructed phase space, where a point in the distance matrix is darkened if the distance is smaller than ϵ and not otherwise. In other words, a Heaviside function is applied to the distances of each pair of time coordinates obtained by the reconstructed phase space. By construction, the main diagonal of the distances matrix is always darkened (and it is called *line of identity* - LOI), and the idea of the RP is that if there is a significant amount of determinism in the system, then its phase-space trajectory will visit previous regions and, thus, the RP will show lines parallel to the main diagonal (LOI).

4.1.2 Lorenz System Example

The Lorenz system is a system of ordinary differential equations known for its chaotic behaviour. More specifically, it is both highly sensitive to initial conditions and able to generate complex orbits, although relatively simple and deterministic. The Lorenz equations are defined as

$$\dot{x} = \sigma(y - x) \tag{4.1a}$$

$$\dot{y} = x(\rho - z) - y \tag{4.1b}$$

$$\dot{z} = xy - \beta z \tag{4.1c}$$

where the notation $\dot{a}$ stands for $\frac{da}{dt}$, t represents the time unit, x, y, and z are the three-dimensional coordinates, and σ, ρ, and β are the system parameters. Following [77], figure 4.1 shows three two-dimensional perspectives of 100 simulation steps of the Lorenz system using $\sigma = 10$, $\rho = 28$, and $\beta = \frac{8}{3}$. The system exhibit chaotic solutions for these parameter values.

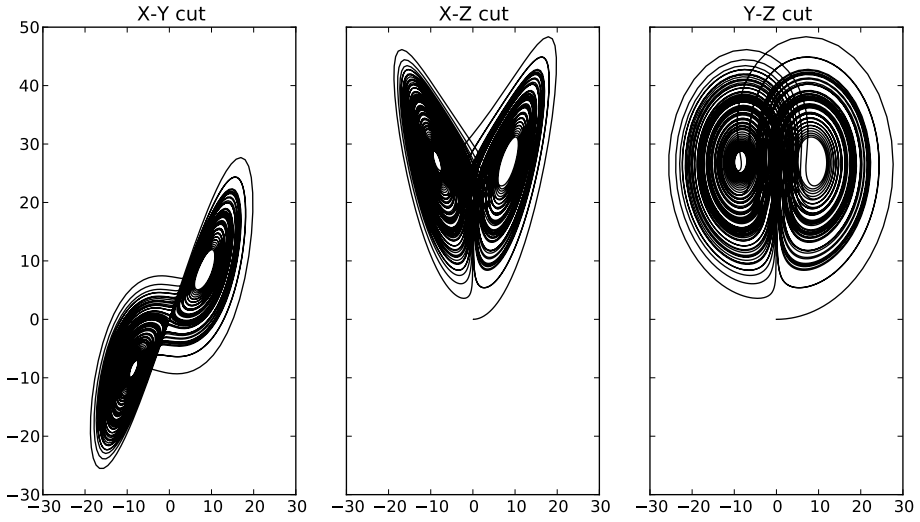

FIGURE 4.1: Three two-dimensional perspectives of 100 simulation steps of the Lorenz system using $\sigma = 10$, $\rho = 28$, and $\beta = \frac{8}{3}$. The system exhibit chaotic solutions for these parameter values

As an example, let us consider 1200 observations generated by the Lorenz system, which are presented together with its RP on the right panel of figure 4.2. On the left panel, the same experiment was reproduced, but the time series was randomly shuffled in order to break all existing structures. In the same way as in [78], here we have considered an embedding dimension $m = 5$, time delay $\tau = 5$, and critical distance value $\epsilon = 5$.

[78] summarizes three different structures that can be found in an RP, namely isolated dots, vertical lines, and diagonal lines. Single dots appear when states are rare or do not last enough time. A diagonal line occurs when a trajectory visits the same region

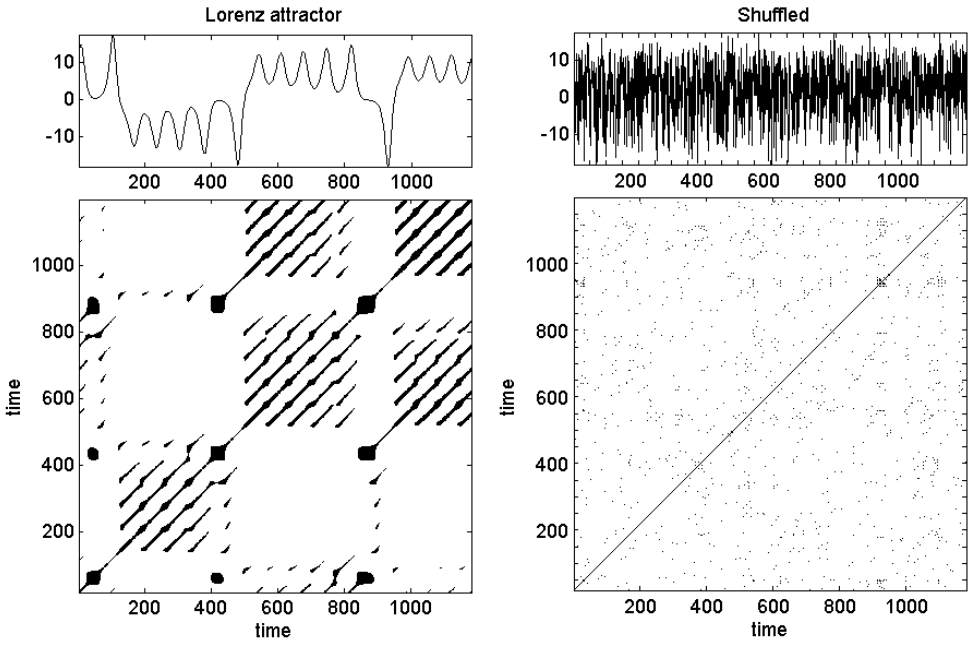

FIGURE 4.2: On the right panel, 1200 observations generated from the Lorenz's Attractor (upper panel) and its respective recurrence plot (lower panel), with embedding dimension $m = 5$, time delay $\tau = 5$, and critical distance value $\epsilon = 5$. On the left panel, the same experiment was performed, but with shuffled time series.

of phase space that it was in the past. Finally, a vertical line appears when the state of the system does not move, or moves too slowly, for a period of time.

4.2 Complexity Measures Based on the Recurrence Plot

Having seen that the recurrence plot is a powerful tool for analyzing dynamic systems, the *RQA* deals with measures which attempt to quantify the insights provided by the *RP*s. For instance, it is clear from figure 4.2 that the cyclical component of the Lorenz attractor is captured by the long diagonal lines shown in the lower left panel. [74] developed some measures based on the density and the diagonal structures of the *RP*, and [78] extended some of these measures considering vertical structures. In a *RP*, diagonal lines suggest that the system orbits two regions of the phase space in parallel for some time, while vertical lines indicate that only one region of the phase space is being visited during that period.

REC - Recurrence Rate

It consists of summing all darkened dots in the RP and dividing them by the total number of dots. Mathematically,

$$REC(m, \tau, \epsilon) = \frac{1}{N^2} \sum_{i,j=1}^{N} R_{i,j}^{m,\epsilon} \tag{4.2}$$

where N is the length of the RP, and R is the binary distance matrix.

As it can be seen in the equation above, REC measures the density of the RP. It is worth stressing that the REC measure can be adjusted by the radius ϵ defined in the previous section. Obviously, if one sets $\epsilon = 0$, then the RP will have no darkened points at all. On the other hand, if ϵ is set sufficiently large, then all points in the RP will be darkened. Apart from other options for choosing ϵ as just described, it is also a common approach to fix ϵ so that the REC measure of the RP equals a predetermined level. This approach will be developed in the surrogate non-linearity test of the next section.

DET - Determinism

This measure is calculated by dividing the sum of all darkened points that belong to a diagonal structure by the total number of darkened points. For deciding whether a recurrence point belongs or not to a diagonal structure, one has to additionally define a minimal line length l_{min}. The idea is that a deterministic system produces longer diagonal lines than stochastic ones. Thus, we have

$$DET(m, \tau, \epsilon, l_{min}) = \frac{\sum_{l=l_{min}}^{N} lp^{\epsilon}(l)}{\sum_{i,j=1}^{N} R_{i,j}^{m,\epsilon}} \tag{4.3}$$

where $p^{\epsilon}(l)$ is the frequency distribution of diagonal line lengths. It should be stressed that if $l_{min} = 1$ (that is, every isolated recurrence point belongs to a line of length 1), then $DET = 1$.

$RATIO$ - Ratio between DET and REC

The $RATIO$ measure is simply the ratio of DET and REC, as shown below

$$RATIO(m, \tau, \epsilon, l_{min}) = \frac{DET(m, \tau, \epsilon, l_{min})}{REC(m, \tau, \epsilon)} \tag{4.4}$$

In the extreme case where $l_{min} = 1$ (and, thus, $DET = 1$), $RATIO$ is equal to the reciprocal of REC. According to [79], in certain circumstances, this measure can be used to study phase transitions, because REC can decrease without a correspondent change in DET.

L - Average Diagonal Length

This measure gives an impression about how much time two trajectories remain close to each other, and is simply calculated by obtaining the average value of the line lengths defined by l_{min}. Therefore, we have

$$L(m, \tau, \epsilon, l_{min}) = \frac{\sum_{l=l_{min}}^{N} lp^{\epsilon}(l)}{\sum_{l=l_{min}}^{N} p^{\epsilon}(l)} \tag{4.5}$$

In this sense, the more often the system shows longer periods of recurrent orbits, the longer the average length of the diagonal lines.

L_{max} - Maximal Diagonal Length

This measure is simply given by the maximal diagonal line length in the RP. According to [79], it is related to the largest positive Lyapunov exponent.

$$L_{max}(m, \tau, \epsilon, l_{min}) = \max_{l=l_{min}}^{N} lp^{\epsilon}(l) \tag{4.6}$$

DIV - Divergence

Divergence is the reciprocal of L_{max}. The smallest the divergence, the longer is the maximal recurrent orbit in the system.

$$DIV(m, \tau, \epsilon, l_{min}) = \frac{1}{L_{max}} \tag{4.7}$$

ENT - Entropy

This measure consists of calculating Shannon entropy to the frequency distributions of diagonal line lengths and interpreting this as the complexity of the deterministic structure of the system. Thus, we have

$$ENT(m, \tau, \epsilon, l_{min}) = -\sum_{l=l_{min}}^{N} P(l) \ln P(l) \tag{4.8}$$

where

$$P(l) = \frac{p^{\epsilon}(l)}{\sum_{l=l_{min}}^{N} p^{\epsilon}(l)} \tag{4.9}$$

In this sense, ENT indicates the diversity of visited regions of the phase space. For instance, if the system visits very often a few specific regions of the phase space, and only occasionally lots of others regions, ENT will be low. In the extreme case of all regions being equally visited, ENT reaches its maximum value given by $N \log(N)$. However, as stated by [78], ENT depends heavily on l_{min} (that is, the bin size for creating the frequency distribution of line lengths).

LAM - Laminarity

This measure is analogous to DET, but with regard to vertical lines. Vertical structures in a Recurrence Plot indicate stationarity in a specific region of the phase space. It is calculated by dividing the sum of all darkened points that belong to a vertical structure by the total number of darkened points. Thus, we have

$$LAM(m, \tau, \epsilon, v_{min}) = \frac{\sum_{v=v_{min}}^{N} v p^{\epsilon}(v)}{\sum_{i,j=1}^{N} R_{i,j}^{m,\epsilon}} \tag{4.10}$$

where v_{min} is the minimal length to define a vertical line.

V_{max} - Maximal Vertical Length

This measure is simply given by the maximal vertical line length in the Recurrence Plot.

$$V_{max}(m, \tau, \epsilon, v_{min}) = \max_{v=v_{min}}^{N} vp^{\epsilon}(v) \tag{4.11}$$

4.2.1 Logistic Map Example

The logistic map is an early example of an apparently simple mathematical model presenting very complicated dynamics [80]. It consists of a polynomial mapping of degree 2 in the following form:

$$x_{n+1} = rx_n(1 - x_n) \tag{4.12}$$

where x_n is defined in $[0, 1]$ and can be interpreted as the ratio between some current population at time n and the environment total capacity, which is assumed to be fixed. The initial population ratio x_0 has also to be assumed. The growth parameter r can be any positive number, although the population ratio interpretation only holds for $r \leq 4$. For higher values of r, x does not respect the $[0, 1]$ range.

Figure 4.3 shows different realizations of two hundred observations of the logistic map for varying values of r. It can be seen that for values of r below 3 there is always a fixed point as long term value, while for values higher than 3 periodic orbits of increasing order start to appear. Finally, for values higher than about 3.57 the logistic map exhibits chaotic behavior. This value is the onset of chaos; most values beyond this threshold (except from some islands of stability such as for $r = 3.83$) present extreme sensitivity to initial conditions and the orbit periods are no longer finite.

These facts are also illustrated by the bifurcation diagram depicted in figure 4.4. Note that the bifurcation diagram shows the possible long term outcomes of x_n in the vertical axis with respect to different values of the bifurcation parameter (which here is r) in the horizontal axis. It can be seen period-doubling bifurcations for values of r higher than 3, while for values higher than about 3.57 the orbit periods are no longer finite.

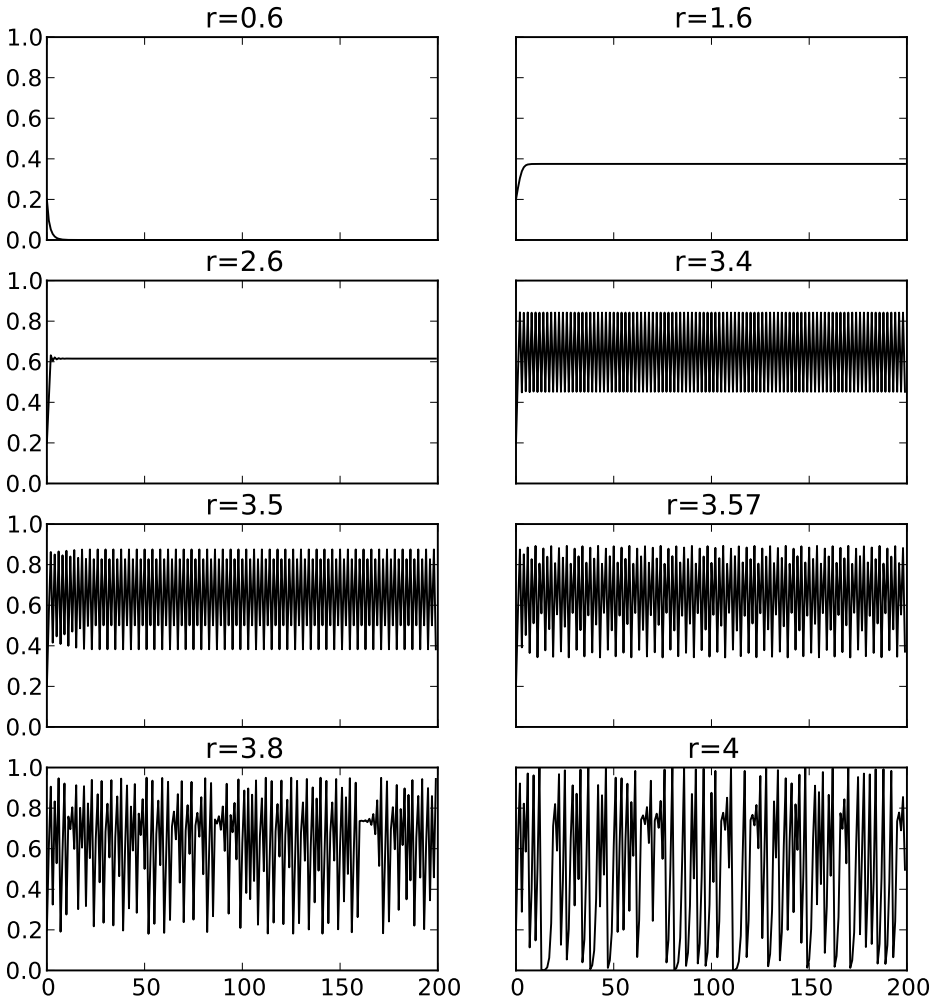

FIGURE 4.3: Different realizations of two hundred observations of the logistic map for varying values of r. It can be seen that for values of r below 3 there is always a fixed point as long term value, while for values higher than 3 periodic orbits of increasing order start to appear.

As an illustration, figure 4.5 shows the time series generated by the logistic map with four different values of the growth parameter, their respective RP, and selected RQA measures. The respective calculated values are shown in table 4.1. It can be seen that for the stable value $r = 3.83$ the majority of the RQA measures are different from the other three chaotic values.

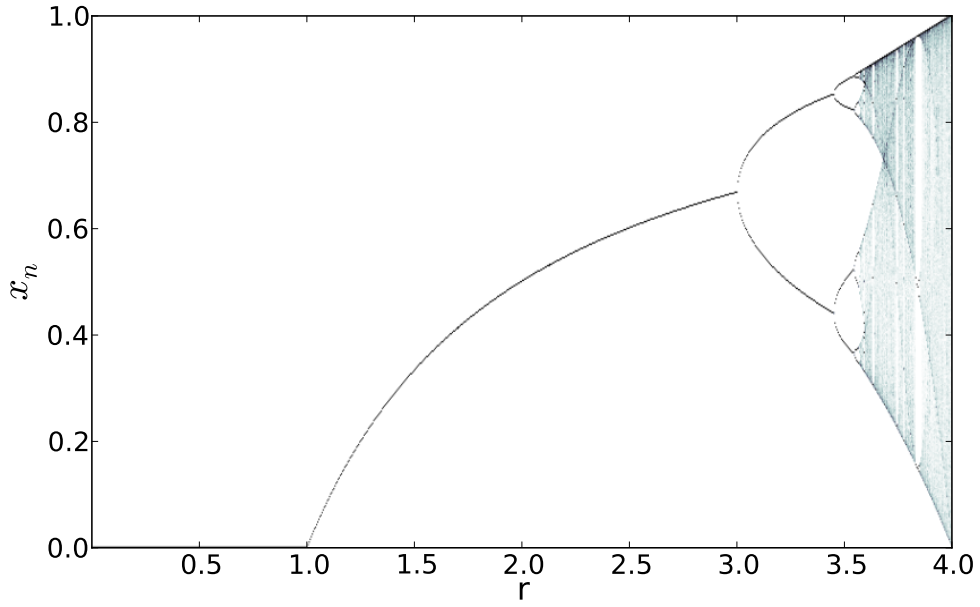

FIGURE 4.4: Bifurcation diagram showing the possible long term outcomes of x_n in the vertical axis with respect to different values of the bifurcation parameter (which here is r) in the horizontal axis. It can be seen period-doubling bifurcations for values of r higher than 3, while for values higher than about 3.57 the orbit periods are no longer finite.

TABLE 4.1: Selected *RQA* complexity measures for four time series generated by different growth parameters of the logistic map. It can be seen that for the stable value $r = 3.83$ the majority of the *RQA* measures are different from the other three chaotic values.

	$r = 3.679$	$r = 3.72$	$r = 3.83$	$r = 4$
REC	0.072	0.051	0.333	0.039
DET	0.817	0.751	1.000	0.552
L_{max}	19	13	195	7
DIV	0.053	0.077	0.005	0.143
$RATIO$	11.281	14.807	2.999	14.285
LAM	0.536	0.092	0.000	0.005
V_{max}	8	9	1	3
ENT	2.783	2.762	6.000	1.786

4.3 Surrogate Linearity Test Based on Recurrence Quantification

This section presents details of the application of surrogated non-linearity tests on the data generated by two different artificial market models (proposed by [4] and [6]). According to [78], a satisfying theoretical study on the properties of the measures described in the previous section is yet to be developed. However, with regard to stationary time

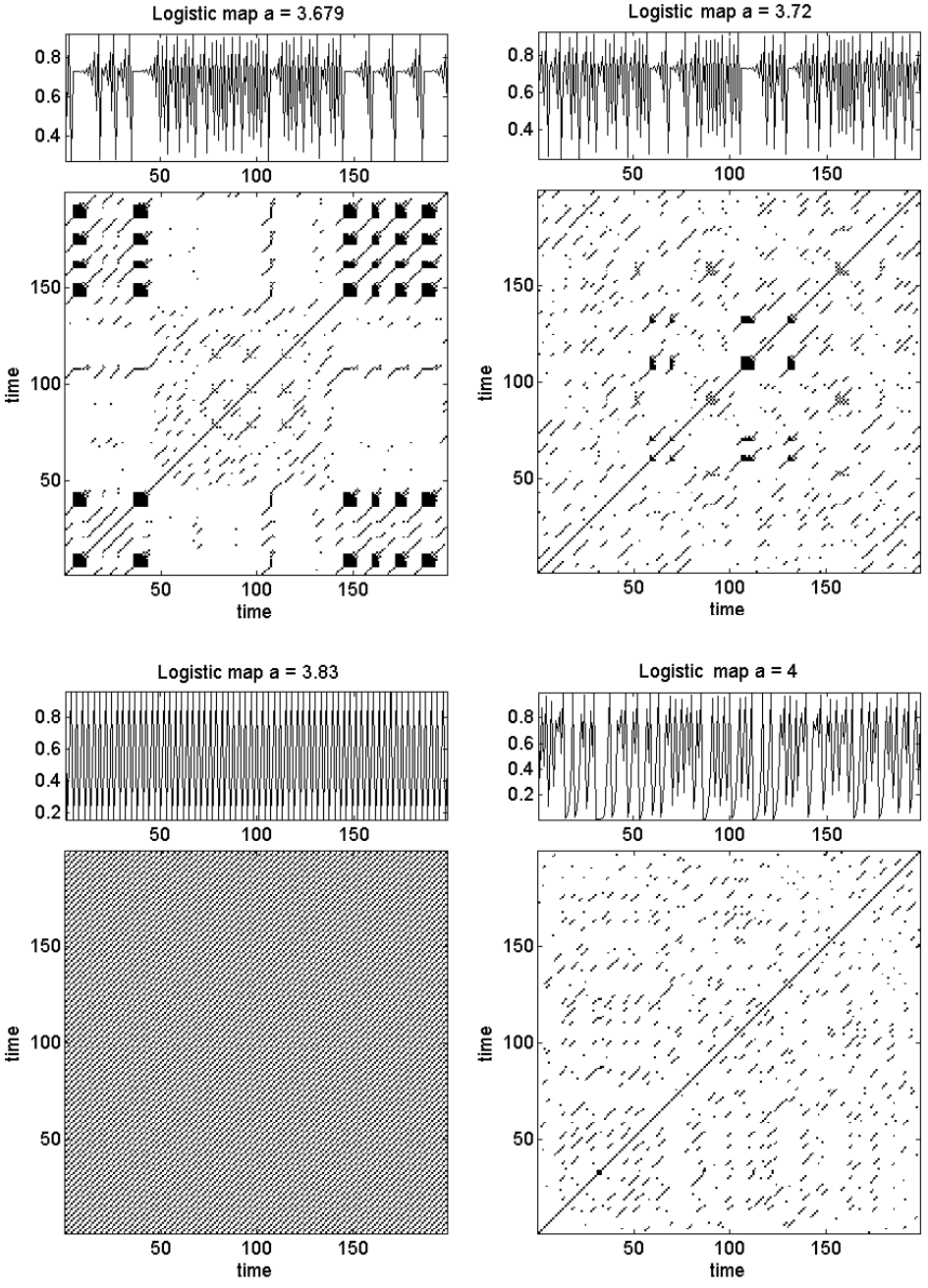

FIGURE 4.5: Time series generated by four different growth parameters of the logistic map and their respective recurrence plots.

series, significance levels of RQA measures can be assessed by means of surrogate tests. Here, the method described by [81] called *Iterative Amplitude Adjusted Fourier Transform* is applied to generate the surrogate copies.

Following [2] when testing for linearity on artificial financial data generated by Lux-Marcehsi model [6], a total sample size of $40,000$ observations was created and divided into 20 subsamples of $2,000$ each. For each of these subsamples, 20 surrogate copies were produced, and their RQA measures were then compared with the original subsamples. Here, again as in [2], focus was given to four of the RQA measures, namely REC, DET, ENT and L_{max}. The parameters for all tests are $m = 15$, $\tau = 1$, ϵ is endogenously determined aiming a fixed 5% REC in the original series [78], and $l_{min} = 3$. The null hypothesis of linearity is rejected with regard to one of these measures if all surrogated copies from a specific subsample present values smaller than the value from their respective subsample. Results are summarized in tables 4.2 and 4.3.

It can be seen that the null hypothesis of linearity is rejected 19 times out of 20 subsamples when considering the REC and DET measures, 17 times when considering ENT, and 15 times for L_{max}. According to the conclusions provided by [2], the RQA approach seems to be a very promising test for complexity in the financial time series. These results add evidence to support the rejection of linearity or low dimensional chaotic motion in the artificial financial time series generated from both microscopic models analysed here.

As can be seen from tables 4.2 and 4.3, results from both tests are similar within subperiods, but are are not within subsamples. Interestingly, comparing test results with the visual appearance of the relevant parts of the time series, there seems to be a general tendency towards rejection in periods with larger fluctuations, while in periods with moderate volatility linearity is not rejected in both models.

For instance, in the same way as pointed out by [3] and [2], both acceptance and rejection of linearity are found in different realizations of the same model. However, different complexity measures usually agree within subperiods, suggesting both that the two models are able to reproduce the empirically observed alternating periods of high and low volatility and that the RQA measures are able to discriminate between these periods, as shown in figure 4.6. It can be seen that, for both models, the null hypothesis

of linearity is accepted if subsample volatility is low, and rejected otherwise.

Figures 4.7, 4.8, 4.9, and 4.10 show Recurrence Plots of four subsamples from the time series depicted in figure 4.6. For instance, considering the Lux-Marchesi model, the null hypothesis of linearity is rejected by all measures in the subsample 8, and not rejected by all measures in subsample 19. Their Recurrence Plots are shown respectively in figures 4.9 and 4.10. In the SSV model, this same difference is higlighted by the Recurrence Plots of the subsamples 5 (null rejected by all measures) and 20 (null not rejected by all measures) (shown respectively in figures 4.7 and 4.8). It can be seen that, as also found by [2] and [3], the null hypothesis of linearity is often rejected in periods presenting high volatility dominated by speculative trading. During periods of low volatility, lower complexity os captured by the RQA measures and, thus, it is easier to accept the null hypothesis of linearity.

In addition, it is also stressed that the hypothesis of chaos or linearity is rejected for the majority of the subsamples, indicating that, if there is a deterministic process ruling the data, it is more complicated than the dynamics from low dimensional chaotic systems. When considering the RQA results for the Lux-Marchesi model presented here, it can be seen a great deal of aligment with tose results presented by [2]. For instance, the null hypothesis of linearity is rejected here 15 out of 20 with respect to the complexity measure REC (recurrence), while in the results presented by the aforementioned authors this number is 18. The same number of rejections (15) is found here and in their article when considering the DET (determinism)) measure. When considering the ENT (entropy) measure the results presented here show 2 rejections less than the authors (15 against 17), and when considering the L_{max} (maximum diagonal length) measure this difference is of 3 rejections (10 and 13).

Conclusion

The main interest in this chapter was to contrast the results presented by [3] with those computed here based on the Recurrence Quantification Analysis (RQA). More specifically, [3] tested for non-linearity or the presence of low dimensional chaos in artificial

TABLE 4.2: Results of non-linearity tests based on *RQA* complexity measures for the *SSV* model. It can be seen that results from different tests are similar within most subperiods. Comparing test results with the visual appearance of the relevant parts of the time series 4.6, there seems to be a general tendency towards rejection in periods with larger fluctuations.

Subsample	*REC*	*DET*	*ENT*	L_{max}
1	Reject	Reject	Reject	Reject
2	Reject	Accept	Reject	Accept
3	Reject	Reject	Reject	Reject
4	Reject	Reject	Reject	Reject
5	Reject	Reject	Reject	Reject
6	Reject	Reject	Reject	Reject
7	Reject	Reject	Reject	Reject
8	Reject	Reject	Reject	Accept
9	Reject	Reject	Reject	Reject
10	Reject	Reject	Reject	Reject
11	Reject	Reject	Reject	Reject
12	Reject	Reject	Reject	Reject
13	Reject	Reject	Reject	Reject
14	Reject	Reject	Reject	Reject
15	Reject	Reject	Reject	Reject
16	Reject	Accept	Reject	Accept
17	Reject	Reject	Reject	Reject
18	Reject	Reject	Reject	Reject
19	Reject	Reject	Reject	Accept
20	Accept	Accept	Accept	Accept

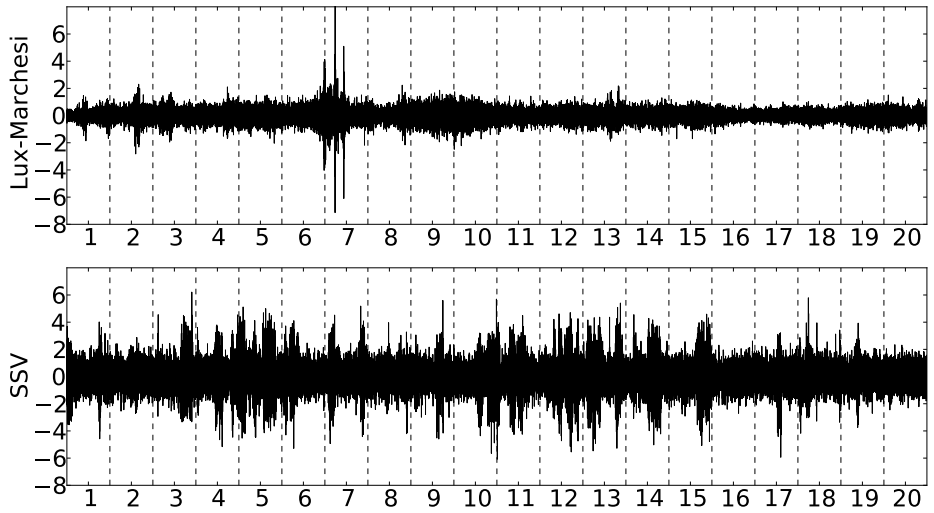

FIGURE 4.6: Artificial returns for the Lux-Marchesi and the *SSV* models. It can be seen in tables 4.2 and 4.3 that results from different tests are similar within most subperiods. Comparing test results with the visual appearance of the relevant parts of the time series, there seems to be a general tendency towards rejection in periods with larger fluctuations.

TABLE 4.3: Results of non-linearity tests based on RQA complexity measures for the Lux-Marchesi model. It can be seen that results from different tests are similar within most subperiods. Comparing test results with the visual appearance of the relevant parts of the time series 4.6, there seems to be a general tendency towards rejection in periods with larger fluctuations.

Subsample	REC	DET	ENT	L_{max}
1	Reject	Reject	Reject	Reject
2	Reject	Reject	Reject	Reject
3	Reject	Reject	Reject	Reject
4	Reject	Reject	Reject	Accept
5	Accept	Accept	Accept	Accept
6	Reject	Reject	Reject	Reject
7	Reject	Reject	Reject	Reject
8	Reject	Reject	Reject	Reject
9	Reject	Reject	Reject	Accept
10	Reject	Reject	Reject	Reject
11	Accept	Accept	Accept	Accept
12	Reject	Reject	Reject	Accept
13	Reject	Reject	Reject	Reject
14	Accept	Accept	Accept	Accept
15	Reject	Reject	Reject	Accept
16	Reject	Reject	Reject	Reject
17	Accept	Accept	Accept	Accept
18	Reject	Accept	Reject	Accept
19	Accept	Accept	Accept	Accept
20	Reject	Reject	Reject	Reject

financial data generated from the Lux-Marchesi model by means of the BDS and Kaplan tests. Here, the same methodology described in [2] is applied to artificial data from the Lux-Marchesi model, and also for the Structural Stochastic Volatility (SSV) model detailed in the previous chapter. In the first two sections the RQA approach was shown to be powerful by presenting how it allows one to discriminate between the different periods of periodic orbits and chaotic motion of the logistic map. Finally, it was shown that the RQA approach is able to discriminate between periods of high and low volatility in artificial financial data, in the same way as pointed out by [3] using tradicional non-linearity tests.

Again in agreement with [3], it could be seen that the hypothesis of linearity is rejected for the majority of the subsamples of data generated from the Lux-Marchesi model. In this sense, this chapter extends and supports the results presented by [3] using a different non linearity test based on the RQA, and by checking if such results are confirmed in a different artificial market model (SSV). Finally, the final section of this chapter

brings evidence in agreement with [3] and [2] to support the rejection of linearity or low dimensional chaotic motion in the artificial financial time series generated from the two different microscopic models considered here.

Appendix D. Testing for non-linear structures in artificial financial data: A Recurrence Quantification Approach

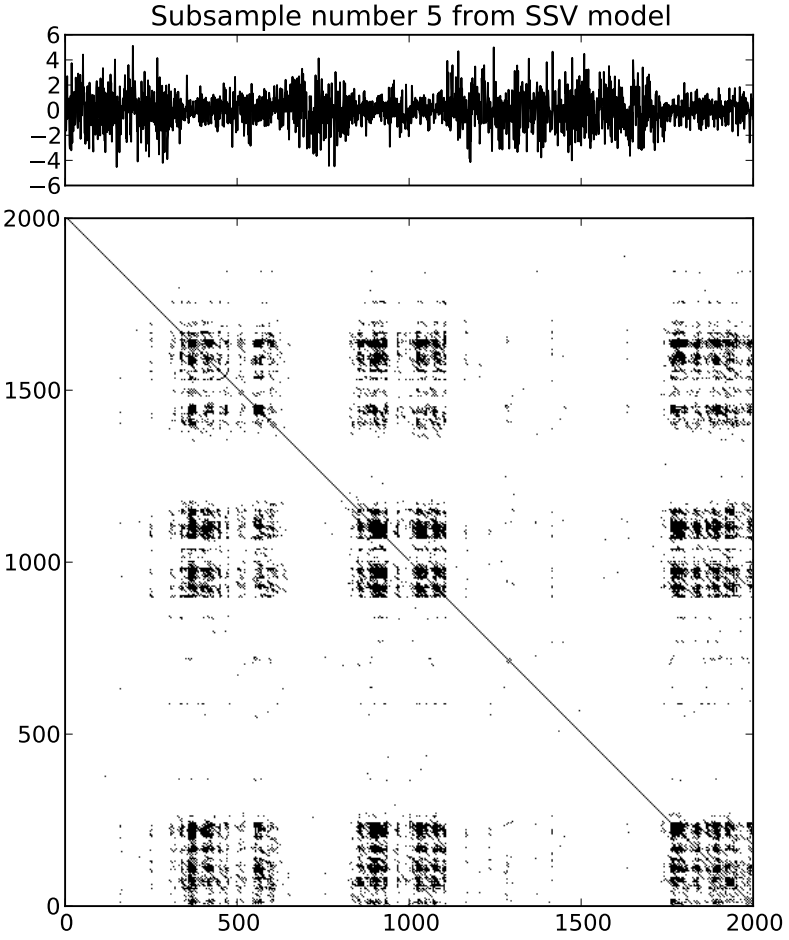

FIGURE 4.7: Subsample number 5 and its Recurrence Plot from the SSV model time series depicted in figure 4.6. The difference between this subsample and subsample number 20 is higlighted in their Recurrence Plots and in table 4.2. In subsample number 5, the null hypothesis of linearity is rejected by all four measures, while in the subsample number 20 the null is not rejected by any of the measures. It can be seen that, as also found by [2] and [3], the null hypothesis of linearity is more often rejected in periods presenting high volatility dominated by speculative trading. During periods of low volatility, the lower complexity of the time series is captured by the RQA measures, thus, making it is easier to the null hypothesis of linearity for being accepted.

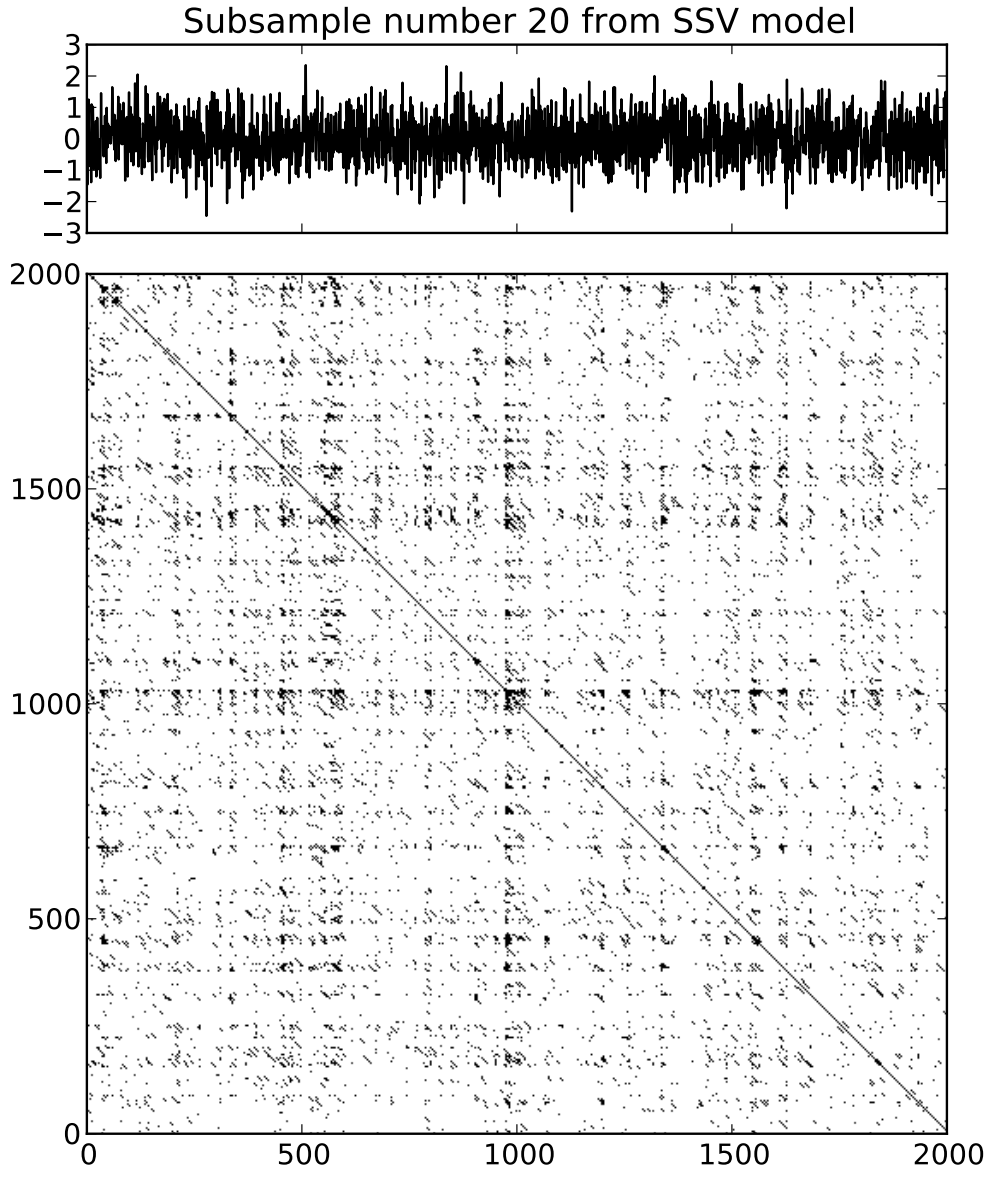

FIGURE 4.8: Subsample number 20 and its Recurrence Plot from the *SSV* model time series depicted in figure 4.6. The difference between this subsample and subsample number 5 is higlighted in their Recurrence Plots and in table 4.2. In subsample number 20, the null hypothesis of linearity is not rejected by any of the four measures, while in the subsample number 5 the null is rejected by all the measures. It can be seen that, as also found by [2] and [3], the null hypothesis of linearity is more often rejected in periods presenting high volatility dominated by speculative trading. During periods of low volatility, the lower complexity of the time series is captured by the *RQA* measures, thus, making it is easier to the null hypothesis of linearity for being accepted.

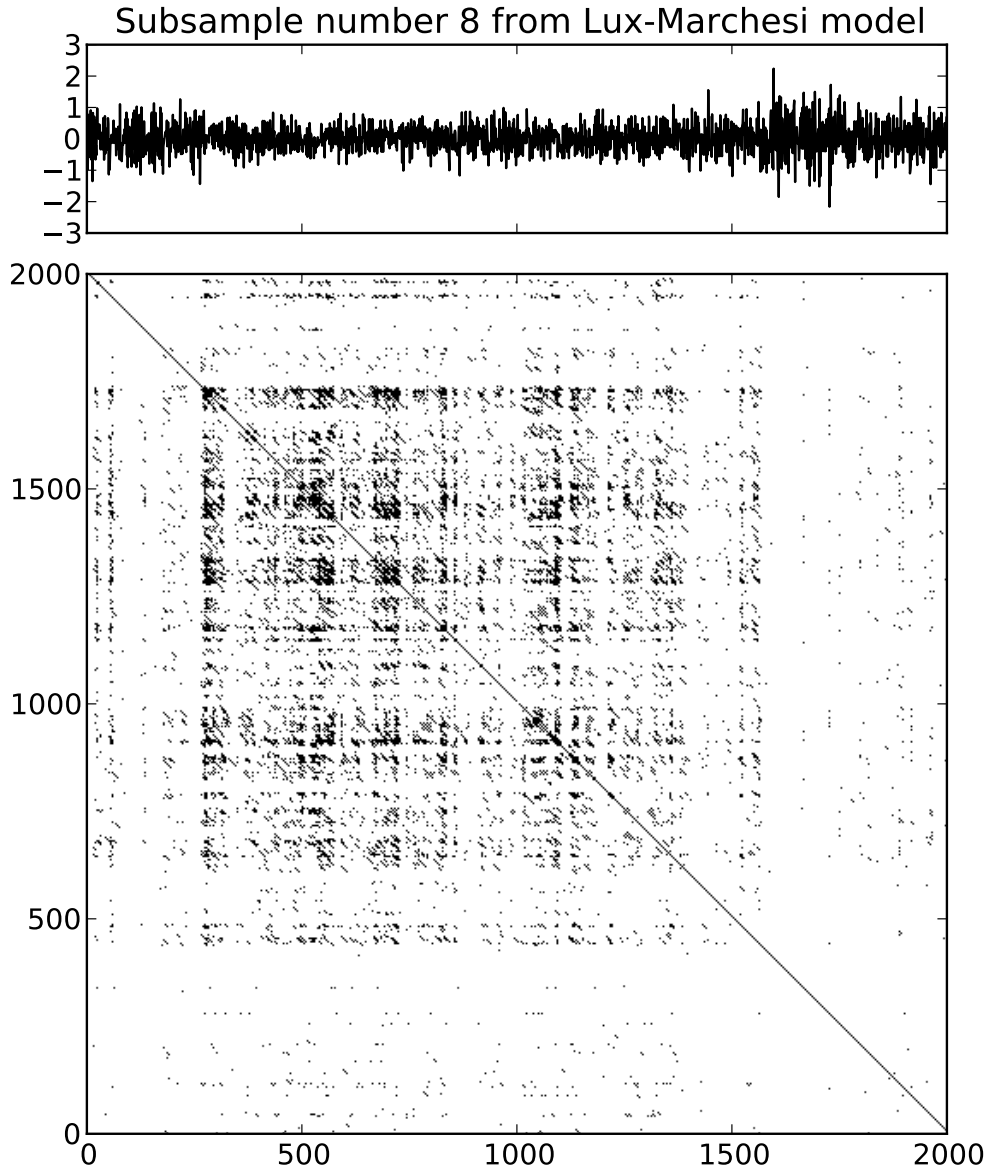

FIGURE 4.9: Subsample number 8 and its Recurrence Plot from the Lux-Marchesi model time series depicted in figure 4.6. The difference between this subsample and subsample number 19 is higlighted in their Recurrence Plots and in table 4.3. In subsample number 8, the null hypothesis of linearity is rejected by all four measures, while in the subsample number 19 the null is not rejected by any of the measures. It can be seen that, as also found by [2] and [3], the null hypothesis of linearity is more often rejected in periods presenting high volatility dominated by speculative trading. During periods of low volatility, the lower complexity of the time series is captured by the *RQA* measures, thus, making it is easier to the null hypothesis of linearity for being accepted.

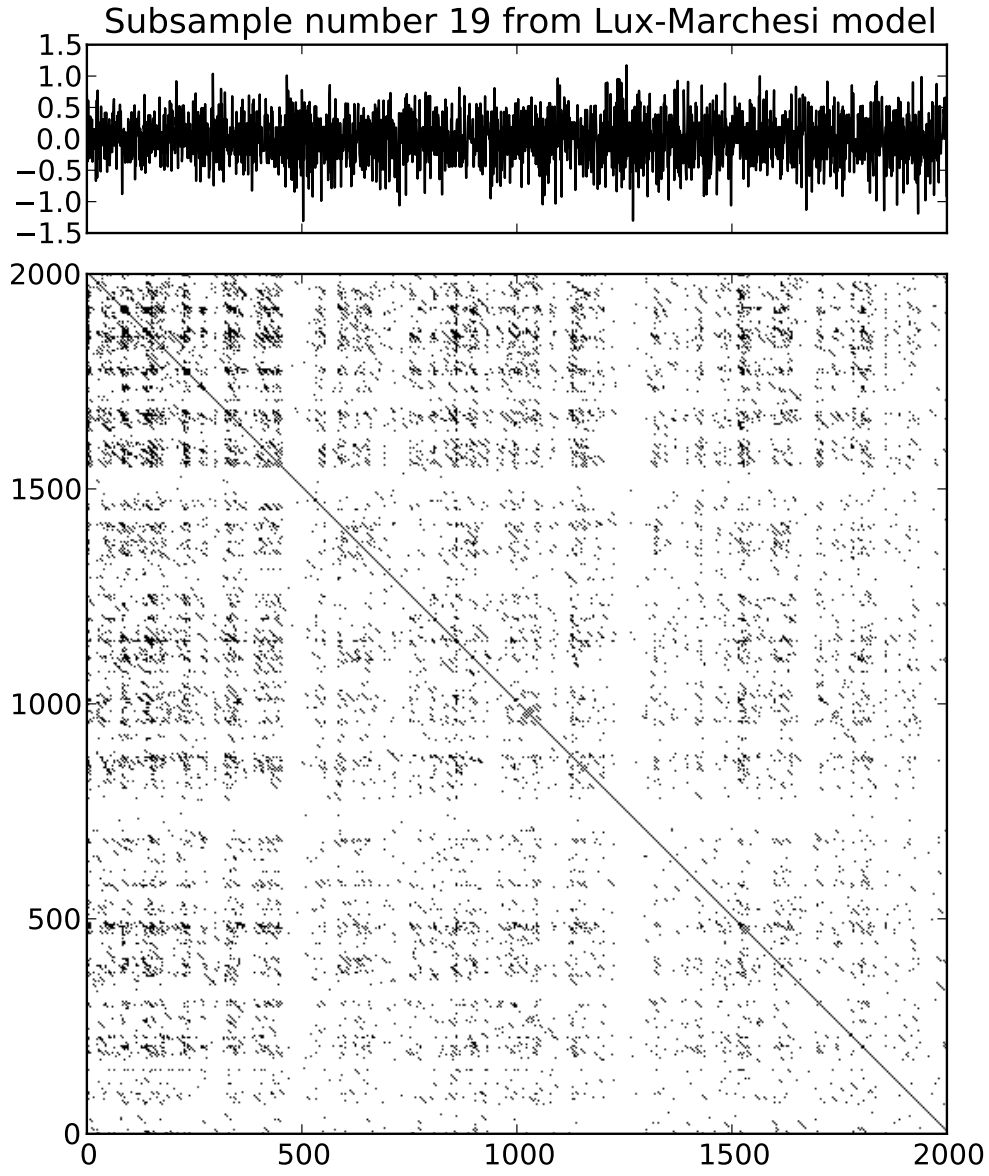

FIGURE 4.10: Subsample number 19 and its Recurrence Plot from the Lux-Marchesi model time series depicted in figure 4.6. The difference between this subsample and subsample number 8 is higlighted in their Recurrence Plots and in table 4.3. In subsample number 19, the null hypothesis of linearity is not rejected by any of the four measures, while in the subsample number 8 the null is rejected by all the measures. It can be seen that, as also found by [2] and [3], the null hypothesis of linearity is more often rejected in periods presenting high volatility dominated by speculative trading. During periods of low volatility, the lower complexity of the time series is captured by the *RQA* measures, thus, making it is easier to the null hypothesis of linearity for being accepted.

Conclusion

In the first chapter of this thesis several features of the networks formed by interlocking directorates were presented as stylized facts, meaning that their existence is widespread over a large and diverse set of economies. For instance, it could be seen that the accumulation of board positions by single individuals cannot be described by the simple random assignment of positions to directors, and, thus, other forces might drive its dynamics. It was also shown that interlocking networks present a large connected component, although this is not totally unexpected when a random graph is used as a benchmark.

Afterwards, the dichotomy between order and randomness presented in the Watts-Strogatz small world graphs was shown to account for the small world phenomena presented in empirical networks, and the preferential attachment process from the Barabási-Albert models able to account for the highly skewed degree distributions. In addition, it could also be seen that some countries engage in the global network of board members differently from the others. For instance, it was observed that a great deal of the absolute number of board directors, and the majority of the most central actors, are based in North Atlantic countries. With respect to the profile of the firms engaging in international interlocks, the lower country assortativity levels observed in companies with high degrees indicate that very well connected firms are responsible for sustaining a connected global network, while smaller and less connected firms usually engage only in domestic interlocking.

The special role of financial institutions could also be observed, mainly by means of their higher average centrality. Financial institutions also present a much larger board on average (up to 40% larger), meaning that for them it might be more worthwhile to engage in interlocks than for non financial institutions. Finally, evidence was shown

supporting that the rich club phenomenon is also a stylized fact of board membership networks, which is not accounted for by any of the random models described here. As in the case of the accumulation of board positions by individuals not being explained by a simple chance process, the higher level of intra-hub connectivity (the rich club phenomena) cannot be explained by the traditional models of preferential attachment, and thus, other factors might have influence on them.

The *rich-gets-richer* effect was used as an explanation for the existence of a very well connected core in the networks of interlocking directorates, a natural consequence of adding nodes at random and attaching them to already well connected nodes [49]. The main contribution of this essay is to show that the high levels of intra hub connectivity presented in real world interlocking networks cannot plausibly be seen as an outcome of chance (at least not from the preferential attachment scheme), and thus proper explanation for the phenomena is still required.

In the second chapter it was shown that all stylized facts described in the first chapter (such as smallworldness, the existence of a large connected component, and rich club phenomena) still hold in the Spanish specific case, considering a wider time span from 2004 to 2010. It was also shown that the network core persists over time regardless of personal turnover, and that the accumulation patterns of board positions by individuals observed in empirical data cannot be explained by a simple random binomial procedure.

By using firm specific data on profitability and leverage, no significant relation between network centrality and profitability could be observed. However, a negative significant relation between centrality and leverage was observed, indicating that interlocks might have been misused to guarantee special lending conditions not justifiable only by economic means. In addition, the chapter dealt with the highly capitalized Ibex companies as prominent actors of the network, the effective but not sufficient impact of a new gender equality regulation, and finally the advantage politicians have to jump from having one to two board positions.

In the third chapter of this thesis the possible effects of the simulation horizon one allows an agent based model to run was subject of investigation. More specifically, the main objective was to validate the following hypothesis: if the simulation horizon is not

sufficiently large, the resulting distribution may present frequent extreme points, which can lead to inaccurate results when one tries to compare different models. In order to answer to this question, a model contest was carried out using different simulation horizons to assess the difference in goodness of fit when inactive traders are introduced in one of the Structural Stochastic Volatility models proposed by [5].

It could be observed that the smaller values of the objective function being minimized suggest that longer simulation horizons increase the ability of the model in reproducing the stylized facts. However, such results also show that the center of the distributions does not change (that is, the mean locations remain the same) when the model is simulated for a longer time horizon. While observing that there is no bias introduced by reducing the simulation horizon, it is then argued that simulating the model 10 times longer than the empirical time horizon (as assumed in [5]) is sufficient for the proposed model contest purposes.

The second objective of the investigation was to check for possible improvements in goodness of fit brought by the inclusion of inactive traders in one of the Structural Stochastic Volatility (SSV) models. By allowing agents also to hold their positions instead of going to the market every day, the model yields better goodness of fit when compared to the standard two agent types model, as pointed by the smaller values of the objective function shown. By allowing agents to be inactive for some periods of time, the model gains a more realistic feature, and, hence, is able to better reproduce the stylized facts represented by the selected moments of interest.

Finally, in the last chapter, the attention was turned to the existence of non-linearity or chaos in artificial financial data generated from the Lux-Marchesi model, and from the Structural Stochastic Volatility (SSV) model detailed in the third chapter. According to [3], early applications of empirical methods from chaos theory arguably pointed to the existence of low-dimensional chaotic motion in empirical financial data. However, it is now believed that the search for low dimensional chaos in empirical financial data was not successful. This suggests that prices in financial markets do not behave in a perfectly random manner, although their hidden structures seem more complex than those produced by low dimensional chaotic systems.

The main objective of this chapter is to contrast the results presented by [3] with those using the Recurrence Quantification Analysis (RQA) approach. For doing so, two simple chaotic systems (the logistic map and the Lorenz's attractor) are introduced in order to highlight the properties of the Recurrence Quantification Analysis (RQA) for detecting non-linearity or chaos in time series. It could be seen, for instance, that the hypothesis of chaos or linearity is rejected for the majority of the subsamples, indicating that, if there is a deterministic process ruling the data, it is more complicated than the dynamics from low dimensional chaotic systems.

Bibliography

[1] A. Barrat and M. Weigt. On the properties of small-world network models. *The European Physical Journal B-Condensed Matter and Complex Systems*, 3(13):547–56, 1999.

[2] J. Belaire-Franch. Testing for non-linearity in an artificial financial market: a recurrence quantification approach. *Journal of Economic Behavior and Organization*, 54:483–494, 2003.

[3] S. Chen, T. Lux, and M. Marchesi. Testing for non-linear structure in an artificial financial market. *Journal of Economic Behavior and Organization*, 46(3):327–342, 2001.

[4] R. Franke and F. Westerhoff. Structural stochastic volatility in asset pricing dynamics: Estimation and model contest. *Christian-Albrechts-Universität zu Kiel. Department of Economics*, (Working Paper):1195–227, 2011.

[5] R. Franke and F. Westerhoff. Validation of a structural stochastic volatility model of asset pricing. *Christian-Albrechts-Universität zu Kiel. Department of Economics*, 2009.

[6] T. Lux and M. Marchesi. Scaling and criticality in a stochastic multi-agent model of a financial market. *Nature*, (387):498–500, 1999.

[7] A. Barabási and R. Albert. Emergence of scaling in random networks. *Science*, (286):509–512, 1999.

[8] G. Caldarelli. Scale-free networks: Complex webs in nature and technology. *Oxford University Presss*, pages 1236–1239, 2007.

[9] G. Davis, M. Yoo, and W. Baker. The small world of the american corporate elite, 1982-2001. *Strategic organization*, 1(3):301–326, 2003.

[10] J. McAuley, L. Costa, and T. Caetano. Rich-club phenomenon across complex network hierarchy. *Applied Physics Letters*, 91(8), 2007.

[11] J. McAuley, L. Costa, and T. Caetano. The rich-club phenomenon in the internet topology. *Communications Letters, IEEE*, 8(3):180–182, 2004.

[12] V. Colizza, A. Flammini, M. Serrano, and A. Vespignani. Detecting rich-club ordering in complex networks. *Nature physics*, 2(2):110–1815, 2004.

[13] N. Kashtan and A. Uri. Spontaneous evolution of modularity and network motifs. *Proceedings of the National Academy of Sciences of the United States of America*, 39(102):13773–13778, 2009.

[14] N. Kashtan and A. Uri. Boards of directors as an endogenously determined institution: A survey of the economic literature. *National Bureau of Economic Research*, (w8161), 2001.

[15] P. Haunschild and C. Beckman. When do interlocks matter? Alternate sources of information and interlock influence. *Administrative Science Quarterly*, pages 815–844, 1998.

[16] D. Palmer, B. Barber, X. Zhou, and Y. Soysal. The friendly and predatory acquisition of large US corporations in the 1960s: The other contested terrain. *American Sociological Review*, pages 469–499, 1995.

[17] C. Andres and M. Lehmann. Is busy really busy? Board governance revisited. *Working paper, WHU-Otto Beisheim Graduate School of Management*, pages 469–499, 2011.

[18] M. Mizruchi. What do interlocks do? An analysis, critique, and assessment of research on interlocking directorates. *Annual review of sociology*, pages 271–298, 1996.

[19] P. Haunschild. Interorganizational imitation: The impact of interlocks on corporate acquisition activity. *Administrative science quarterly*, pages 564–592, 1993.

[20] M. Useem. The inner circle: Large corporations and the rise of business political activity in the US and UK. *Oxford University Press*, pages 564–592, 1984.

[21] S. Tolbert and L. Zucker. Institutional sources of change in the formal structure of organizations: The diffusion of civil service reform, 1880-1935. *Administrative science quarterly*, 28:22–39, 1983.

[22] M. Milaković, M. Raddant, and L. Birg. Persistence of a network core in the time evolution of interlocking directorate. *Economics working paper/Christian-Albrechts-Universität Kiel, Department of Economics*, (10), 2009.

[23] K. Carroll, M. Fennema, and E. Heemskerk. Constituting corporate europe: A study of elite social organization. *Antipode*, 4(42):811–843, 2010.

[24] K. Carroll and M. Fennema. Is there a transnational business community? *International Sociology*, 3(17):393–419, 2002.

[25] C. Papadimitriou and M. Sideri. On the Floyd–Warshall algorithm for logic programs. *The Journal of Logic Programming*, 41(1):129–137, 1999.

[26] A. Hagberg, P. Swart, and D. Chult. Exploring network structure, dynamics, and function using networkx. *Los Alamos National Laboratory (LANL)*, (LA-UR-08-05495), 2008.

[27] M. Milaković, S. Alfarano, and T. Lux. The small core of the german corporate board network. *Kiel Institute for the World Economy Working Paper*, (1446):60–67, 2008.

[28] S. Milgram. The small world problem. *Psychology today*, 1(2):60–67, 1967.

[29] D. Newman, D. Watts, and S. Strogatz. Random graph models of social networks. *Proc. Natl. Acad. Sci. USA 99*, pages 2566–2572, 2002.

[30] P. Erds and A. Rnyi. On random graphs i. *Publ. Math. Debrecen*, (6):290–297, 1959.

[31] P. Erds and A. Rnyi. On the evolution of random graphs. *Publ. Math. Inst. Hungar. Acad. Sci.,*, (5):17–61, 1960.

[32] S. Granovetter. The strength of weak ties. *American journal of sociology*, pages 1360–1380, 1973.

[33] A. Rapoport and W. Horvath. A study of a large sociogram. *Behavioral Science*, 6 (4):279–291, 1961.

[34] M. Newman. Mixing patterns in networks. *Phys. Rev. Lett.*, 208701(89), 2002.

[35] R. Kroszner and P. Strahan. Throwing good money after bad? Board connections and conflicts in bank lending. *National Bureau of Economic Research*, (w8694), 2001.

[36] N. Fligstein and P. Brantley. Bank control, owner control, or organizational dynamics: Who controls the large modern corporation? *American Journal of Sociology*, pages 280–307, 1992.

[37] J. Bearden and B. Mintz. The structure of class cohesion: the corporate network and its dual. *Intercorporate relations: the structural analysis of business*, pages 187–207, 1987.

[38] R. Ratcliff. Banks and corporate lending: an analysis of the impact of the internal structure of the capitalist class on the lending behavior of banks. *American Sociological Review*, pages 553–570, 1980.

[39] D. Watts and M. Strogatz. Collective dynamics of small-world networks. *Nature*, (393):440–442, 1998.

[40] J. Alstott, E. Bullmore, and D. Plenz. powerlaw: a Python package for analysis of heavy-tailed distributions. *arXiv:1305.0215v1 [physics.data-an]*, 2013.

[41] A. Clauset, C. Shalizi, and M. Newman. Power-law distributions in empirical data. *SIAM review*, 4(51):661–703, 2009.

[42] L. Adamic and B. Huberman. Power-law distribution of the world wide web. *Science*, 5461(287):661–703, 2000.

[43] R. Mondragón and S. Zhou. Random networks with given rich-club coefficient. *The European Physical Journal B*, 9(85):1–6, 2012.

[44] M. van den Heuvel and O. Sporns. Rich-club organization of the human connectome. *The Journal of Neuroscience*, 31(44):15775–15786, 2011.

[45] R. Milo, S. Kashtan, M. Itzkovitz, M. Newman, and U. Alon. On the uniform generation of random graphs with prescribed degree sequences. *Available at http://arxiv.org/abs/cond-mat/0312028*, 2004.

[46] S. Borgatti and M. Everett. Models of core/periphery structures. *Social Networks*, 21(4):375–395, 2000.

[47] S. Lip. A fast algorithm for the discrete core/periphery bipartitioning problem. *ArXiv e-prints*, 2011. URL `http://adsabs.harvard.edu/abs/2011arXiv1102.5511L`.

[48] D. Fricke. Trading strategies in the overnight money market: Correlations and clustering on the e-MID trading platform. *Physica A: Statistical Mechanics and its Applications*, 24(391):6528–6542, 2012.

[49] M. Buchanan. Nexus: small worlds and the groundbreaking theory of networks. *WW Norton and Company*, 2003.

[50] R. Aguilera. Directorship interlocks in comparative perspective: The case of Spain. *European Sociological Review*, 14(4):319–342, 1998.

[51] J. Pueyo. Interlocking directorates in spanish banking in the twentieth century. *Departament d'Economia i Empresa, Universitat Pompeu Fabra, Working Paper*, (391), 2006.

[52] P. Ferris, M. Jagannathan, and A. Pritchard. Too busy to mind the business? Monitoring by directors with multiple board appointments. *Journal of Finance*, 58 (3):1087–1111, 2003.

[53] E. Fich and A. Shivdasani. Are busy boards effective monitors? *Journal of Finance*, 61(2):689–724, 2006.

[54] Bureau van Dijk. Sistema de análisis de balances ibéricos. 2012.

[55] M. Stephens. Edf statistics for goodness of fit and some comparisons. *Journal of the American Statistical Association*, 69:730–737, 1974.

[56] S. Zhou and R. Mongragón. Random networks with given rich-club coefficient. *IEEE Commun. Lett.*, (8):180–182, 2004.

[57] T. Hoshi, A. Kashyap, and D. Scharfstein. Corporate structure, liquidity, and investment: Evidence from japanese industrial groups. *The Quarterly Journal of Economics*, 106(1):33–60, 1991.

[58] R. Rajan and L. Zingales. Which capitalism? lessons form the east asian crisis. *Journal of Applied Corporate Finance*, 11(3):40–48, 1998.

[59] J. Horton, Y. Millo, and G. Serafeim. Too busy to mind the business? Monitoring by directors with multiple board appointments. *Journal of Business Finance and Accounting*, 39(3):399–426, 2012.

[60] C. Drago, F. Millo, R. Ricciuti, and P. Santella. Corporate governance reforms, interlocking directorship networks and company value in Italy (1998-2007). *CESifo working paper: Industrial Organisation*, (3322), 2011.

[61] A. Kirman, P. Bourgine, and J. Nadal. The structure of economic interaction: individual and collective rationality. *In Cognitive economics: an interdisciplinary approach. Heidelberg: Springer-Verlag*, pages 293–312, 2004.

[62] H. Amman, D. Kendrick, and J. Rust. Agent-based computational finance. *Handbook of computational economics. Elsevier*, (2), 1996.

[63] E. Samanidou, E. Zschischang, D. Stauffer, and T. Lux. Agent-based models of financial markets. *Reports on Progress in Physics*, 70(3), 2007.

[64] B. LeBaron. Agent-based computational finance. *Handbook of computational economics*, (2):1187–1233, 2006.

[65] S. Chen. Computational intelligence in agent-based computational economics. *In: Fulcher, J., Jain. L. (eds.), Computational intelligence: a compendium, Springer*, pages 517–594, 2008.

[66] T. Lux. Stochastic behavioral asset pricing models and the stylized facts. *Handbook of financial markets: Dynamics and evolution*, 161(1), 2009.

[67] S. Grossman and J. Stiglitz. On the impossibility of informationally efficient markets. *The American Economic Review*, 3(70):393–408, 1980.

[68] B. Mandelbrot. Forecasts of future prices, unbiased markets, and martingale models. *Journal of Business*, (1):242–255, 1966.

[69] W. Arthur, J. Holland, B. LeBaron, R. Palmer, and P. Tyler. Asset pricing under endogenous expectations in an artificial stock market. *In: Arthur, W., Durlauf, S., and Lane, D. (eds.), The Economy as an Evolving Complex System II. Reading, Mass.: Addison-Wesley*, pages 15–44, 1997.

[70] W. Brock and C. Hommes. Heterogeneous beliefs and routes to chaos in a simple asset pricing model. *Journal of Economic dynamics and Control*, 89(22):1235–1274, 1998.

[71] B. LeBaron. Agent-based computational finance. *Journal of Economic dynamics and Control*, (2):1187–1233, 2006.

[72] F. Westerhoff. The use of agent-based financial markets to test the effectiveness of regulatory policies. *Journal of Economics and Statistics*, (228):1195–227, 2008.

[73] J. Eckmann, S. Kamphorst, and D. Ruelle. Recurrence plots of dynamical systems. *Europhysics Letters*, 5(9):973–977, 1987.

[74] P. Zbilut and C. Webber Jr. Embeddings and delays as derived from quantification of recurrence plots. *Physics Letters A*, 171(3-4):199–203, 1992.

[75] F. Takens. Detecting strange attractors in turbulence. *in: Dynamical Systems and Turbulence Springer Berlin*, pages 973–977, 1981.

[76] P. Zbilut, J. Zaldivar-Comenges, and F. Strozzi. Recurrence quantification based liapunov exponents for monitoring divergence in experimental data. *Physics Letters A*, 297(3-4):173–181, 2002.

[77] E. Lorenz. Deterministic nonperiodic flow. *Journal of the Atmospheric Sciences*, 20(2):130–141, 1963.

[78] N. Marvan. Encounters with neighbours – current developments of concepts based on recurrence plots and their applications. *Ph.D. Thesis, University of Potsdam*, 2003.

[79] C. Webber Jr. and J. Zbilut. Dynamical assessment of physiological systems and states using recurrence plots strategies. *Journal of Applied Physiology*, 76(2):965–973, 1994.

[80] R. May. Simple mathematical models with very complicated dynamics. *Nature*, 261 (5560):459–467, 1976.

[81] T. Schreiber and A. Schmitz. Improved surrogate data for nonlinearity tests. *Physical Review Letters*, 77:635–638, 1996.

Affirmation

I, Ricardo Giglio, declare that this thesis titled, 'Essays on Interlocking Directorates and Speculative Dynamics' and the work presented in it are my own. I confirm that:

- This work was done wholly or mainly while in candidature for a research degree at this University.
- Where any part of this thesis has previously been submitted for a degree or any other qualification at this University or any other institution, this has been clearly stated.
- Where I have consulted the published work of others, this is always clearly attributed.
- Where I have quoted from the work of others, the source is always given. With the exception of such quotations, this thesis is entirely my own work.
- I have acknowledged all main sources of help.
- Where the thesis is based on work done by myself jointly with others, I have made clear exactly what was done by others and what I have contributed myself.

Signed:

Date: